Damage identification techniques on beam bridges under moving vehicle loads

written by:

MENELAOS PAPAMICHELAKIS

MSc Structural Engineering

September, 2021

TU Delft

[*This page intentionally left blank*]

Damage identification techniques on beam bridges under moving vehicle loads

MSc Thesis written by

Menelaos Papamichelakis

to obtain the degree of Master of Science

in Structural Engineering

at Delft University of Technology

to be defended on 28 September, 2021

Project duration:	November 2020 – September 2021		
Thesis committee:	Chair	Dr. ir. Alice Cicirello	TU Delft
	Member	Prof. dr. ir. Andrei Metrikine	TU Delft
	Member	Dr. ir. Eliz-Mari Lourens	TU Delft

Author Information

Author: Menelaos Papamichelakis
Student number: 5122953

An electronic version of this thesis is available at *https://repository.tudelft.nl/*

Cover: Ponte Morandi collapse – theguardian.com

[*This page intentionally left blank*]

Acknowledgements

This thesis is the last step in order to obtain the Master of Science degree in Structural Engineering in the faculty of Civil Engineering and Geosciences at Delft University of Technology.

At this point, I would like to express my gratitude to my committee members: Dr. ir. Alice Cicirello, Dr. ir. Eliz-Mari Lourens and Prof. dr. ir. Andrei Metrikine for their guidance and support during the whole period I was working on this thesis. It was because of their valuable opinions and suggestions for my topic that I comprehended every detail of this project, enhancing my understandings not only of the numerical models but also of the physics in the different methods included in this thesis. Also, I am greatly indebted to my daily supervisor and chair of this committee, Dr. ir. Alice Cicirello, for her patience and encouragement not only in my research progress but in my personal development, during the whole thesis period.

Last but not least, to the people who have accompanied me on this journey, they know who they are (and I will keep reminding them!), thank you for being a part of my life.

Abstract

The dynamic behavior of structural components can largely change in the presence of damages. Understanding this behavior is of particular importance for critical engineering systems, and in particular bridges. Damage identification methods forms a key objective in structural health monitoring of bridges so many researches have been conducted in this area. In this thesis, damage identification techniques on beam bridges under moving vehicle loads will be presented in order to produce useful conclusions about the assessment of existing bridges by investigating various numerical applications of different scenarios.

The first objective of this thesis is to derive the analytical expressions needed to be able to predict the dynamic response of many different cases of bridges so that as many real scenarios as possible can be treated. This means that these expressions would be used to investigate damaged beam bridges that can be modelled as an assembly of beams with any number of different material properties, any type of interface or boundary conditions and any number of cracks. For this reason an approach to analyze the bridge as an assembly of n piecewise homogeneous damaged Euler-Bernoulli beams jointed at their edges, will be presented, using the generalized functions to obtain a single expression of the solution which depends on the 4 integration constants associated with the boundary conditions. The closed-form expressions of these 4 constants will be provided. Furthermore, in the presence of internal or externals springs, translational or rotational, additional constants representing the discontinuities have to be taken into account and are computed by considering one additional condition for each discontinuity. The feasibility of this approach and the corresponding analytical formulations is shown with two numerical applications that include all the different capabilities mentioned. Moreover, the implementation of these expressions in a deterministic approach for damage localization is presented, mainly as another example of the many possibilities of the use of analytical formulations instead of other approaches and as an introduction of the so called Inverse Problem with deterministic and probabilistic methods.

The second objective concerns the optimization of damage identification on bridges by comparing different quantities that are evaluated while measuring the response of the bridge (direct monitoring) and the response of the moving vehicle when it passes along the bridge (indirect monitoring). First, the governing equations for the dynamic response of these models are derived, considering the crack(s) as a rotational spring, the bridge as an Euler-Bernoulli beam (or multiple with different properties) and the moving vehicle as a spring-mass system. In this manner, the dynamic response of the bridge is calculated (modal characteristics and displacement) as well as the one of the moving oscillator (displacement and acceleration) and the reaction force acting on the surface of the beam from the moving vehicles. Numerical applications with different beam properties and different number of cracks are performed, using MATLAB for the analytical expressions and SAP2000 for the finite element model, to derive the optimal quantity to be used for damage identification. Lastly, the results are validated by considering and comparing an alternative way of modelling crack, namely as a zone with reduced rigidity, for the same numerical examples, leading to the same conclusions about the crack(s) identification.

Last but not least, the third objective of this thesis is to be able deal not only with the widely used time-invariant damages, namely the always-open crack model, but also with time-variant damages and in this case with the switching crack model. To achieve this, the analytical expressions for the closed-form solutions of the mode shapes derived for the always-open crack are modified to be able to tackle the switching crack model by introducing a Boolean switching crack array which identifies open cracks, modelled as rotational springs. These new expressions would still be able to be used for any number of Euler-Bernoulli beams, any type of interface or boundary conditions and any number of switching cracks. Then, the governing equations for the dynamic response of this model are derived, considering the moving vehicles as moving masses in order to

validate the approach with numerical examples existing in the literature and then by introducing its new capabilities. Further, as the computational strategy has been validated, a comparison between time-variant and time-invariant damages is performed concerning crack identification, so that the reader would recognize the importance of understanding the dynamic behavior of different ways of modelling damage in complicate engineering systems like bridges.

Contents

List of Figures

List of Tables

[*This page intentionally left blank*]

Chapter 1

1. Introduction

1.1 Background

Damage identification forms a key objective in structural health monitoring. Specifically for bridges, visual inspection for maintenance purposes happens on a regular basis, with main objective the short and long-term structural integrity, safety and resiliency. But as visual inspection can be useful for detecting surface damages such as concrete spalling, corrosions of steel members or even partially failed components, it is limited at detecting embedded and/or minor cracks such as fatigue cracks, corrosion of embedded reinforcement and delamination. That is the reason many state-of-the-art papers regarding the progress in the area of damage identification methods for bridge structures are published every year, and the theoretical developments, the laboratory-scale implementations and the full-scale experiments become more and more sophisticated and advanced. This master thesis is also one of these attempts to provide useful remarks, by providing results and conclusions that are validated, in the spectrum of structural damage detection, localization and quantification and condition assessment of bridges.

Moreover, in the field of damage identification, there is an ongoing discussion about the way of considering the crack itself in structures. In literature, there are many different ways to treat damages in bridges making the need of robust identification techniques, able to localize and quantify crack(s) in every scenario, more important than ever. This is also because there are examples of damages like capillary cracks which can open or closed depending on the vibration amplitude and side where the damage is located (top or bottom fibers). In this thesis damages with both time-variant and time-invariant parameters would be considered, to predict the dynamic behavior of the bridge, as well as a comparison between them in terms of damage identification purposes.

In the next sections, the already available knowledge about the process of the inspection of bridges and its limitations will be discussed as well as a comparison of direct and indirect monitoring which are linked with the objectives of this thesis about deriving the optimal quantity from all the available measurements. Then, the ways of modelling and considering, in this thesis, the bridge, the vehicle loads and the damage would be explained, adding another final section about the assumptions and the limitations of the specific model.

1.2 Inspection of the bridge

As already noted visual inspection is really common when damage identification is concerned in bridges. But the visual inspection process can be [1]:

- labor-intensive
- costly
- time consuming
- many times unreliable because its inherent reliance on the inspector's judgment

These limitations leads to lack of effectivity of the inspection processes and combined with the alarming aging state of transportation infrastructures makes the bridge maintenance and operation problem really challenging.

The solution comes from adding a new inspection paradigm that exploits the availability of sensor data and measurements, a strategy known as structural health monitoring. In this field the use of advanced transducers, data acquisition and transmission systems, signal processing techniques and more, have introduced new capabilities for damage identification and remaining useful life prediction of bridges. These reasons led to the progress of physics and/or data-driven techniques enabling the decision-making process of advanced SHM systems that are also, nowadays, becoming economically viable [1]. One can say that SHM will play a crucial role in future management and of transportation infrastructure.

1.3 Direct and Indirect Monitoring

Another important discussion mentioned in a lot of papers in the literature and that a lot of researchers investigate is the decision of using measurements on the bridge (direct monitoring) versus on the vehicle (indirect monitoring). Advantages and disadvantages for each side could be find in a large number of different papers ([2], [3], [4]) and they are also summarized in this master thesis, comparing directly the two approaches.

- Direct monitoring is more expensive and time-consuming than indirect monitoring as the equipment (e.g. sensors) should be ordered and then placed carefully along the bridge.
- The understanding of the dynamic behavior of the bridge can be more clear with direct monitoring where lots of information can be recorded, in contrast with indirect monitoring where it is difficult to distinguish between the vehicle and the bridge induced vibrations.
- With indirect monitoring it becomes more challenging to get a complete picture of the bridge behavior in contrast with direct monitoring where influence lines, eigenfrequencies and mode shapes could be provided understanding how the bridge responds to traffic loading.
- The advantage of indirect monitoring is that the inspection can be on-going for a longer period and the same approach can be used for different bridges in contrast with direct monitoring where a different setup is needed for each one of them .
- For both methods, another disadvantage is that the measurements might be ill-posed due to “external” factors (operational / environmental variability) that cause uncertainties in the response.

The last point is important to be explored further as these factors, introducing uncertainties to the measurements, cause serious problems in the existing structural health monitoring techniques. In the paper [5] the effects of environmental and operational variabilities are explained. A few examples of them are mentioned below:

Environmental variability caused from:

- Temperature
- Humidity
- Wind

Temperature, for example, affects not only the material stiffness, but also alters the boundary conditions of a system. Moreover, structures exhibit daily and seasonal temperature variations (a 5% change in fundamental frequency has been documented for bridges during the 24hours cycle and 10% seasonal changes in frequencies were repeatedly observed for years). Finally, when temperature falls below freezing point, 43-76% variations have been documented.

Operational variability caused from:

- Ambient loading conditions
- Operational speed
- Mass loading

In order to tackle these kind of uncertainties, data normalization was introduced, a procedure where data sets are normalized so that signal changes caused by environmental and operational variations can be separated from structural changes of interest.

Looking at the advantages and disadvantages of each approach, one should be really careful about the its limitations and whenever one of them is chosen, the corresponding precautions have to be taken into consideration.

1.4 Problem statement

Now, that a general overview about the reasons that make inspection challenging and damage identification techniques so important, has been provided, this section is dedicated to describe how the modelling of the bridge, the moving vehicles and the damage are considered in this thesis, in order to provide qualitative outcomes. Each one of these considerations was carefully selected after examining similar research topics in the literature, and they are described appropriately in the next paragraphs.

1.4.1 Modelling of the bridge

In the current thesis, the moving load-bridge interaction problem is treated by using the well-established model of an Euler-Bernoulli beam subject to moving vehicle loads. The governing equations that describe the dynamic response of the beam, taking into account time-varying mass, stiffness and damping matrices are presented in this work. Moreover, one novel thing of this master thesis will be the derivation of analytical expressions in order to be able to deal not only with the, commonly-used in the literature, simply supported beam-type bridges but with beams with increased complexity. The complexity rises by considering the bridge as one engineering system that can be modelled as an assembly of beams with different materials and cross-sections, with internal rotational and/or translational springs and external translational springs at the interfaces.

To be able to deal with multi-span beam-type bridges and overcome specific limitations like, (i) computational efficiency in dealing with any number of step changes in material and cross-section, (ii) taking into account efficiently internal and external springs at the discontinuities and (iii) numerical errors in the evaluation of high-order modes for jointed beams, the approach implemented in paper [6] will also be used in this project to derive the new analytical expressions for the mode shapes of the model under investigation. This is necessary as other widely-used methods are not able to overcome these limitations. Specifically, the “classic method” of considering an assembly of n Euler-Bernoulli beams jointed at their edges is based on writing a set of n governing equations and impose $4(n-1)$ continuity conditions (one of each interface). As this approach needs the evaluation of $4(n-1)$ integration constants, it gets time-consuming when the number of the Euler-Bernoulli beams is increased. Another approach not able to tackle this type of problem efficiently is the Finite Element Method (FEM) where the accuracy of the results will depend on the density of the mesh, and as a denser mesh is required for each interface, the computational effort is also increased when the number of discontinuities is increased. Furthermore, the above-mentioned approaches cannot be easily used for exploring the performance of different designs.

Other approaches for evaluating the dynamic response of an assembly of Euler-Bernoulli beams with mechanical or geometrical discontinuities are, a “matrix approach” used in paper [7] to couple two separate uniform EB beams at the discontinuity by imposing specific continuity conditions but taking into account only ideal joints, a “transfer matrix” method used in paper [8] to evaluate the free vibration of jointed EB beams with step changes in cross-sections with ideal joints, a “lumped-mass” approximation used in paper [9] employing exact influence coefficients by defining some ad-hoc Green’s functions and solving efficiently the eigenvalue problem and the “element impedance” method in paper [10] where each beam section is modelled as a free-free section plus an input impedance at one end and an output impedance at the other, and then they are all coupled to form an overall stepped beam structure, a method which is computationally efficient as it avoids matrix operations of large dimensions.

Moreover, it is worth noting that the evaluation of the natural frequencies can be affected by numerical instabilities due to the presence of the hyperbolic functions in the closed-form solutions of the free vibrations, to the point of being able to compute accurately up to 12 modes depending on the boundary conditions, see paper [11]. To overcome this limitation in this project, as it was described in the paper [12], the governing equations of each segment of the jointed EB beam with step changes in material properties will be written in its local coordinate systems and by coupling them with interface conditions at the interface points. In this manner (using local coordinate systems) the expression of the frequency determinant (characteristic equation) of the jointed beam is simplified and leads to largely avoiding numerical round-off errors and consequently improving the accuracy on the evaluation of the higher modes.

To sum up, for the dynamic response of the jointed Euler-Bernoulli beam with step changes in material with rotational and translational internal springs and external translational springs at the interfaces, an approach using generalized functions and local coordinate systems will be used in order to obtain a singe expression of the solution (in terms of deflection or mode shapes) which depends only on 4 integration constants associated with the boundary conditions and one additional constant for each internal or external spring at the interfaces. All the closed-form expressions for the integration constants will be provided.

1.4.2 Modelling of the vehicle

As far as the moving vehicle load is concerned, there are, indeed, different ways to consider the moving vehicle in a model ([14]) and there are simple as well as other more advanced designs mentioned in the literature. One of them is like a moving concentrated force, which especially for the Finite Element Method might be the

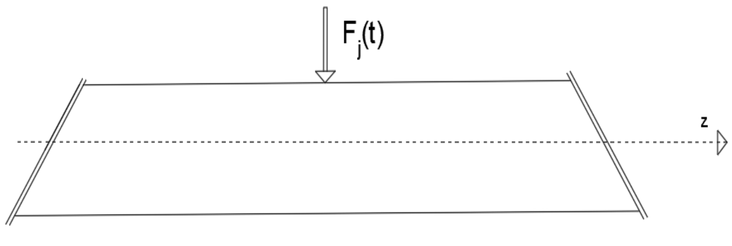

Figure 1. 1: Moving vehicle load as a concentrated force

simplest one but one can lose part of the physics of the model as the inertial effect is completely neglected (see figure 1.1).

Another way of modelling the moving vehicle is like a mass moving on top of the surface of the bridge but also in this case the coupling stiffness with the beam tends to infinity and this does not corresponds precisely in the physics of the real problem.

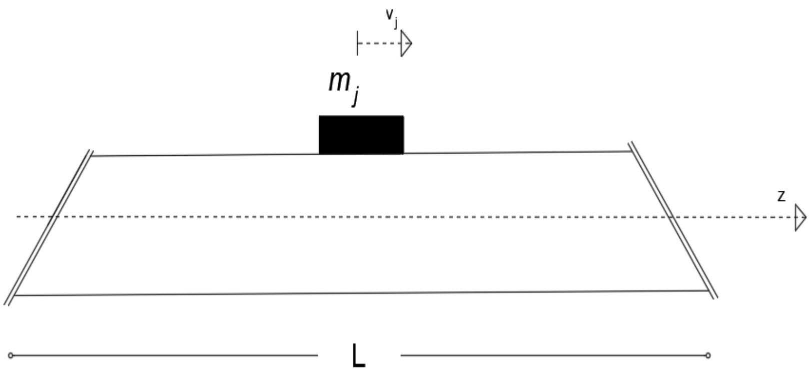

Figure 1. 2: Moving vehicle load as a moving mass

Lastly, one way of modelling the moving vehicle is as a sprung mass system (moving oscillator), where significant inertial of the vehicle is present and the coupling stiffness is also finite. In this case, the mass of the vehicle is not just sliding on top of the beam but it could be designed with an oscillatory motion at a desired frequency.

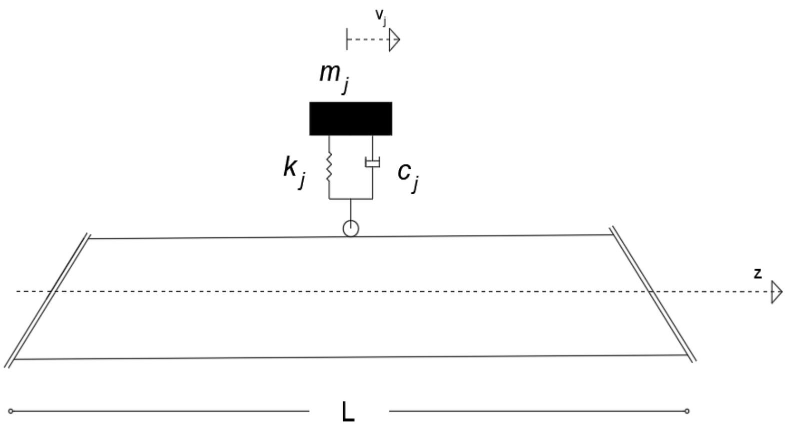

Figure 1. 3: Moving vehicle load as a spring-mass system

In the current master thesis, the governing equations of motion for both modelling the vehicle as a moving mass and as a moving oscillator will be presented so that the reader will be able to judge from the results which model to follow for other investigations.

1.4.3 Modelling of the crack

The final part of the model concerns the way of modelling the damage in the Euler-Bernoulli beam. Also in this case there are different ways that one could find available in the literature. The presence of damage is often tackled by using a discrete spring model ([13]). This model usually provides the best trade-off between model accuracy and computational cost compared to local stiffness reduction models and to 2D/3D Finite Element models which include crack initiation and propagation ([15]). On the other hands, using this model as in paper [16], which means modelling the crack as a massless rotational spring and writing the governing equations for each undamaged pieces between two consecutive cracks, the size of the problem increases with the number of cracks, since a set of continuity conditions need to be imposed at each crack location. The flexibility model, developed by [17], is used for other investigations like the one in [18], considering separately the conditions when the load is moving over the crack or over the undamaged section.

In this master thesis modelling the crack as both a massless rotational spring and with a local reduction model will be treated in a manner, using analytical expressions, that make both approaches equally fast and accurate (see figures 1.4, 1.5).

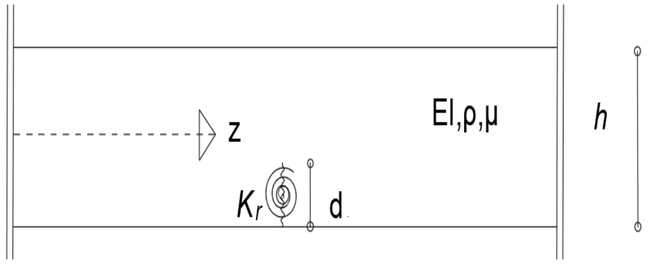

Figure 1. 5: Crack modelled as a rotational spring

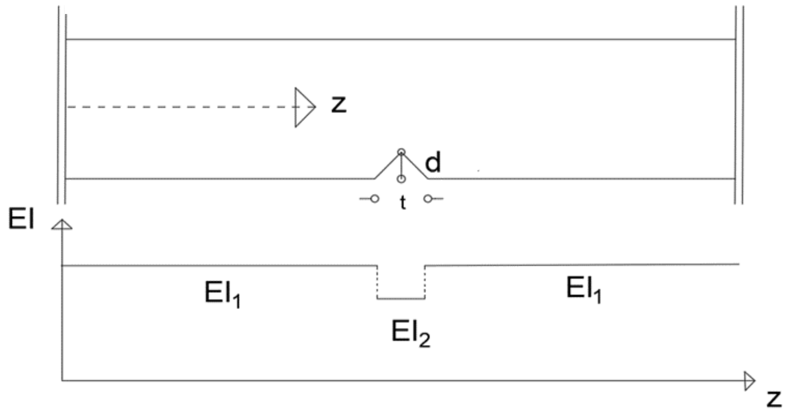

Figure 1. 4: Crack modelled as an influenced zone with reduced rigidity

Damage could be treated with time-variant or time-invariant properties. The always-open crack model, widely adopted for engineering applications, belongs to the category of cracks with time-invariant parameters, and many methods of treating these cracks can be found in the literature. But the always open crack model can lead to inaccurate results in the presence of capillary cracks, which can be open or closed depending on the vibration amplitude and side where the damage is located (either bottom or top fibers). These time-variant parameters can be accounted by employing the switching crack model [19] or the breathing model [20]. While the former accounts for the closed crack condition and the residual cross section stiffness when the crack is open, the latter accounts for progressive variations of the cross section stiffness.

In this master thesis the switching crack model will be implemented in Chapter 4, considering the crack as a rotational spring which can open or close depending on the elastic axial strain at the center of the crack. The differences of this model comparing it with the always-open crack model and the undamaged case are presented in Chapter 4, as well as the comparison of this model when damage identification techniques are concerned.

1.5 Assumptions of the model

In this section, according to the modelling part described above, the assumptions of the model are presented. These assumptions have been chosen carefully in order to simplify the model in specific parts, where it was needed, without the cost of deviating from realistic scenarios, leading to inaccuracies. Limitations, because of these assumptions are also included briefly, but a more detailed discussion about them is given in the last chapter of this thesis. The assumptions and limitations of the model are:

- The surface of the bridge is considered as smooth, meaning the roughness of the bridge has not been considered in the governing equations of motion
- The moving vehicle mass effect will not be taken into account as this would result into time-varying mode shapes which depend on the vehicle's position, therefore not allowing the application of the mode superposition method
- Given the relative small size of the interaction problem, the friction force is neglected
- The vehicle is travelling with known direction and speed along the z-axis
- The vibration of the beam occurs only in the transversal direction
- The mass and the beam are always in contact

Each one of the points describes an assumption either about the interaction of the moving vehicle and the bridge or the properties of the bridge and all of them contribute to the specifications of the model and the derivation of the equations that describe its motion.

1.6 Research questions

An introduction to the field of structural damage detection on bridges has been presented, including many of the existing limitations of structural health monitoring on bridges and the need of advanced methods to predict propagation of cracks or even failure of primary structural elements. Then, the way that the problem of damage identification on beam bridges under moving vehicle loads will be treated in this thesis, has been indicated by explaining how every part (bridge, damage, vehicle loads) will be modelled. Finally, assumptions and limitations of the model were also presented.

Now, that the model became more clear and the research gaps due to all the uncertainties in the procedure are self-evident, the research questions that this thesis will focus on, in every chapter, are introduced. First, the main objective of the current master thesis, related to everything has already been said so far, is:

"How to model and identify damages with time-variant and invariant parameters on multi-span beam-type bridges under moving vehicle loads modelled as a spring-mass system".

The main objective describes what would one important outcome of this thesis, which would be able to tackle damages with both time-variant and time-invariant parameters. Moreover, in this thesis, the number of different beam segments of different properties that describe the bridge will not be a problem, as well as the number of cracks and the boundary and interface conditions. All these specifications will be considered in the derivation of the analytical expressions in the 2nd Chapter, in order to be able to deal with any possible real case scenario of a beam-type bridge.

Throughout this thesis and in the process of answering the main research question, other research sub-questions will also be answered in each Chapter.

Chapter 2, "*Dynamic response of damaged beams with time-invariant parameters under moving loads*":

1) How to model the crack(s) in the Euler-Bernoulli beam?
2) How to obtain a closed-form solution for the mode shapes for any number of cracks, multiple step changes in material, arbitrary boundary conditions and internal/external translational and rotational springs?
3) How to improve the numerical stability (higher order modes) and accuracy of the closed form expressions?
4) How to use only the closed-form solutions for the mode shapes to detect a crack?

Chapter 3, "*Cracks identification (location, intensity)*":

1) Which is the optimal measured quantity to detect a crack?
2) What would be the size of a crack with respect to the size of the cross section to be identifiable?
3) Would the model of the crack affect the identification?
4) Would the number of cracks affect the identification?
5) Would the complexity of the beam-type bridge (varying rigidity) affect the identification?

Chapter 4, "*Dynamic response of beams with switching cracks under moving masses*":

1) How to model the switching crack in the Euler-Bernoulli beam?
2) How to exploit closed-form solutions of the mode shapes to account for the switching cracks?
3) How to evaluate the open cracks distribution at a time instant?
4) Are the always-open or always-closed crack distributions the boundaries for the switching crack model?
5) What would be the differences in damage identification when using the switching crack model instead of the widely adopted always-open crack model?

Each one of these questions demands a comprehensive answer that will be able to make the reader realize every aspect of the specific model and to also lead to an outcome that will provide useful knowledge in the field of structural damage detection that could be used for other similar future projects.

1.7 Report Structure

This thesis report is divided into 4 main chapters and the final chapter about the discussions and conclusions of the whole thesis work.

Chapter 1 explains the background of the research and states the problem of interest. Specifications about the modelling part and its assumptions are provided as well as the research goals and research questions that will be covered in this thesis work.

Chapter 2 contains the entire procedure of the derivation of novel analytical expressions for the mode shapes of the model, in order to obtain a single expression of the solution which depends only on 4 integration constants associated with the boundary conditions and one additional condition for each external or internal spring at the discontinuities. Closed-form solutions of these 4 integration constants are also provided. Then, the new expressions are validated by comparing them with the results of two FE (Finite Element) models in SAP2000, achieving the accuracy needed. Finally, the same expressions are also used as a powerful tool in deterministic model updating and the so called Inverse Problem, in order to identify the location of a crack along a bridge, knowing only its intensity. The findings of this chapter are an example of the importance of using analytical expressions instead of only FE models, as a parameter investigation could be accomplished much faster and with the same accuracy and less computational effort.

Chapter 3 focuses on the comparison of different quantities obtained after the direct and indirect monitoring of the bridge in order to conclude to the optimal one in terms of crack(s) identification. To do that, first the governing equations that describe the dynamic response of the model were derived, assuming the moving vehicles as spring-mass systems (oscillators) and then, the results of the modal characteristics of the bridge, the dynamic response of the beam-type bridge, the reaction force acting on top of the bridge because of the moving oscillator and the response of the oscillator itself (displacement, acceleration) were calculated for different numerical applications and compared. The conclusion in this chapter about the optimal quantity for crack identification, was tested not only for the widely-used simply supported beam with one crack, but for different ways of modelling the crack, for the presence of 2 cracks at different locations and for increased complexity of the model, meaning a multi-span beam-type bridge with different properties along the bridge. At the same time, while comparing the different quantities, a lot of damage scenarios (varying the depth of the crack) were tested so that a good estimation of the minimum depth of a crack to be identifiable along the bridge, was also presented.

Chapter 4 exploits the analytical expressions already derived for the mode shapes, to account for cracks with time-variant parameters, in this case, the switching crack model. First, the governing equations that describe the dynamic response of the model were derived, assuming the moving vehicles as moving masses and then a computational strategy is presented that is able to deal with the opening/closing of the crack during the analysis by computing an open cracks distribution at every time instant. To accomplish that, a Boolean variable is introduced that specified if the crack is open or closed depending on the sign of the axial strain at the location of the crack. This computational strategy is first verified by comparing its results with the ones from FE models in SAP2000, and then it is used to compare the switching crack model with the undamaged case and the always-open crack model. Finally, the damage identification techniques presented in the 3rd Chapter are also used for the switching cracks, showing the importance of understanding their behavior.

The final chapter presents the discussions of the results and conclusions of the whole thesis work, where research questions are answered. Limitations and recommendations for future are also discussed.

The following flowchart summarized the main thesis work:

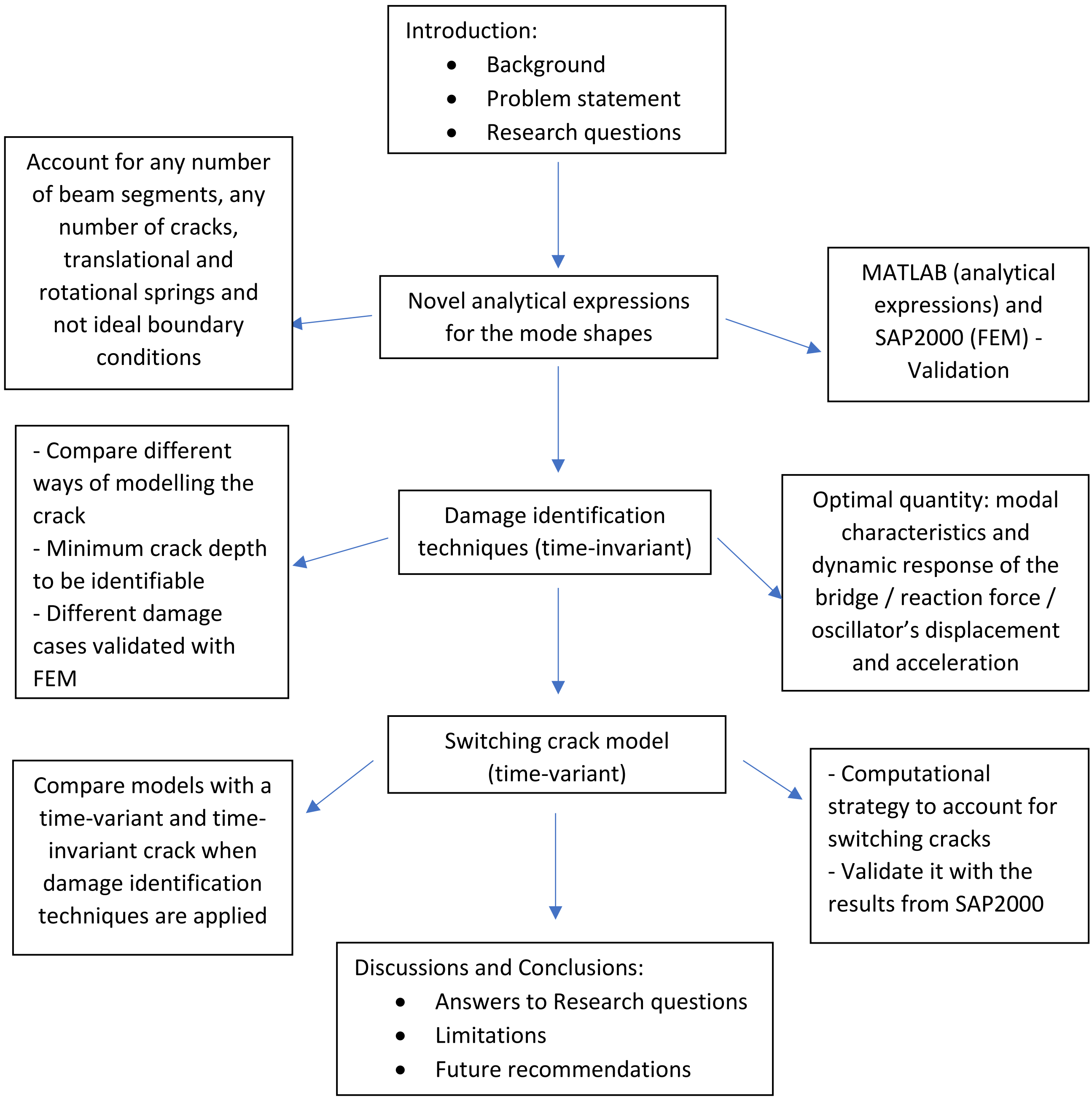

Figure 1. 6: Flowchart of the main thesis work

Chapter 2

2. Dynamic response of damaged beams with time-invariant parameters under moving loads

In this chapter the dynamic response of damaged beams with time-invariant parameters under moving loads will be examined by producing new analytical formulations for the dynamic characteristics of the model. These expressions are, indeed, novel in terms of similar research approaches in literature, and they will be used in this thesis as a tool for the investigation of damage identification techniques in the next chapters.

Therefore, in this chapter, the entire procedure of the derivation of novel analytical expressions for the mode shapes of the model, in order to obtain a single expression of the solution which depends only on 4 integration constants associated with the boundary conditions and one additional condition for each external or internal spring at the discontinuities. Closed-form solutions of these 4 integration constants are also provided. Then, the new expressions are validated by comparing them with the results of two FE (Finite Element) models in SAP2000, achieving the accuracy needed.

Finally, the same expressions are also used as a powerful tool in deterministic model updating and the so called Inverse Problem, in order to identify the location of a crack along a bridge, knowing only its intensity. The findings of this chapter are an example of the importance of using analytical expressions instead of only FE models, as a parameter investigation could be accomplished much faster and with the same accuracy and less computational effort.

It is important to derive analytical expressions for this problem as we can handle with:

- Parameter investigation (different designs much faster than FEM).
- Avoid remodeling, remeshing (denser mesh close to each crack, discontinuity).
- Less computational effort (FEM could be time-consuming).
- FEM limitations in handling switching cracks (time-varying) – to be explained further in next chapters.

Meanwhile, in this chapter, the following research sub-questions will be answered:

- How to model the crack(s) in the Euler-Bernoulli beam?
- How to obtain a closed-form solution for the mode shapes for any number of cracks, multiple step changes in material, arbitrary boundary conditions and internal/external translational and rotational springs?
- How to improve the numerical stability (higher order modes) and accuracy of the closed form expressions?
- How to use only the closed-form solutions for the mode shapes to detect a crack?

2.1 How to obtain a closed-form solution for the mode shapes for any number of cracks, multiple step changes in material and arbitrary boundary conditions?

<u>Main objective</u>: *A single expression of the solution which depends only on <u>4 integration constants</u> associated with the boundary conditions*.

<u>Steps</u>:

1. Consider ways to deal with the numerical errors / instabilities and time-consuming solutions
2. Closed-form expressions of these 4 constants will be derived
3. The solution will be verified using the Finite Element Method

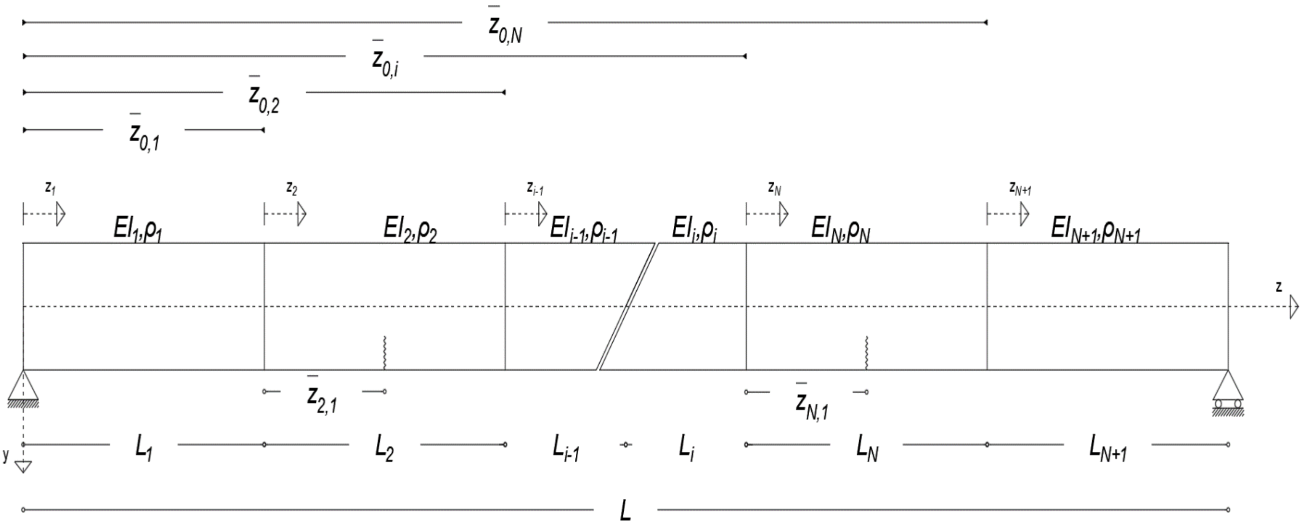

Figure 2. 1: Euler-Bernoulli beam with multiple step changes in material and multiple cracks

Natural frequencies and mode shapes of Euler-Bernoulli beams with multiple cracks:

Let's consider the governing equation describing the response of the *i*th EB beam with uniform flexural rigidity, cross-section and density at its local coordinate system z_i,, with length L_i, so that, $0 \leq z_i \leq L_i$:

$$\frac{\partial^2}{\partial z_i^2}\left[EI(z_i)\frac{\partial^2 u(z_i,t)}{\partial z_i^2}\right] + \rho_i A_i \frac{\partial^2 u(z_i,t)}{\partial t^2} = 0 \qquad \textit{Eq. 1}$$

The mode superposition method can be applied by considering the mode shapes of a damaged beam as:

$$u(z_i,t) = \sum_{r=1}^{\infty} \Phi_{i,r}(z_i) q_{i,r}(t) \qquad \textit{Eq. 2}$$

where $\Phi_{i,r}(z_i)$ is the rth mode shape of the *i*th damaged beam with open cracks and $q_{i,r}(t)$ is the rth generalized coordinate. Considering a modal truncation:

$$u(z_i,t) \cong \sum_{r=1}^{N} \Phi_{i,r}(z_i) q_{i,r}(t) \qquad \textit{Eq. 3}$$

Where N is the number of modes which are included in the modal expansion and a sufficient number should be included to minimize the error in the response calculation. As a rule-of-thumb N can be chosen as twice the number of modes that would be excited by the load acting on the beam.

Substituting in the governing equation:

$$\sum_{r=1}^{N}\left[EI(z_i)\Phi_{i,r}''(z_i)q_{i,r}(t)\right]'' + \rho_i A_i \sum_{r=1}^{N}\Phi_{i,r}(z_i)\ddot{q}_{i,r}(t) = 0 \qquad \text{Eq. 4}$$

The flexibility model is now introduced to the transversally vibrating damaged beam. The dimensionless bending flexibility of the beam:

$$\widetilde{EI}(z_i) = \frac{EI(z_i)}{EI_{i,0}} \qquad \text{Eq. 5}$$

where $EI_{i,0}$ is a convenient reference value of the flexural stiffness of the ith beam, is defined as:

$$\widetilde{EI}(z_i)^{-1} = 1 + \sum_{j=1}^{n}\alpha_{i,j}\delta(z_i - \bar{z}_{i,j}) \qquad \text{Eq. 6}$$

where n is the number of cracks, the jth one occurring at the abscissa $\bar{z}_{i,j}$, $\delta(z_i - \bar{z}_{i,j})$ is the Dirac delta function centered at the jth crack position; $\alpha_{i,j}$ is a parameter related to the severity of the damage at $z_i = \bar{z}_{i,j}$ and is given as:

$$\alpha_{i,j} = \frac{EI_{i,0}}{K_{i,j}} \qquad \text{Eq. 7}$$

where $K_{i,j}$ is the elastic stiffness of the rotational spring of the jth crack of the ith beam.

Back to the governing equation, after simple multiplications, this equation [1] can be rewritten for each r-mode

$$\frac{\left[EI(z_i)\widetilde{\Phi}_{i,r}''(z_i)\right]''}{\rho_i A_i \widetilde{\Phi}_{i,r}(z_i)} = -\frac{\ddot{q}_{i,r}(t)}{q_{i,r}(t)} = \omega_{i,r}^2 \qquad \text{Eq. 8}$$

Since one ratio is a function of z_i only and the other one is a function of t only, both of them must be equal to a positive constant $\omega_{i,r}^2$ which is the square value of the natural frequency related to the rth mode shape.

Therefore, the two differential equations that we obtain are:

$$\ddot{q}_{i,r}(t) + \omega_{i,r}^2 q_{i,r}(t) = 0 \qquad \text{Eq. 9}$$

$$\left[EI(z_i)\widetilde{\Phi}_{i,r}''(z_i)\right]'' - \omega_{i,r}^2\rho_i A_i \widetilde{\Phi}_{i,r}(z_i) = 0 \qquad \text{Eq. 10}$$

The latter equations can be rewritten considering the flexibility model of crack as:

$$\left[\widetilde{EI}(z_i)\widetilde{\Phi}_{i,r}''(z_i)\right]'' - \beta_{i,r}^4\widetilde{\Phi}_{i,r}(z_i) = 0 \qquad \text{Eq. 11}$$

where,

$$\beta_{i,r}^4 = \frac{\omega_{i,r}^2\rho_i A_i}{EI_{i,0}} \qquad \text{Eq. 12}$$

2.1.1 Undamaged case: Consider the case of an assembly of Euler-Bernoulli beams with no damages

In this case: $\widetilde{EI}(z_i) = 1$, therefore the governing equation [Eq. 1] is rewritten as:

$$\left[\widetilde{\Phi}_{i,r}''(z_i)\right]'' - \beta_{i,r}^4 \widetilde{\Phi}_{i,r}(z_i) = 0 \qquad \text{Eq. 13}$$

And its well-known solution as a combination of trigonometric and hyperbolic functions is:

$$\widetilde{\Phi}_{i,r}(z_i) = \frac{C_{i,r}^{(1)}}{2}\left(cos(\beta_{i,r}z_i) + cosh(\beta_{i,r}z_i)\right) + \frac{C_{i,r}^{(2)}}{2\beta_{i,r}}\left(sin(\beta_{i,r}z_i) + sinh(\beta_{i,r}z_i)\right) - \frac{C_{i,r}^{(3)}}{2\beta_{i,r}^2}\left(cos(\beta_{i,r}z_i) - cosh(\beta_{i,r}z_i)\right) - \frac{C_{i,r}^{(4)}}{2\beta_{i,r}^3}\left(sin(\beta_{i,r}z_i) - sinh(\beta_{i,r}z_i)\right) \qquad \text{Eq. 14}$$

which could be derived by computing the Laplace transform and then its inverse.

The coefficients $C_{i,r}^{(1)}, C_{i,r}^{(2)}, C_{i,r}^{(3)}, C_{i,r}^{(4)}$ are the 4 integration constants dependent on $\beta_{i,r}$ and which can be computed by imposing 4 boundary conditions of the ith beam

In the case of an assembly of beams, the 4 integration constants and the frequency parameter of the mode shape of each ith beam can be expressed as *a function of the preceding beam* by explicitly enforcing the continuity conditions at each interface. As a result each mode shape of the jointed beam depends only on 4 constants and m frequency parameters (being m the mode number). Moreover, each frequency parameter $\beta_{i,r}$ will be expressed as function of the natural frequencies ω_r of the entire jointed beam.

To derive the recursive expression of the 4 constants using generalized functions:

$$\widetilde{\Psi}_{i,r}(z_i) = \widetilde{\Phi}_{i,r}'(z_i) \qquad \text{Eq. 15}$$

$$\widetilde{M}_{i,r}(z_i) = -EI_i \widetilde{\Phi}_{i,r}''(z_i) \qquad \text{Eq. 16}$$

$$\widetilde{T}_{i,r}(z_i) = -EI_i \widetilde{\Phi}_{i,r}'''(z_i) \qquad \text{Eq. 17}$$

where $\widetilde{\Psi}_{i,r}(z_i)$ the slope; $\widetilde{M}_{i,r}(z_i)$ the bending moment; $\widetilde{T}_{i,r}(z_i)$ the shear force.

Now, with the enforcement of the continuity conditions at each interface in terms of the mode shape deflection, the slope, the bending moment and shear force:

$$\widetilde{\Phi}_{i,r}(z_{0,i}) = \widetilde{\Phi}_{i+1,r}(0) \qquad \text{Eq. 18}$$

$$\widetilde{\Psi}_{i,r}(z_{0,i}) = \widetilde{\Psi}_{i+1,r}(0) \qquad \text{Eq. 19}$$

$$\widetilde{M}_{i,r}(z_{0,i}) = \widetilde{M}_{i+1,r}(0) \qquad \text{Eq. 20}$$

$$\widetilde{T}_{i,r}(z_{0,i}) = \widetilde{T}_{i+1,r}(0) \qquad \text{Eq. 21}$$

Which enables to reduce the 4N unknown coefficients (where N the number of the modes taken into account) to 4 unknown coefficients which can be found by imposing the 4 boundary conditions only:

$$C_{i+1,r}^{(1)} = \frac{1}{2\beta_{i,r}^3}\left(\beta_{i,r}^3 C_{i,r}^{(1)} \Gamma_{i,r}^{(1)} + \beta_{i,r}^2 C_{i,r}^{(2)} \Gamma_{i,r}^{(3)} + \beta_{i,r} C_{i,r}^{(3)} \Gamma_{i,r}^{(2)} + C_{i,r}^{(4)} \Gamma_{i,r}^{(4)}\right) \qquad \text{Eq. 22}$$

$$C_{i+1,r}^{(2)} = \frac{1}{2\beta_{i,r}^2}\left(\beta_{i,r}^3 C_{i,r}^{(1)} \Gamma_{i,r}^{(4)} + \beta_{i,r}^2 C_{i,r}^{(2)} \Gamma_{i,r}^{(1)} + \beta_{i,r} C_{i,r}^{(3)} \Gamma_{i,r}^{(3)} + C_{i,r}^{(4)} \Gamma_{i,r}^{(2)}\right) \qquad \text{Eq. 23}$$

$$C_{i+1,r}^{(3)} = \frac{1}{2\tilde{\gamma}_i\beta_{i,r}}\left(\beta_{i,r}^3 C_{i,r}^{(1)}\Gamma_{i,r}^{(2)} + \beta_{i,r}^2 C_{i,r}^{(2)}\Gamma_{i,r}^{(4)} + \beta_{i,r} C_{i,r}^{(3)}\Gamma_{i,r}^{(1)} + C_{i,r}^{(4)}\Gamma_{i,r}^{(3)}\right) \quad \text{Eq. 24}$$

$$C_{i+1,r}^{(4)} = \frac{1}{2\tilde{\gamma}_i}\left(\beta_{i,r}^3 C_{i,r}^{(1)}\Gamma_{i,r}^{(3)} + \beta_{i,r}^2 C_{i,r}^{(2)}\Gamma_{i,r}^{(2)} + \beta_{i,r} C_{i,r}^{(3)}\Gamma_{i,r}^{(4)} + C_{i,r}^{(4)}\Gamma_{i,r}^{(1)}\right) \quad \text{Eq. 25}$$

where the functions $\Gamma_{i,r}^{(1)}, \Gamma_{i,r}^{(2)}, \Gamma_{i,r}^{(3)}, \Gamma_{i,r}^{(4)}$ are defined as:

$$\Gamma_{i,r}^{(1)} = cos(\beta_{i,r}L_i) + cosh(\beta_{i,r}L_i) \quad \text{Eq. 26}$$

$$\Gamma_{i,r}^{(2)} = cosh(\beta_{i,r}L_i) - cos(\beta_{i,r}L_i) \quad \text{Eq. 27}$$

$$\Gamma_{i,r}^{(3)} = sinh(\beta_{i,r}L_i) + sin(\beta_{i,r}L_i) \quad \text{Eq. 28}$$

$$\Gamma_{i,r}^{(4)} = sinh(\beta_{i,r}L_i) - sin(\beta_{i,r}L_i) \quad \text{Eq. 29}$$

and the dimensionless quantity:

$$\tilde{\gamma}_i = \frac{EI_{i+1}}{EI_i} \quad \text{Eq. 30}$$

The locations $(z_{0,i})$ are the ones of the discontinuities along the length of the beam, the points that separates two beams of uniform flexural rigidity, cross-section and density.

In the case of an assembly of Euler-Bernoulli beams, the time-dependent deflection of the jointed beam was given as:

$$W(z,t) = W_1(z_1,t) + \sum_{i=2}^{N+1}[W_i(z,t) - W_{i-1}(z,t)]H(z - \bar{z}_{0,i-1}) \quad \text{Eq. 31}$$

Since $W_i(z,t)$ can be expressed as the sum of the product of the mode shapes and the generalized coordinates, the Heaviside's unit step function will affect only the mode shapes.

So, the rth mode shape of the jointed Euler-Bernoulli beam is expressed as:

$$\tilde{\Phi}_r(z) = \tilde{\Phi}_{1,r}(z) + \sum_{i=2}^{N+1}\left[\tilde{\Phi}_{i,r}(z - \bar{z}_{0,i-1}) - \tilde{\Phi}_{i-1,r}(z - \bar{z}_{0,i-2})\right]H(z - \bar{z}_{0,i-1}) \quad \text{Eq. 32}$$

where, $z_1 = z$, $z_2 = z - \bar{z}_{0,1}$,...., $z_i = z - \bar{z}_{0,i-1}$

In the same manner the slope $\tilde{\Psi}_{i,r}(z) = \tilde{\Phi}_{i,r}{}'(z)$, the bending moment $\tilde{M}_{i,r}(z) = -EI_i\tilde{\Phi}_{i,r}{}''(z)$ and the shear force $\tilde{T}_{i,r}(z) = -EI_i\tilde{\Phi}_{i,r}{}'''(z)$ are given for the rth mode shape of the whole jointed EB beam as:

$$\tilde{\Psi}_r(z) = \tilde{\Psi}_{1,r}(z) + \sum_{i=2}^{N+1}\left[\tilde{\Psi}_{i,r}(z - \bar{z}_{0,i-1}) - \tilde{\Psi}_{i-1,r}(z - \bar{z}_{0,i-2})\right]H(z - \bar{z}_{0,i-1}) \quad \text{Eq. 33}$$

$$\tilde{M}_r(z) = \tilde{M}_{1,r}(z) + \sum_{i=2}^{N+1}\left[\tilde{M}_{i,r}(z - \bar{z}_{0,i-1}) - \tilde{M}_{i-1,r}(z - \bar{z}_{0,i-2})\right]H(z - \bar{z}_{0,i-1}) \quad \text{Eq. 34}$$

$$\tilde{T}_r(z) = \tilde{T}_{1,r}(z) + \sum_{i=2}^{N+1}\left[\tilde{T}_{i,r}(z - \bar{z}_{0,i-1}) - \tilde{T}_{i-1,r}(z - \bar{z}_{0,i-2})\right]H(z - \bar{z}_{0,i-1}) \quad \text{Eq. 35}$$

2.1.2 Damaged case: Consider the case of an assembly of Euler-Bernoulli beams with damages

In this case, $\widetilde{EI}(z_i)^{-1} = 1 + \sum_{j=1}^{n} \alpha_{i,j}\delta(z_i - \bar{z}_{i,j})$, therefore the governing equation is defined as:

$$\left[\widetilde{EI}(z_i)\widetilde{\Phi}''_{i,r}(z_i)\right]'' - \beta_{i,r}^4 \widetilde{\Phi}_{i,r}(z_i) = 0 \qquad \text{Eq. 36}$$

Considering the ith beam the following procedure is used. First a double integration of the governing equation yields:

$$\left[\widetilde{EI}(z_i)\widetilde{\Phi}''_{i,r}(z_i)\right] - \beta_{i,r}^4 \widetilde{\Phi}_{i,r}^{[2]}(z_i) = C_A z + C_B \qquad \text{Eq. 37}$$

where C_A, C_B are two unknown integration constants, while $\widetilde{\Phi}_{i,r}^{[m]}(z_i)$ stands for the primitive (or anti-derivative) of order m of $\widetilde{\Phi}_{i,r}(z_i)$ given by m consecutive indefinite integrations. By setting:

$$\widetilde{W}_i(z_i) = \beta_{i,r}^4 \widetilde{\Phi}_{i,r}^{[2]}(z_i) - C_A z - C_B \qquad \text{Eq. 38}$$

which leads to rewrite the governing equation as:

$$\left[\widetilde{EI}(z_i)\widetilde{W}_{i,r}''''(z_i)\right] - \beta_{i,r}^4 \widetilde{W}_{i,r}(z_i) = 0 \qquad \text{Eq. 39}$$

or equally,

$$\left[1 + \sum_{j=1}^{n} \alpha_{i,j}\delta(z_i - \bar{z}_{i,j})\right]^{-1} \widetilde{W}_{i,r}''''(z_i) - \beta_{i,r}^4 \widetilde{W}_{i,r}(z_i) = 0 \qquad \text{Eq. 40}$$

$$\widetilde{W}_{i,r}''''(z_i) = \left[1 + \sum_{j=1}^{n} \alpha_{i,j}\delta(z_i - \bar{z}_{i,j})\right] \beta_{i,r}^4 \widetilde{W}_{i,r}(z_i) \qquad \text{Eq. 41}$$

By applying the Laplace Transform in a specific rth mode shape to simplify the notation:

$$s^4 \mathcal{L}\langle \widetilde{W}_i(z_i)\rangle - \widetilde{W}_i'''(0) - s\widetilde{W}_i''(0) - s^2\widetilde{W}_i'(0) - s^3\widetilde{W}_i(0) = \mathcal{L}\left\langle \left[1 + \sum_{j=1}^{n} \alpha_{i,j}\delta(z_i - \bar{z}_{i,j})\right] \beta_i^4 \widetilde{W}_i(z_i)\right\rangle \qquad \text{Eq. 42}$$

where $\mathcal{L}\langle\blacksquare\rangle$ stands for the Laplace's transform operator; while s is the Laplace's variable associated with the dimensionless abscissa ζ_i. Isolating the term $\widetilde{U}_i(s) = \mathcal{L}\langle \widetilde{W}_i(z_i)\rangle$ and introducing the integration constants $C_1 = \widetilde{W}_i(0)$, $C_2 = \widetilde{W}_i'(0)$, $C_3 = \widetilde{W}_i''(0)$ and $C_4 = \widetilde{W}_i'''(0)$, leads to:

$$\widetilde{U}_i(s) = \frac{1}{s^4 - \beta_i^4}\left\{ s^3 C_1 + s^2 C_2 + sC_3 + C_4 + \sum_{j=1}^{n} \beta_i^4 \alpha_{i,j} e^{-z_{i,j}s}\, \widetilde{W}_i(\bar{z}_{i,j}) \right\} \qquad \text{Eq. 43}$$

Inverse Laplace transform leads to:

$$\begin{aligned}\widetilde{W}_i(z_i) = \frac{1}{2\beta_i^3}&[\beta_i(C_1\beta_i^2 - C_3)\cos(\beta_i z) + \beta_i(C_1\beta_i^2 + C_3)\cosh(\beta_i z) + (C_2\beta_i^2 + C_4)\sinh(\beta_i z) \\ &+ (C_2\beta_i^2 - C_4)\sin(\beta_i z)] \\ &+ \frac{\beta_i}{2}\sum_{j=1}^{n} \alpha_{i,j}\widetilde{W}_i(\bar{z}_{i,j})[\sinh(\beta_i(z_i - \bar{z}_{i,j})) - \sin(\beta_i(z_i - \bar{z}_{i,j}))]\,\mathcal{H}(z_i - \bar{z}_{i,j})\end{aligned} \qquad \text{Eq. 44}$$

To obtain the mode shape function with open cracks, the second derivative is calculated as:

$$\widetilde{\Phi}_i(z_i) = \frac{1}{2\beta_i}[\beta_i(C_3 - C_1\beta_i^2)\,cos(\beta_i z_i) + \beta_i(C_1\beta_i^2 + C_3)\,cosh(\beta_i z_i) + (C_2\beta_i^2 + C_4)\,sinh(\beta_i z_i) + (C_4 - C_2\beta_i^2)\,sin(\beta_i z_i)] + \frac{\beta_i^3}{2}\sum_{j=1}^{n}\alpha_{i,j}\widetilde{W}_i(\bar{z}_{i,j})\left[sinh(\beta_i(z_i - \bar{z}_{i,j})) - sin(\beta_i(z_i - \bar{z}_{i,j}))\right]\mathcal{H}(z_i - \bar{z}_{i,j}) \quad \text{Eq. 45}$$

where,

$$\widetilde{W}_i(\bar{z}_{i,j}) = \frac{1}{2\beta_i^3}[\beta_i(C_1\beta_i^2 - C_3)\,cos(\beta_i\bar{z}_{i,j}) + \beta_i(C_1\beta_i^2 + C_3)\,cosh(\beta_i\bar{z}_{i,j}) + (C_2\beta_i^2 + C_4)\,sinh(\beta_i\bar{z}_{i,j}) + (C_2\beta_i^2 - C_4)\,sin(\beta_i\bar{z}_{i,j})] + \frac{\beta_i}{2}\sum_{k=1}^{j-1}\alpha_{i,k}\widetilde{W}_i(\bar{z}_{i,k})\left[sinh(\beta_i(\bar{z}_{i,j} - \bar{z}_{i,k})) - sin(\beta_i(\bar{z}_{i,j} - \bar{z}_{i,k}))\right]\mathcal{H}(\bar{z}_{i,j} - \bar{z}_{i,k}) \quad \text{Eq. 46}$$

Considering the same procedure for an assembly of jointed Euler-Bernoulli beams, but in this case with the presence of damages, the unknown integration constants will be reduced from $4N$ to 4 unknown coefficients, by enforcing the continuity conditions at each interface in terms of the mode shapes, which can be solve by imposing the boundary conditions.

The results in this scenario are:

$$C_{i+1,r}^{(1)} = \frac{1}{2\tilde{\gamma}_{i,r}\delta_{i,r}^4}\left(C_{i,r}^{(1)}\Gamma_{i,r}^{(1)} + \frac{1}{\beta_{i,r}}C_{i,r}^{(2)}\Gamma_{i,r}^{(3)} + \frac{1}{\beta_{i,r}^2}C_{i,r}^{(3)}\Gamma_{i,r}^{(2)} + \frac{1}{\beta_{i,r}^3}C_{i,r}^{(4)}\Gamma_{i,r}^{(4)}\right) + \Pi_{i,r}^{(1)} \quad \text{Eq. 47}$$

$$C_{i+1,r}^{(2)} = \frac{1}{2\tilde{\gamma}_{i,r}\delta_{i,r}^4}\left(\beta_{i,r}C_{i,r}^{(1)}\Gamma_{i,r}^{(4)} + C_{i,r}^{(2)}\Gamma_{i,r}^{(1)} + \frac{1}{\beta_{i,r}}C_{i,r}^{(3)}\Gamma_{i,r}^{(3)} + \frac{1}{\beta_{i,r}^2}C_{i,r}^{(4)}\Gamma_{i,r}^{(2)}\right) + \Pi_{i,r}^{(2)} \quad \text{Eq. 48}$$

$$C_{i+1,r}^{(3)} = \frac{1}{2}\left(\beta_{i,r}^2C_{i,r}^{(1)}\Gamma_{i,r}^{(2)} + \beta_{i,r}C_{i,r}^{(2)}\Gamma_{i,r}^{(4)} + C_{i,r}^{(3)}\Gamma_{i,r}^{(1)} + \frac{1}{\beta_{i,r}}C_{i,r}^{(4)}\Gamma_{i,r}^{(3)}\right) + \Pi_{i,r}^{(3)} \quad \text{Eq. 49}$$

$$C_{i+1,r}^{(4)} = \frac{1}{2}\left(\beta_{i,r}^3C_{i,r}^{(1)}\Gamma_{i,r}^{(3)} + \beta_{i,r}^2C_{i,r}^{(2)}\Gamma_{i,r}^{(2)} + \beta_{i,r}C_{i,r}^{(3)}\Gamma_{i,r}^{(4)} + C_{i,r}^{(4)}\Gamma_{i,r}^{(1)}\right) + \Pi_{i,r}^{(4)} \quad \text{Eq. 50}$$

where the functions $\Gamma_{i,r}^{(1)}, \Gamma_{i,r}^{(2)}, \Gamma_{i,r}^{(3)}, \Gamma_{i,r}^{(4)}$ are defined again as:

$$\Gamma_{i,r}^{(1)} = cos(\beta_{i,r}L_i) + cosh(\beta_{i,r}L_i) \quad \text{Eq. 51}$$

$$\Gamma_{i,r}^{(2)} = cosh(\beta_{i,r}L_i) - cos(\beta_{i,r}L_i) \quad \text{Eq. 52}$$

$$\Gamma_{i,r}^{(3)} = sinh(\beta_{i,r}L_i) + sin(\beta_{i,r}L_i) \quad \text{Eq. 53}$$

$$\Gamma_{i,r}^{(4)} = sinh(\beta_{i,r}L_i) - sin(\beta_{i,r}L_i) \quad \text{Eq. 54}$$

and the dimensionless quantities:

$$\tilde{\gamma}_i = \frac{EI_{i+1}}{EI_i} \quad \text{Eq. 55}$$

$$\tilde{\delta}_i = \frac{\beta_{i+1}}{\beta_i} \quad \text{Eq. 56}$$

Moreover, the functions $\Pi_{i,r}^{(1)}, \Pi_{i,r}^{(2)}, \Pi_{i,r}^{(3)}$ and $\Pi_{i,r}^{(4)}$ are defined as:

$$\Pi_{i,r}^{(1)} = \frac{1}{2\tilde{\gamma}_{i,r}\delta_{i,r}^{4}}\left[\sum_{j=1}^{n_i}\left\{\alpha_{i,j}\widetilde{W}_i(\bar{z}_{i,j})\beta_i\left[sinh\left(\beta_i(L_i - \bar{z}_{i,j})\right) - sin(\beta_i(L_i - \bar{z}_{i,j}))\right]\right\}\right] - \frac{\beta_{i+1}}{2}\sum_{j=1}^{n_{i+1}}\left\{\alpha_{i+1,j}\widetilde{W}_{i+1}(\bar{z}_{i+1,j})\left[sinh\left(\beta_{i+1}(\bar{z}_{i+1,j})\right) - sin(\beta_{i+1}(\bar{z}_{i+1,j}))\right]\right\} \quad \text{Eq. 57}$$

$$\Pi_{i,r}^{(2)} = \frac{1}{2\tilde{\gamma}_{i,r}\delta_{i,r}^{4}}\left[\sum_{j=1}^{n_i}\left\{\alpha_{i,j}\widetilde{W}_i(\bar{z}_{i,j})\beta_i^2\left[cosh\left(\beta_i(L_i - \bar{z}_{i,j})\right) - cos(\beta_i(L_i - \bar{z}_{i,j}))\right]\right\}\right] - \frac{\beta_{i+1}^2}{2}\sum_{j=1}^{n_{i+1}}\left\{\alpha_{i+1,j}\widetilde{W}_{i+1}(\bar{z}_{i+1,j})\left[cosh\left(\beta_{i+1}(\bar{z}_{i+1,j})\right) - cos(\beta_{i+1}(\bar{z}_{i+1,j}))\right]\right\} \quad \text{Eq. 58}$$

$$\Pi_{i,r}^{(3)} = \frac{1}{2}\left[\sum_{j=1}^{n_i}\left\{\alpha_{i,j}\widetilde{W}_i(\bar{z}_{i,j})\beta_i^3\left[sinh\left(\beta_i(L_i - \bar{z}_{i,j})\right) + sin(\beta_i(L_i - \bar{z}_{i,j}))\right]\right\}\right] - \frac{\beta_{i+1}^3}{2}\sum_{j=1}^{n_{i+1}}\left\{\alpha_{i+1,j}\widetilde{W}_{i+1}(\bar{z}_{i+1,j})\left[sinh\left(\beta_{i+1}(\bar{z}_{i+1,j})\right) + sin(\beta_{i+1}(\bar{z}_{i+1,j}))\right]\right\} \quad \text{Eq. 59}$$

$$\Pi_{i,r}^{(4)} = \frac{1}{2}\left[\sum_{j=1}^{n_i}\left\{\alpha_{i,j}\widetilde{W}_i(\bar{z}_{i,j})\beta_i^4\left[cosh\left(\beta_i(L_i - \bar{z}_{i,j})\right) + cos(\beta_i(L_i - \bar{z}_{i,j}))\right]\right\}\right] - \frac{\beta_{i+1}^4}{2}\sum_{j=1}^{n_{i+1}}\left\{\alpha_{i+1,j}\widetilde{W}_{i+1}(\bar{z}_{i+1,j})\left[cosh\left(\beta_{i+1}(\bar{z}_{i+1,j})\right) + cos(\beta_{i+1}(\bar{z}_{i+1,j}))\right]\right\} \quad \text{Eq. 60}$$

where n_i and n_{i+1}, are the number of cracks for the ith and $(i+1)$th beam respectively.

Finally, $\mathcal{H}(z_i)$ denotes the Heaviside unit step function (which also corresponds to the primitive of the Dirac delta function centered at zero):

$$\mathcal{H}(z_i) = \delta_i^{[1]}(z_i) = \int_{-\infty}^{\zeta}\delta(\xi_i)d\xi_i = \begin{cases} 0, & z_i < 0; \\ \frac{1}{2}, & z_i = 0; \\ 1, & z_i > 0. \end{cases} \quad \text{Eq. 61}$$

2.1.3 Numerical application (2.1) – Step changes in material:

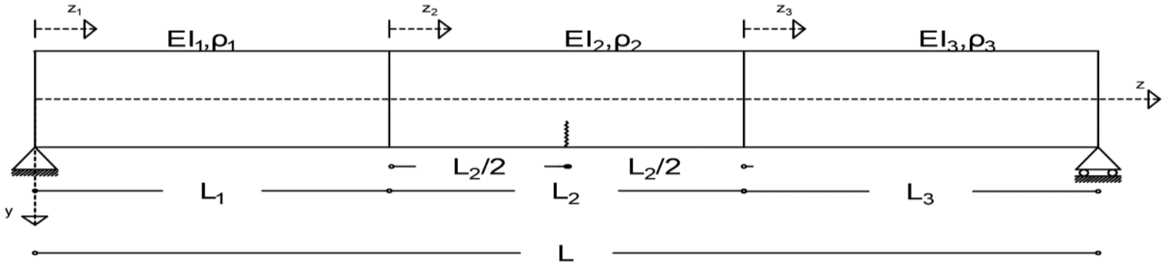

Figure 2. 2: Numerical application (2.1) - Model

The first numerical application, in order to examine the validity of the proposed expressions, is a simply supported beam with three different segments, each one of them described by a different density and Young's modulus, and a single crack at the middle. The properties of the beam-type bridge are:

Table 2. 1: Numerical application (2.1) - Properties of the model

Properties	*Beam 1*	*Beam 2*	*Beam 3*
Length [m]	10	10	10
Density [kg/m^3]	7800	7400	7000
Young's modulus [kN/m^2]	2.10x10^8	2.00x10^8	1.90x10^8

All the beams have a square cross-section of sides $h = 20\ cm$ and the crack has a depth of $d_{2,1} = 0.15\ cm$ located at the 2nd beam at the location $z_2 = 5\ m$. This means that the equivalent stiffness coefficient is equal to $K_{2,1} = 8000\ \mathrm{kN\ m}$, and the corresponding damage parameter is equal to $a_{2,1} = 3.33$.

Boundary Conditions:

$$\widetilde{M}_r(0) = \widetilde{\Phi}_r(0) = 0 \qquad \text{Eq. 62}$$

$$\widetilde{M}_r(L) = \widetilde{\Phi}_r(L) = 0 \qquad \text{Eq. 63}$$

To verify the results of the eigenfrequencies and the mode shapes, a Finite Element (FE) model has been built in SAP2000, by applying a release partial fixity at the crack location. The results of the five first eigenfrequencies for both the Undamaged and Damaged case are:

Table 2. 2: Numerical application (2.1) - Eigenfrequencies from Proposed Expressions and SAP2000 – Undamaged case

Eigenfrequencies Undamaged case	Proposed expressions (rad/sec)	SAP2000 (rad/sec)	Error (%)
1	3.2914	3.2900	-0.0425
2	13.1672	13.1661	-0.0083
3	29.6257	29.6157	-0.0337
4	52.6675	52.6002	-0.1279
5	82.2940	82.2205	-0.0894

Table 2. 3: Numerical application (2.1) - Eigenfrequencies from Proposed Expressions and SAP2000 – Damaged case

Eigenfrequencies Damaged case	Proposed expressions (rad/sec)	SAP2000 (rad/sec)	Error (%)
1	2.9766	2.9755	-0.0369
2	13.1671	13.1635	-0.0273
3	27.1896	27.1770	-0.0463
4	52.6676	52.6201	-0.0898
5	76.3745	76.2489	-0.1647

The results are compared to those yielded by SAP2000, together with the percentage error, defined as:

$$\varepsilon(\%) = \left(\frac{\omega_{SAP2000} - \omega_{proposed}}{\omega_{SAP2000}}\right) * 100 \qquad \text{Eq. 64}$$

where $\omega_{SAP2000}$ is the frequency yielded by SAP2000, while $\omega_{proposed}$ is the one obtained with the proposed method.

The results are in a very good agreement with an error below 0.05% for the first 3 eigenfrequencies and below 0.15% for the 4^{th} and the 5^{th} eigenfrequencies. SAP2000 uses the finite element approach, which provides approximated values of the natural frequencies even if a dense mesh is considered. This means that the proposed expression, that were derived in this thesis project, can predict accurately the eigenfrequencies of this model and consequently of any other similar model with different parameters or number of segments or number of cracks or different boundary conditions. As expected, the 2^{nd} and the 4^{th} eigenfrequencies are hardly affected by the presence of the crack, as the crack is located close to the point where the deflection is always zero (in this case it is not exactly at the middle because of the step changes in material of the bridge). Next step will be to verify the mode shapes, normalized so that the maximum deflection would be equal to one(1). The first 5 mode shapes are presented, calculated with both SAP2000 and the proposed expressions, for the Undamaged case as well as the Damaged case.

The results for the shape of the mode shapes with the proposed expressions seem to coincide with the ones calculated from the finite element model in SAP2000. For the 1^{st} , the 3^{rd} and the 5^{th} mode shape a kink is present exactly at the location of the crack, being the main difference with the Undamaged case. This kink is, of course, more and more noticeable when the intensity of the crack increases. In this case that the depth of the crack is equal to 75% of the beam's height, the difference with the Undamaged case is easily noticed. Another difference, for the 3^{rd} and the 5^{th} mode shapes, is the location of the maximum deflection. For the Undamaged case the maximum value of deflection is located at Beam (3) with the minimum value of Young's modulus, as for the Damaged case that value is observable at the location of the crack, indicating the critical location of the bridge. For the remaining mode shapes, namely the 2^{nd} and the 4^{th} , are the same for the Undamaged and the Damaged cases for the same reason explained before for the eigenfrequencies.

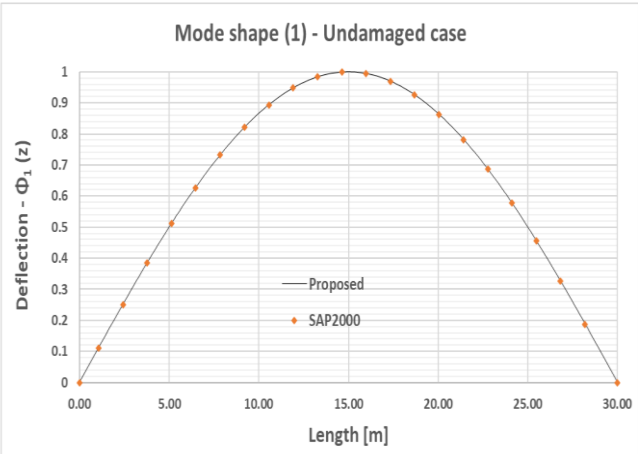

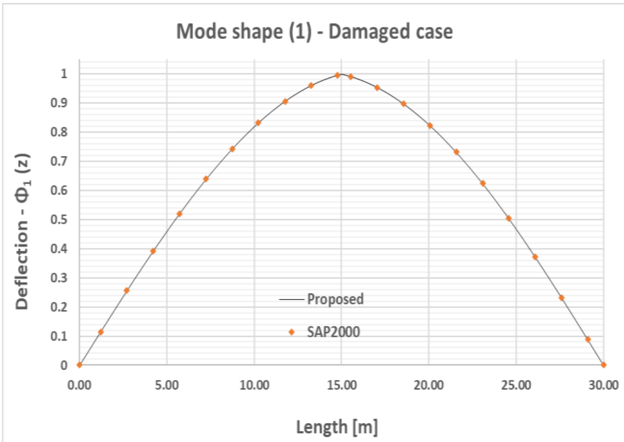

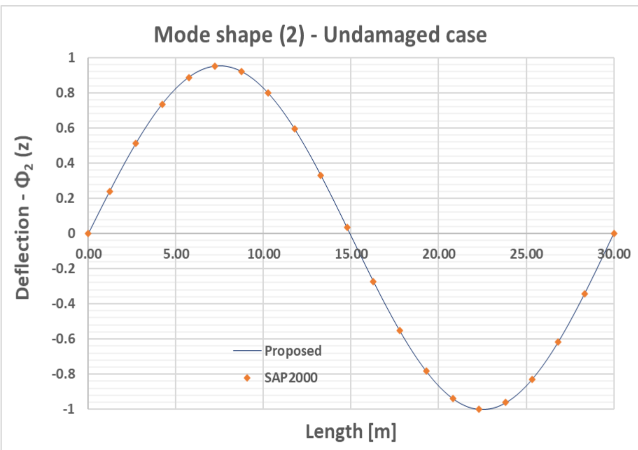

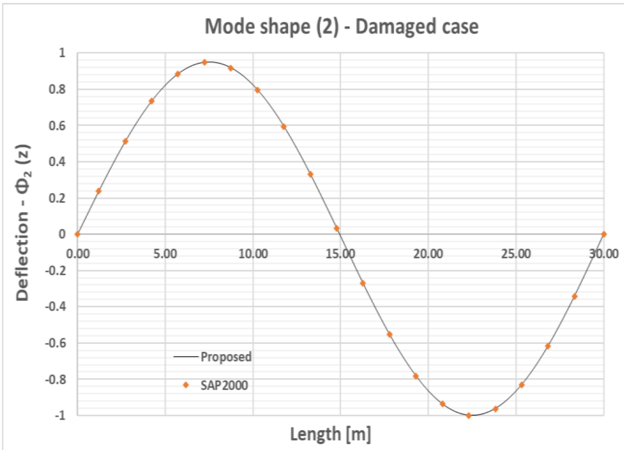

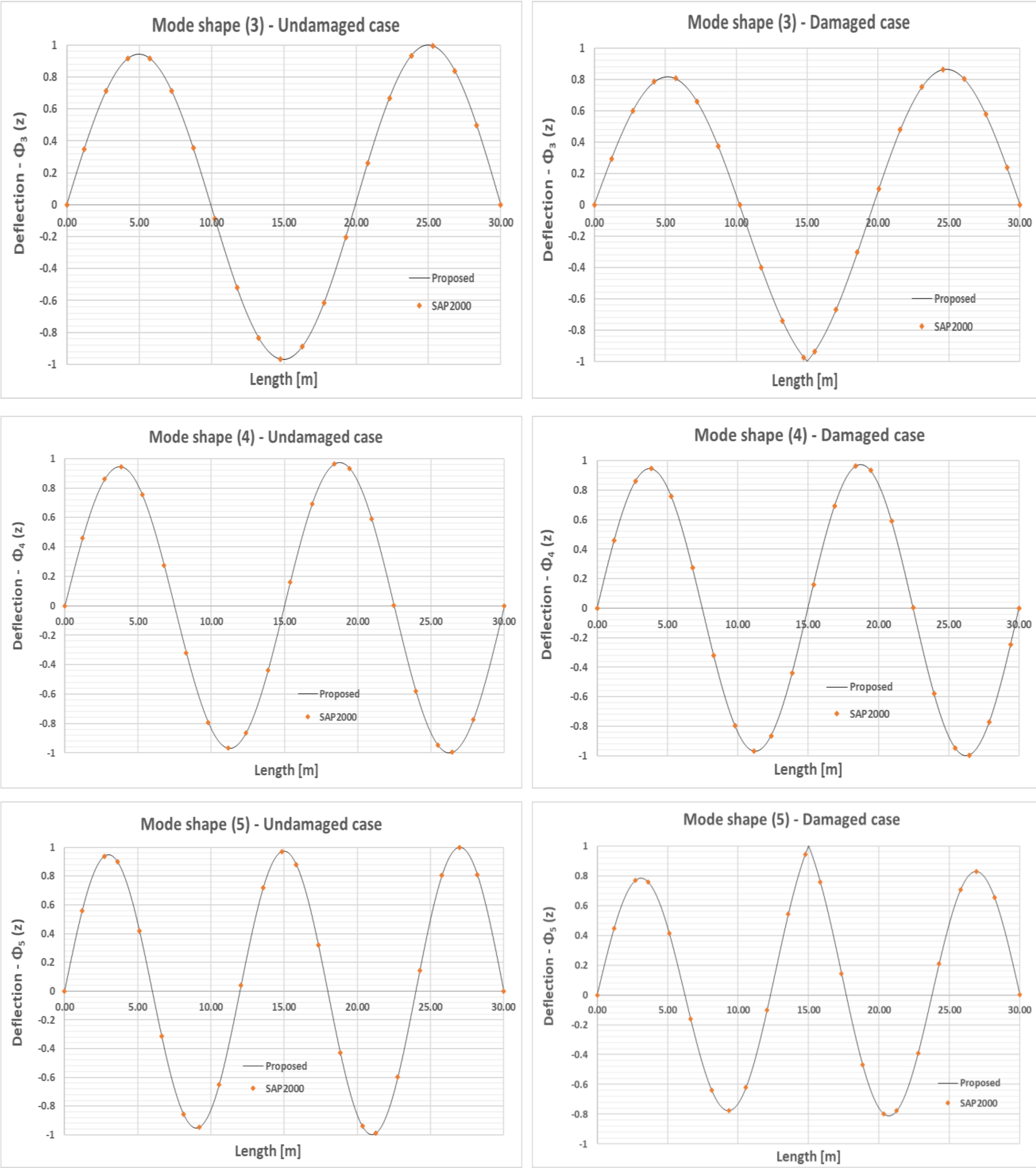

Figure 2. 3: Deflection of the first 5 mode shapes - Comparison: Proposed expressions - SAP2000

2.2 How to obtain a closed-form solution for the mode shapes for any number of cracks, multiple step changes in material, arbitrary boundary conditions and internal/external translational and rotational springs?

2.2.1 Main objective: A single expression of the solution which depends only on 4 integration constants associated with the boundary conditions and one additional condition for each external or internal spring at the discontinuities.

Steps:

1. Closed-form expressions of these 4 constants will be derived
2. The solution will be verified using the Finite Element Method

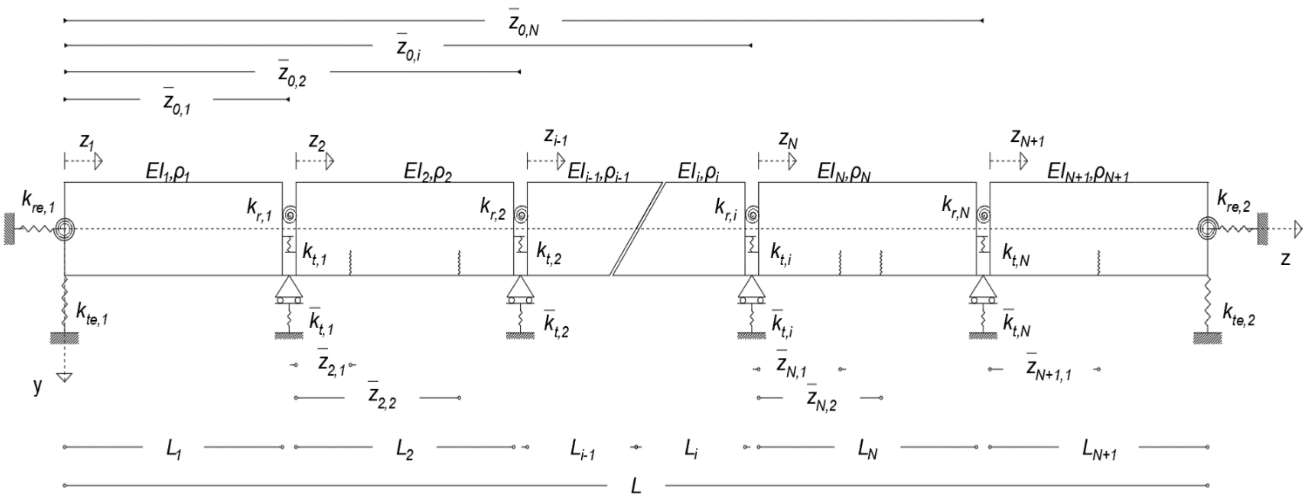

Figure 2. 4: Jointed EB beam with multiple step changes in material, arbitrary boundary conditions, along-axis springs and internal rotational and translational springs at the discontinuities

Natural frequencies and mode shapes of Euler-Bernoulli beams with multiple cracks and flexible boundary and interface conditions:

Consider now a jointed damaged Euler-Bernoulli beam with step changes in flexural stiffness with arbitrary boundary conditions, rotational and/or translational internal springs and/or external translational springs at the interface points. The procedure need now to be particularized to include the presence of internal translational, internal rotational and along-axis external translational springs which cause unknown variations of $\tilde{\Phi}_{i,r}(z_{0,i}), \tilde{\Psi}_{i,r}(z_{0,i}), \tilde{T}_{i,r}(z_{0,i})$ at the interface points. These unknown variations can be expressed as $\Delta\Phi_{i,r}$, $\Delta\Psi_{i,r}$ and $\Delta T_{i,r}$ meaning that the coefficients $C_{1,r}^{(1)}, C_{1,r}^{(2)}. C_{1,r}^{(3)}, C_{1,r}^{(4)}, \Delta\Phi_{i,r}, \Delta\Psi_{i,r}\ \Delta T_{i,r}$ are evaluated by imposing the 4 boundary conditions together with one continuity condition for each spring.

The internal rotational springs (stiffness $k_{r,i}$), internal translational springs (stiffness $k_{t,i}$), along-axis external translational springs (stiffness $\bar{k}_{t,i}$) at the discontinuity interfaces can be expressed as:

$$\tilde{M}_{i,r}(z_{0,i}) = k_{r,i}\Delta\Psi_{i,r} \qquad \text{Eq. 65}$$

$$\tilde{T}_{i,r}(z_{0,i}) = k_{t,i}\Delta\Phi_{i,r} \qquad \text{Eq. 66}$$

$$\widetilde{\Phi}_{i,r}(z_{0,i}) = -\frac{\Delta T_{i,r}}{\bar{k}_{t,i}} \quad \text{Eq. 67}$$

The continuity conditions at the interfaces, in this case, can be expressed in terms of the mode shape deflection, the slope, the bending moment and the shear force as:

$$\widetilde{\Phi}_{i,r}(z_{0,i}) + \Delta\Phi_{i,r} = \widetilde{\Phi}_{i+1,r}(0) \quad \text{Eq. 68}$$

$$\widetilde{\Psi}_{i,r}(z_{0,i}) + \Delta\Psi_{i,r} = \widetilde{\Psi}_{i+1,r}(0) \quad \text{Eq. 69}$$

$$\widetilde{M}_{i,r}(z_{0,i}) = \widetilde{M}_{i+1,r}(0) \quad \text{Eq. 70}$$

$$\widetilde{T}_{i,r}(z_{0,i}) + \Delta T_{i,r} = \widetilde{T}_{i+1,r}(0) \quad \text{Eq. 71}$$

Following the same procedure to derive the expressions of the constants, they can now be found as:

$$C_{i+1,r}^{(1)} = \frac{1}{2\tilde{\gamma}_{i,r}\delta_{i,r}^4}\left(C_{i,r}^{(1)}\Gamma_{i,r}^{(1)} + \frac{1}{\beta_{i,r}}C_{i,r}^{(2)}\Gamma_{i,r}^{(3)} + \frac{1}{\beta_{i,r}^2}C_{i,r}^{(3)}\Gamma_{i,r}^{(2)} + \frac{1}{\beta_{i,r}^3}C_{i,r}^{(4)}\Gamma_{i,r}^{(4)}\right) + \Pi_{i,r}^{(1)} \quad \text{Eq. 72}$$

$$C_{i+1,r}^{(2)} = \frac{1}{2\tilde{\gamma}_{i,r}\delta_{i,r}^4}\left(\beta_{i,r}C_{i,r}^{(1)}\Gamma_{i,r}^{(4)} + C_{i,r}^{(2)}\Gamma_{i,r}^{(1)} + \frac{1}{\beta_{i,r}}C_{i,r}^{(3)}\Gamma_{i,r}^{(3)} + \frac{1}{\beta_{i,r}^2}C_{i,r}^{(4)}\Gamma_{i,r}^{(2)}\right) + \Pi_{i,r}^{(2)} - \frac{\Delta T_{i,r}}{\beta_{i+1,r}^4 EI_{i+1}} \quad \text{Eq. 73}$$

$$C_{i+1,r}^{(3)} = \frac{1}{2}\left(\beta_{i,r}^2 C_{i,r}^{(1)}\Gamma_{i,r}^{(2)} + \beta_{i,r}C_{i,r}^{(2)}\Gamma_{i,r}^{(4)} + C_{i,r}^{(3)}\Gamma_{i,r}^{(1)} + \frac{1}{\beta_{i,r}}C_{i,r}^{(4)}\Gamma_{i,r}^{(3)}\right) + \Pi_{i,r}^{(3)} + \Delta\Phi_{i,r} \quad \text{Eq. 74}$$

$$C_{i+1,r}^{(4)} = \frac{1}{2}\left(\beta_{i,r}^3 C_{i,r}^{(1)}\Gamma_{i,r}^{(3)} + \beta_{i,r}^2 C_{i,r}^{(2)}\Gamma_{i,r}^{(2)} + \beta_{i,r}C_{i,r}^{(3)}\Gamma_{i,r}^{(4)} + C_{i,r}^{(4)}\Gamma_{i,r}^{(1)}\right) + \Pi_{i,r}^{(4)} + \Delta\Psi_{i,r} \quad \text{Eq. 75}$$

It looks like that all the expressions are similar with the aforementioned procedure and the constants $C_{1,r}^{(2)}.C_{1,r}^{(3)},C_{1,r}^{(4)}$ are characterized with an additional term related to the local variation. In a similar fashion, other types of discontinuities can be treated, introducing additional terms to the expressions of the constants.

Similarly with the previous procedure, the mode shape expression is used to evaluate the characteristic function and consequently each natural frequency and the corresponding mode shape. The system of equations, now, that need to solved is of $4+m$ equations, being 4 the number of boundary conditions and m equations for the m unknown variations at the interfaces.

Taking into account local reference system, numerical instabilities due to the presence of the hyperbolic functions in the evaluation of high order modes are reduced as it will be shown in the following numerical application.

2.2.2 Numerical application (2.2) – Step changes in material, external/internal translational and rotational springs:

The second numerical example consists of a beam-type bridge with three different concrete segments with a set of different parameters for each one of them. In this case, arbitrary boundary conditions will be examined (fixed left end and flexible right end), as well as the presence of more than one crack (2 cracks along the 1st Beam) and internal translational and rotational springs at the interface points.

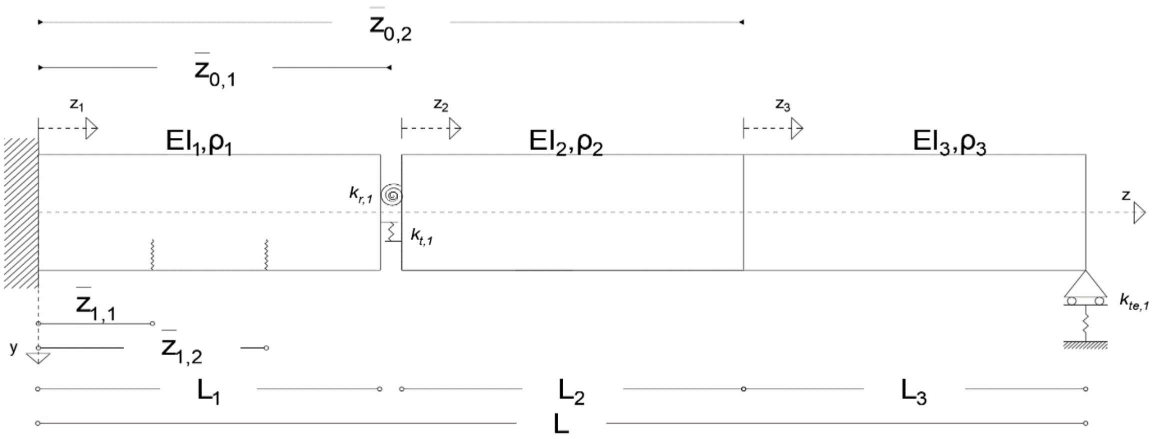

Figure 2. 5: Numerical application (2.2) - Model

Table 2. 4: Numerical application (2.1) - Properties of the model

Properties	Beam 1	Beam 2	Beam 3
Length [m]	7.5	7.5	7.5
Concrete Type	C25/30	C20/25	C20/25
Density [kg/m^3]	2548.54	2548.54	2548.54
Young's modulus [kN/m^2]	3.10x10^7	3.00x10^7	2.90x10^7

All the beams have a square cross-section of sides $h = 50\ cm$ and the cracks have a depth of $d_{1,1} = 0.30\ cm$ and $d_{1,2} = 0.30\ cm$ located at the 1st Beam at the location $\bar{z}_{1,1} = 2.5\ m$ and $\bar{z}_{1,2} = 5\ m$. This means that the equivalent stiffness coefficient for both crack is equal to $K_{1,1} = K_{\ 1,2} = 55357.14\ kN\ m$, and the corresponding damage parameter is equal to $a_{1,1} = a_{2,2} = 2.92$.

<u>Boundary conditions:</u>

$$\widetilde{\Phi}_r(0) = 0 \quad \text{Eq. 76}$$

$$\widetilde{\Psi}_r(0) = 0 \quad \text{Eq. 77}$$

$$\widetilde{M}_r(L) = 0 \quad \text{Eq. 78}$$

$$\widetilde{\Phi}_r(L) = -\frac{\widetilde{T}_r(L)}{k_{te,1}} \quad \text{Eq. 79}$$

<u>Interface conditions:</u>

$$\widetilde{T}_r\left(z_{0,i}\right) = k_{t,1}\Delta\Phi_{1,r} \quad \text{Eq. 80}$$

$$\widetilde{M}_r\left(z_{0,i}\right) = k_{r,1}\Delta\Psi_{1,r} \quad \text{Eq. 81}$$

where: $k_{te,1} = 100200\frac{kN}{m}$; $k_{t,1} = 150\frac{kN}{m}$; $k_{r,1} = 270\frac{kN}{m}$

It is expected that the 2 cracks located at $\bar{\bar{z}}_{1,1} = 2.5\ m$ and $\bar{\bar{z}}_{1,2} = 5m$ would change all the values of the eigenfrequencies this time as well as the shape of the mode shapes.

The results of the five first eigenfrequencies for both the Undamaged and Damaged case are:

Table 2. 5: Numerical application (2.2) - Eigenfrequencies from Proposed Expressions and SAP2000 – Undamaged case

Eigenfrequencies Undamaged case	Proposed expressions (rad/sec)	SAP2000 (rad/sec)	Error (%)
1	6.227	6.263	0.5748
2	32.328	32.457	0.3974
3	35.449	35.397	-0.1469
4	107.053	107.095	0.0392
5	197.028	196.677	-0.1785

Table 2. 6: Numerical application (2.2) - Eigenfrequencies from Proposed Expressions and SAP2000 – Damaged case

Eigenfrequencies Damaged case	Proposed expressions (rad/sec)	SAP2000 (rad/sec)	Error (%)
1	5.980	6.009	0.4826
2	27.615	27.711	0.3464
3	34.853	34.814	-0.112
4	107.051	106.810	-0.2256
5	153.249	153.252	0.0019

The results are compared to those yielded by SAP2000, together with the percentage error, defined as:

$$\varepsilon(\%) = \left(\frac{\omega_{SAP2000} - \omega_{proposed}}{\omega_{SAP2000}}\right) * 100 \qquad \textit{Eq. 82}$$

where $\omega_{SAP2000}$ is the frequency yielded by SAP2000, while $\omega_{proposed}$ is the one obtained with the proposed method.

The eigenfrequencies found from the proposed expressions, derived in this thesis project, are in a very good agreement with the ones calculated using a FEM model in SAP2000. Specifically, the error for almost all the eigenfrequencies is below 0.5%, and this is only because in SAP2000 the approximated values of the natural frequencies are calculated, even if a dense mesh is considered. This means that the analytical expressions proposed in this thesis can also predict the eigenfrequencies of more complicate beam-type bridges, meaning multiple cracks, flexible boundary conditions and along-axis external and/or internal translational and rotational springs at the discontinuities.

Next step will be to also verify the mode shapes, normalized so that the maximum deflection is equal to one(1). The results of the modal displacements for both the Undamaged and Damaged cases are presented:

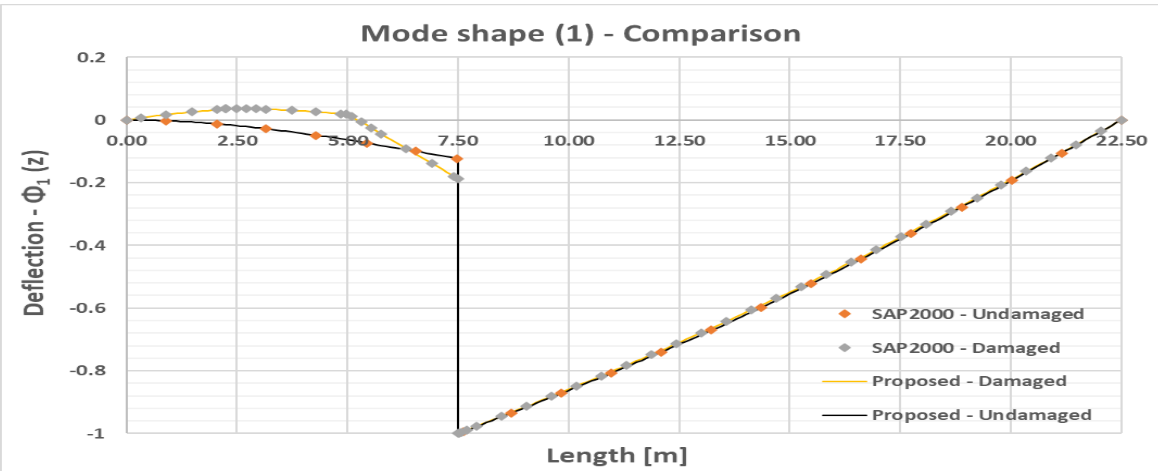

Figure 2. 6: Deflection 1st Mode shape - Comparison: Proposed expressions - SAP2000

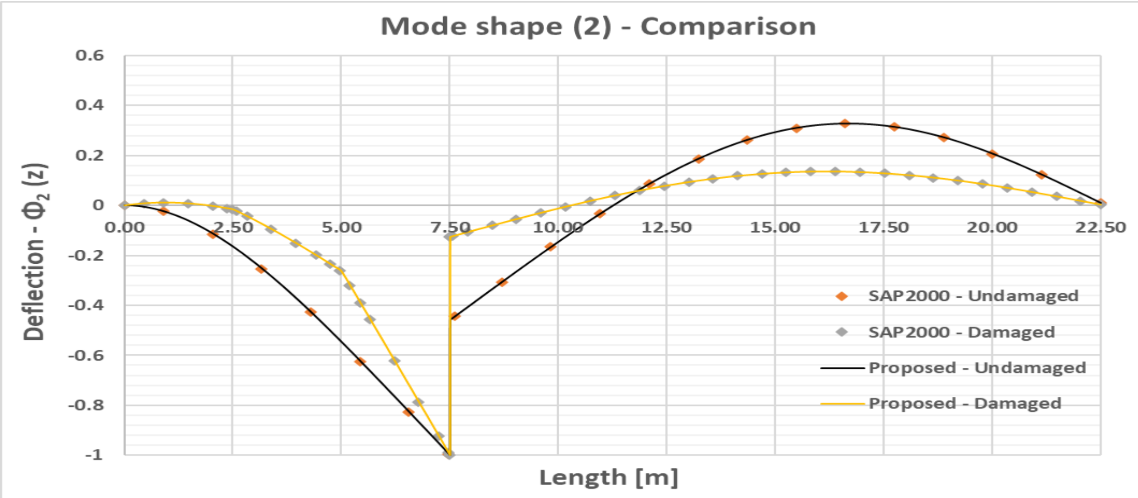

Figure 2. 9: Deflection 2nd Mode shape - Comparison: Proposed expressions - SAP2000

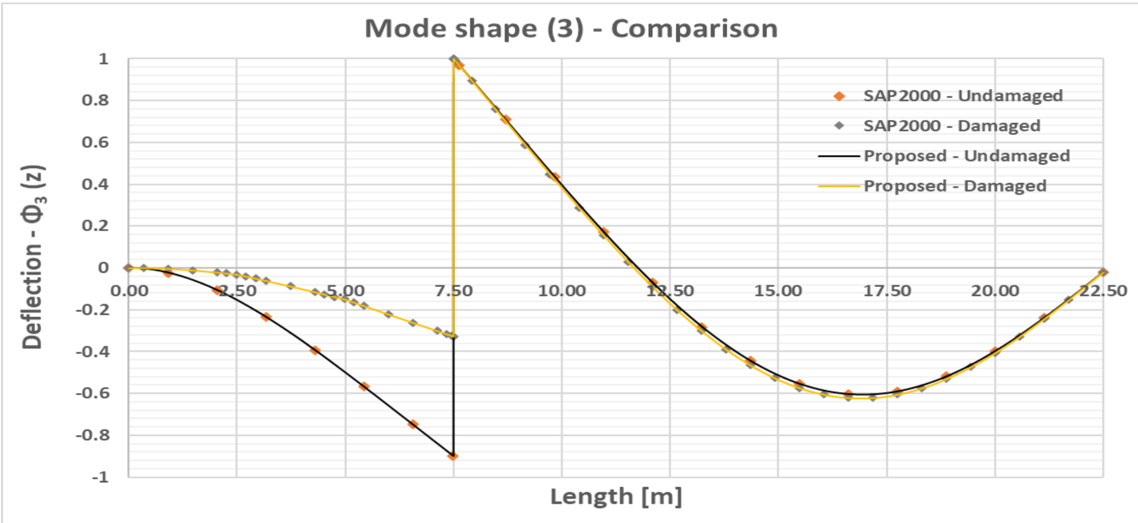

Figure 2. 8: Deflection 3rd Mode shape - Comparison: Proposed expressions - SAP2000

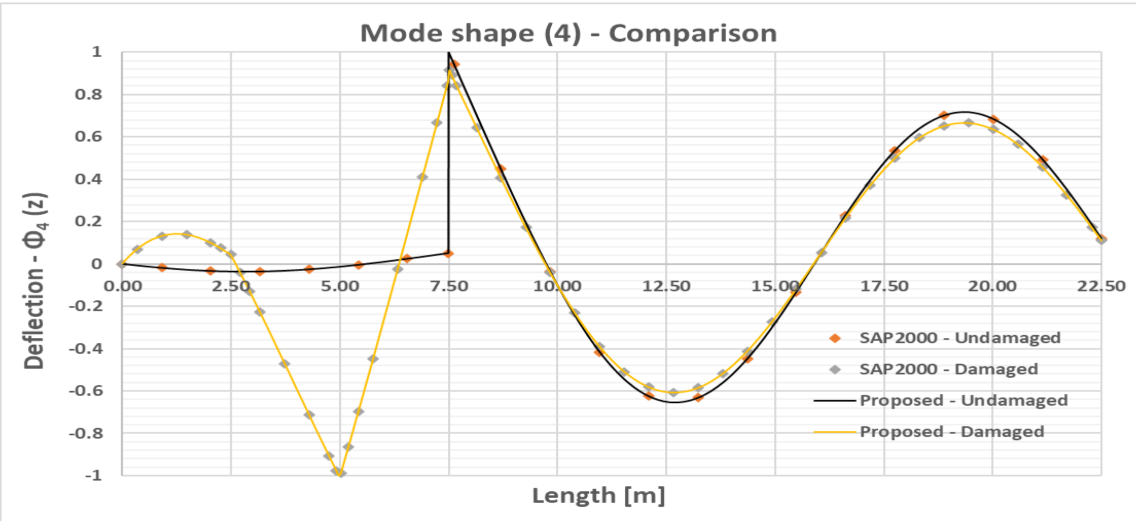

Figure 2. 7: Deflection 4th Mode shape - Comparison: Proposed Expressions - SAP2000

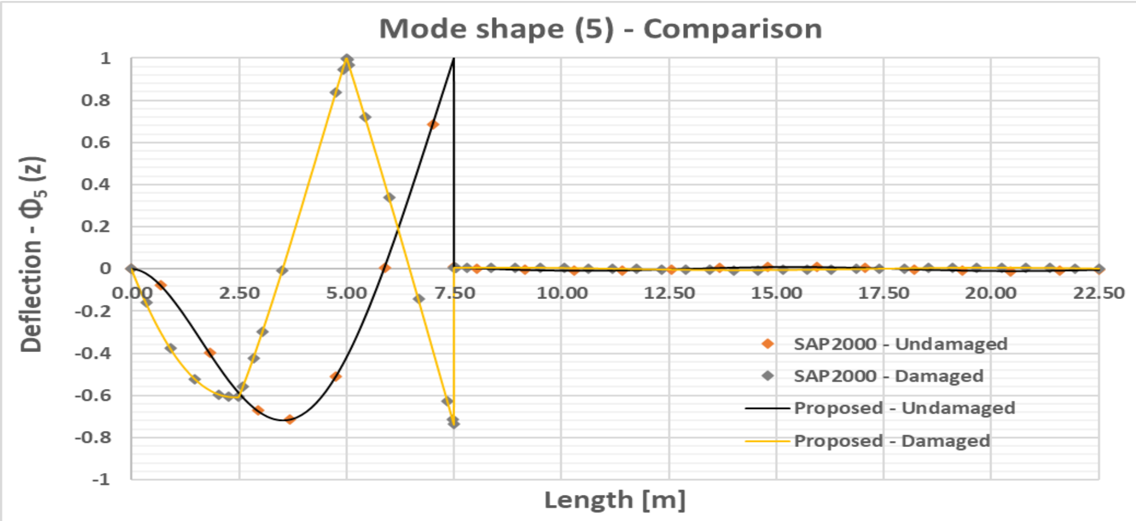

Figure 2. 10: Deflection 5th Mode shape - Comparison: Proposed Expressions - SAP2000

In this numerical application, again, the proposed expressions for the mode shapes can accurately predict the modal response as the results coincide with the ones found using a FEM model in SAP2000. A denser mesh was used, as mentioned before, close to the cracks and the discontinuities in order to be able to predict the results as accurate as possible. In contrast with the Numerical application (1), now all the mode shapes are affected due to the presence of the 2 cracks in the 1st Beam. Specifically, for each one of them, at the locations of the cracks $\bar{\bar{z}}_{1,1} = 2.5\ m$ and $\bar{\bar{z}}_{1,2} = 5m$, there is a change in curvature because of the local reduction of flexural rigidity. These changes depend mainly on the intensity of the cracks, and for a crack's depth of 60% the beam's height as the cracks in this example, they are easily recognizable, meaning that the Damaged mode shapes should always be considered really carefully.

All in all, considering the results of both numerical applications, deriving in this chapter the analytical expressions for the mode shapes, it was achieved to predict really fast and with accuracy, the dynamic characteristics of a beam-type bridges with:

- ✓ Any number of step changes in material properties.
- ✓ Any number of cracks per beam/segment.
- ✓ Any type of boundary and interface conditions (flexible boundary conditions, along-axis springs and internal rotational and translational springs at the discontinuities).

The next section is about using the same expressions in deterministic model updating methods and the so called Inverse Problem. Model updating can be achieved with analytical expressions in a more efficient way and that is the reason they are so commonly used in this field. An example of determining the location of a crack, knowing only its intensity, will follow by minimizing a cost function.

2.3 Inverse Problem- Model updating

2.3.1 How to use only the closed-form solutions for the mode shapes to detect a crack?

In this final part, an introduction of the concepts of model updating and the so called “inverse problem” is presented so that the importance of the findings of this project, as well as the other damage identification techniques is properly demonstrated. The main objective of the Finite Element model updating is to modify the parameters of a FE model such as its output corresponds better with experimental observations of the structural behavior. But modifying the model in any FE software is a task which needs computational time and effort from the user. Every time changes are applied to the model, might be the properties of the beam or the crack(s) or the moving load(s), redesigning is needed as well as remeshing with proper attention. On the other hand, using analytical expressions that have been proven to accurately produce the results coming from any FE model, could be used to adjust the parameters as many times as needed quite faster. This is also the reason parametric design and the use of programming have been really efficient and useful tools for Structural Health Monitoring as well as many other engineering applications.

Inverse problems like model updating and structural health monitoring may be considered as optimization problems, although a characteristic feature of the inverse problems is that they may be ill-posed. In reality, the errors that might be present and give rise to inaccuracies in the model predictions should be considered in order to achieve accurate results. That is the reason the use of probabilistic model updating techniques are really common in the field of SHM to take into account the possible uncertainties coming modelling errors, measurement noise, environmental causes and many more. The reader is advised to search in the literature probabilistic approaches using probability density functions (PDF) to the uncertain parameters to end up in the “posterior” PDF which contains both the uncertainty of the prior information as well as the uncertainty in the experimental data.

Moreover, there are also deterministic model updating methods, where the objective is to determine a set of model parameters, associated with a certain physical model, using information contained in some experimental data. The optimal set of model parameters minimized the misfit between experimental data and model predictions, which is measured by a cost function [26].

In this project, a vibration-based model updating will be followed in order to show the importance of the so called “prior” knowledge coming from the use of analytical expressions to damage localization. Usually, one can produce this “prior” knowledge with analytical expressions by modifying the parameters as many times as possible in order to adjust the real measurements with one set of these parameters used. In this case, the same will happen making use of the expressions for the eigenfrequencies, derived in the beginning of this thesis, for a complicate beam-type damaged beam. The cost function is now modified as:

$$G(a,s)=\sum_i\left(\frac{\Delta\omega_i(a,s)}{\omega_i^U}-\frac{\Delta\omega_{ei}}{\omega_{ei}^U}\right)^2 \qquad \textit{Eq. 83}$$

The solution as mentioned before will come by minimizing the cost function as:

$$\tilde{G}(s)=min\,G(a,s) \qquad \textit{Eq. 84}$$

where, a is the damage parameter described in equation [7] and s is the location of the crack.

In the first part of the summation in the expression of the cost function, $\frac{\Delta\omega_i(a,s)}{\omega_i^U}$, concerns the values coming from the analytical expressions derived in this project, where the nominator is equal to the difference of the eigenfrequency coming from the damaged beam and the one from the undamaged beam and the denominator is equal to the natural frequency of the undamaged beam. The second part of the summation, $\frac{\Delta\omega_{ei}}{\omega_{ei}^{U}}$, describe exactly the same quantities but concerns the values from the experiments of a real scenario.

2.3.2 Deterministic Model Updating – Problem statement

Numerical application (2.3) – Step changes in material – Sensitivity Analysis:

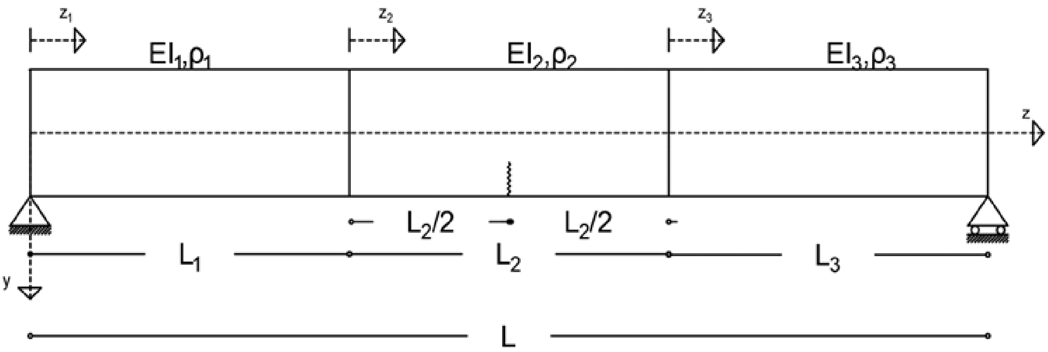

Figure 2. 11: Numerical application (2.3) – Model definition

The properties of the model of this numerical application are the same with the ones of the numerical application (1.1).

The aim of this example is to predict the location of the crack, assumed to be somewhere in the second beam segment (Beam 2), knowing only its intensity a priori. To accomplish that, the cost function as described before should be minimized in order to predict the location. As far as the second part of the summation in the cost function is concerned, because there are no experimental data/measurements available, the results coming from SAP2000 and the Finite Element Method will be used as pseudo-experimental data/measurements to test the reliability of this optimization procedure. These are:

Table 2.7: Numerical application (2.3) – Pseudo-experimental measurements

FEM results	Damaged	Undamaged
ω1=	2.9755	3.29
ω2=	13.1635	13.1661
ω3=	27.177	29.6157
ω4=	52.6201	52.6002
ω5=	76.2489	82.2205

Now, concerning the values coming from the analytical expressions, a sensitivity analysis will be performed, where the natural frequencies will be found for 3 different damage parameters α and 9 different locations along Beam 2. This means that for each mode shape and eigenfrequency 27 values will be collected, something that analytical expressions makes it possible in an easy and really fast manner, in contrast with FE model updating where 27 different analyses should take place, correcting it every time.

In figure [2.12] the first 5 modal shapes of Beam 2 as part of the whole beam-type bridge are presented, normalized so that the maximum modal amplitude is equal to 1, in order to give a first impression of which of them will change, more or less, by placing the crack at a random location.

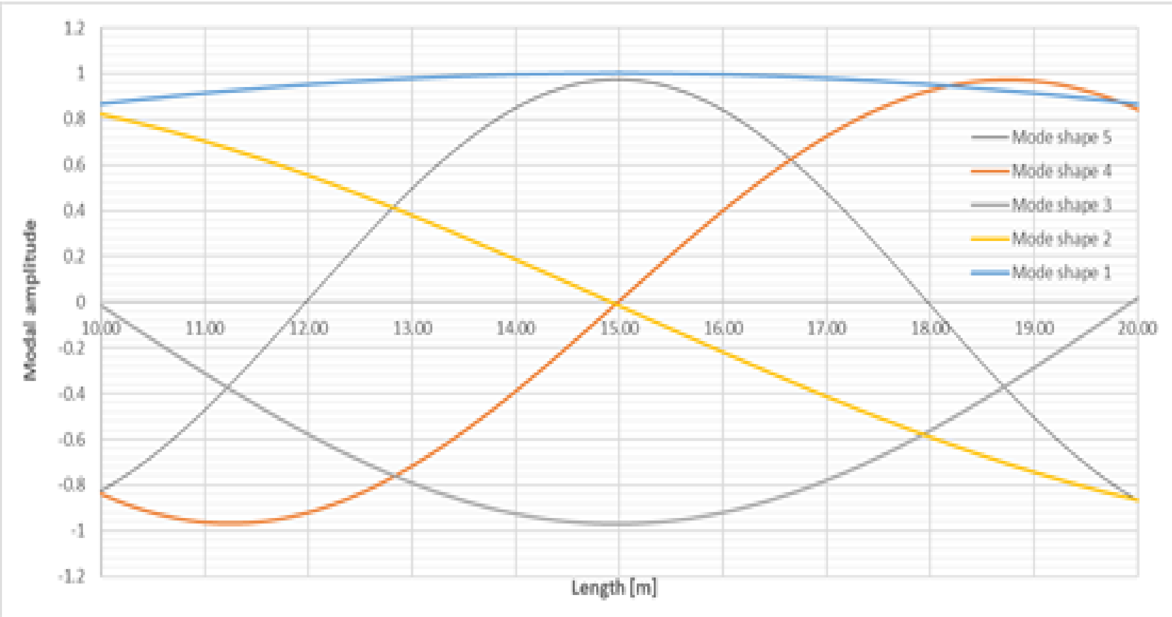

Figure 2. 12: Modal amplitude of the 2nd Beam for the first 5 mode shapes

Now in figure [2.13] the results of the sensitivity analysis are presented, showing in the vertical axis the percentage of the difference of the damaged and the undamaged case, over the value of the undamaged state for each set of damage parameter and crack location, $\frac{\Delta\omega_i(a,s)}{\omega_i^U}$, and in the horizontal axis the normalized crack location z/L, where L is the total length of the bridge.

Three damage parameters a are considered for a different depth of the crack, as:

- $d_{2,1} = 0.14\ cm$ -> $K_{2,1} = 11868$ kN m -> $\alpha_{2,1}$=1.36
- $d_{2,1} = 0.15\ cm$ -> $K_{2,1} = 8000$ kN m -> $\alpha_{2,1}$=3.33
- $d_{2,1} = 0.16\ cm$ -> $K_{2,1} = 5000$ kN m -> $\alpha_{2,1}$=5.93

Nine different points were considered for the location of the crack at Beam 2:

$$z_2 = 1 - 9\ m$$

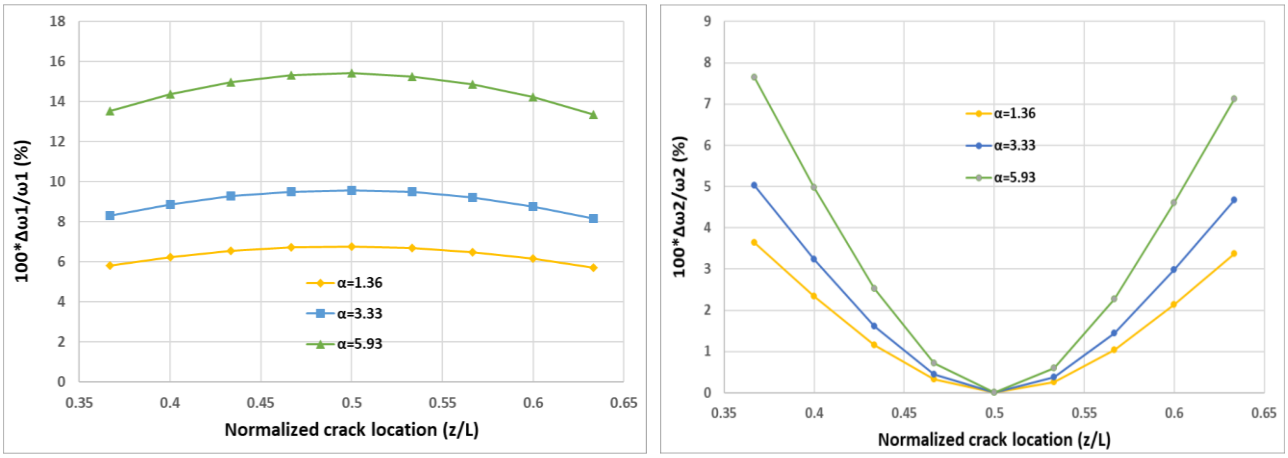

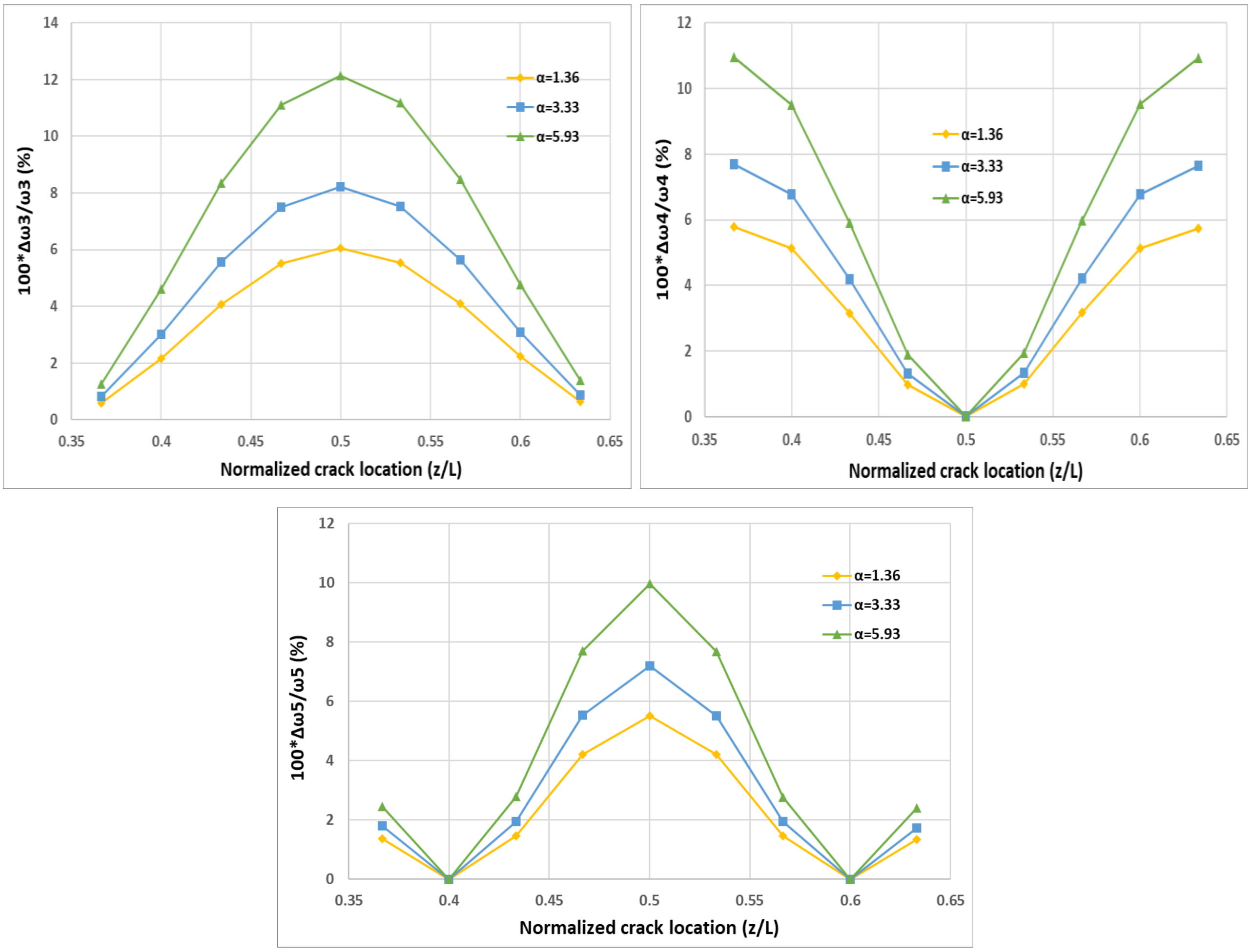

Figure 2. 12: Sensitivity Analysis - The percentage of the difference of the damaged and undamaged eigenfrequency for the first 5 mode shapes versus the normalized crack location of the 2nd Beam

As expected, when the damage parameter increases or equally the depth of the crack increases, then the modal amplitudes also increase. Moreover, it is observed once again that when the crack is located at the midpoint, the changes of the 2nd and the 4th natural frequency are equal to zero for every damage case. The same applies for the 5th mode shape where there are nodal points at the normalized location 0.4 and 0.6 of the total length of the beam so they also remain unaffected when the crack is located at these points.

The next figures will indicate the solution of minimizing the cost function for each location using a different number of mode shapes every time (where i : the number of eigenfrequency considered). Specifically, figure [2.14] where the values of all the 5 first mode shapes were considered in the summation in the formula of the cost function, the value when of $G(a, s)$ is qual to zero at the midpoint. This is exactly the point where the crack is located when the model of SAP2000 was considered and its results were used as pseudo-experimental data. This means that the localization of the damages was accomplished successfully by only knowing “a priori” its intensity.

Figure [2.14] shows that the same conclusion can be derived from only using the 1st , the 3rd and the 5th mode shapes as they are the only ones affected by a crack at the midpoint in contrast of using different combinations of mode shapes, that make localization less feasible.

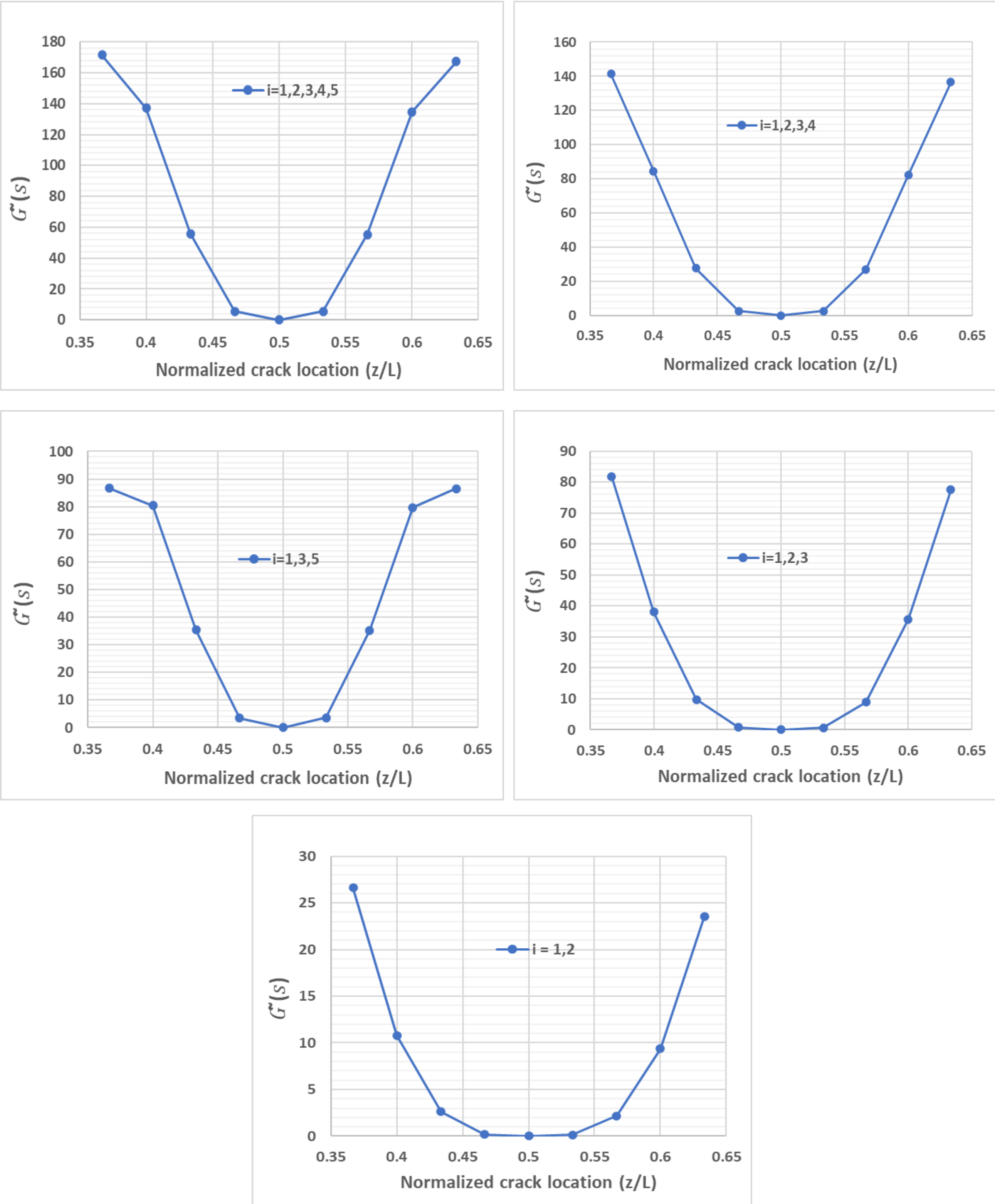

Figure 2. 13: Cost function versus the normalized crack location for the 2nd Beam using a different number of eigenfrequencies (i)

To conclude, the crack's location using a deterministic model updating approach was accurately predicted knowing beforehand its intensity, thanks to the use of the analytical expressions of the eigenfrequencies that made the procedure of modifying the parameters easier and faster. Another remark was that by increasing the number of mode shapes considered, the possibility for accuracy is also increased as mode shapes contain nodal points that makes the identification of the crack more difficult. Finally, for the case that both location and intensity are unknown, or the uncertainties should be included in the analysis, then probabilistic model updating approaches should be considered to judge about the characteristics of the damage (localization, quantification).

Chapter 3

3. Dynamic response of beam-type damaged bridges with time-invariant parameters under moving loads - Cracks identification (location, intensity)

In this chapter, crack identification techniques will be presented in order to be able to draw conclusions about the optimization of the process and understand the differences from different quantities taken from indirect and direct monitoring. Moreover, to compare different ways of modelling damages by testing the same models but with different properties for the crack(s). Finally, to propose damage identification techniques that would not be affected when the complexity of the model increases, meaning the step changes in material that was discussed extensively in the previous chapter.

Overall, the research sub-questions that will be discussed in this chapter are:

- Which is the optimal measured quantity to detect a crack?
- What would be the minimum depth of a crack to be identifiable?
- Would the model of the crack affect the identification?
- Would the number of cracks affect the identification?
- Would the complexity of the beam-type bridge (varying rigidity) affect the identification?

It is important to note that the realization of this chapter was only possible by deriving the new analytical expressions for the mode shapes in the previous chapter. One reason for that is by using these expressions in MAPLE and MATLAB, parameter investigation can be accomplished and many different damage scenarios could be tested in order to produce, as accurate as possible, results and conclusions. Another reason is that for examining the coupled problem of the moving vehicle and the bridge, it requires the calculation of the dynamic characteristics of the bridge and this is also demonstrated in the governing equations derived in this chapter and include the formula of the modal deflection. Finally, by using these expressions it was also possible to compare different ways of modelling the crack as they were derived in order to be able to consider any number of different beam segments and could be used as such to model the crack as a separate segment (influenced zone because of the presence of the crack) with different properties (reduced rigidity) than the rest of the bridge.

3.1 Governing equations

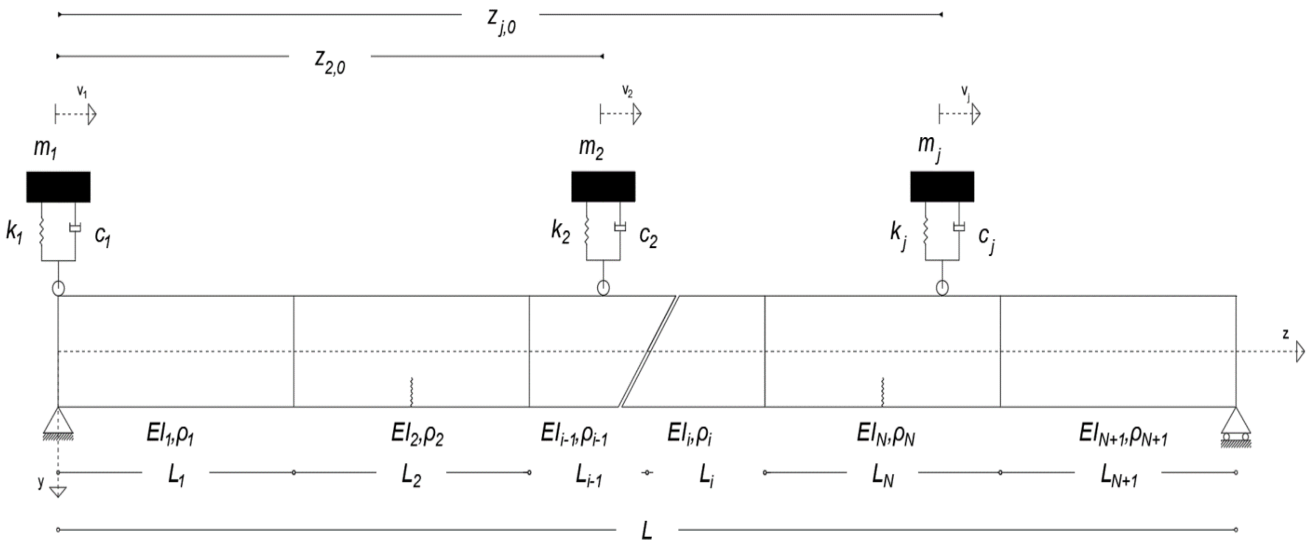

Figure 3. 1: Euler-Bernoulli beam with step changes in material and multiple cracks, subjected to moving vehicle loads modelled as spring-mass systems

In the following part, as the way to deal with multiple step changes in material and stiffness has already be discussed and in order to simplify the notation, a homogeneous Euler-Bernoulli beam is considered, with length L, mass density ρ, cross-section with area A, modulus of elasticity E, second moment of inertia I and equivalent viscous damping coefficient μ. The governing equations for the dynamic response of beam-type damaged bridges with time-invariant parameters under moving loads will be derived, in order to be able to answer the research questions for crack identification (see also [27]).

The equation of motion is given as:

$$EI\frac{\partial^4 u(z,t)}{\partial z^4} + \rho A\frac{\partial^2 u(z,t)}{\partial t^2} + \mu\frac{\partial u(z,t)}{\partial t} = \sum_{j=1}^{n} F_j(z,t) \qquad \textit{Eq. 85}$$

At the right hand side of the equation the vehicle is represented by a moving oscillator with mass m_j, viscous damping c_j and elastic stiffness k_j. The summation term indicates that more than one oscillators might be present along the bridge, and they are supposed to be in permanent contact with the road surface.

Moreover, the loading is equal to:

$$F_j(z_i,t) = U\left[L - \left(z_{j,0} + v_j t\right)\right] f_j(t)\delta(z - v_j t) \qquad \textit{Eq. 86}$$

where t and z denote the time and the spatial coordinate measured along the axis of the beam, respectively; v_j is the moving speed of the oscillator; $z_{j,0}$ is the initial position of the moving oscillator at $t = 0$; $U\left[1 - \left(z_{j,0} + v_j t\right)\right]$ being the unit step function so that $U\left[L - \left(z_{j,0} + v_j t\right)\right] = 0$ when the oscillator reach the end of the bridge, meaning $\left(z_{j,0} + v_j t\right) > L$, and $U\left[L - \left(z_{j,0} + v_j t\right)\right] = 1$ while the oscillator moves along the bridge; f_j is the reaction force transmitted by the jth oscillator and is located at the instantaneous position $z_j(t) = \left(z_{j,0} + v_j t\right)$ and its expression will be given below.

The solution of the governing equation could be obtained once again considering the classical modal analysis, as:

$$u(z,t) = \sum_{r=1}^{\infty} \Phi_r(z) q_r(t) \qquad \textit{Eq. 87}$$

where $\Phi_r(z)$ is the rth undamped mode shape of the damaged beam with the always-open cracks and $q_r(t)$ is the rth generalized coordinate.

and an approximation of the solution considering a modal truncation:

$$u(z,t) \cong \sum_{r=1}^{N} \Phi_r(z) q_r(t) \qquad \textit{Eq. 88}$$

Important to mention is that in order to calculate the dynamic response, for the mode shapes in the aforementioned formulas, the analytical expressions derived in this thesis project will be used for both the Undamaged and Damaged cases of the bridge.

Now, similarly with the moving mass, substituting in the equation of motion, pre-multiplying both sides of the governing equation by $\Phi_r(z)$ and integrating with respect to z between 0 and L, the following expression with the time-dependent generalized coordinates is obtained:

$$\ddot{q}_r(t) + 2\zeta_r \omega_r \dot{q}_r(t) + \omega_r^2 q_r(t) = \sum_{j=1}^{n} U\big[L - \big(z_{j,0} + v_j t\big)\big] f_j(t) \Phi_r(v_j t) \qquad \textit{Eq. 89}$$

where the mode expression after using the Dirac delta properties is equal to: $\Phi_r(v_j t)$; ζ_r is the modal damping ratio and it will be assumed constant in all vibration modes.

The mode shape expression included in the equation above is orthonormal with respect with the mass per unit length ρA. This is just one of the most common procedure of scaling the modes, as well as scaling the modes such that the maximum value of the amplitude is unitary. This means that there is a free choice on the way of normalizing the eigenmodes as the final solution to the force problem is independent of the chosen method of normalization.

The equation of motion of the jth moving oscillator, in terms of absolute displacement is given as:

$$m_j \ddot{u}_{v,j}(t) = -c_j\big[\dot{u}_{v,j}(t) - \dot{u}_{w,j}(t)\big] - k_j\big[u_{v,j}(t) - u_{w,j}(t)\big] \qquad \textit{Eq. 90}$$

where $u_{v,j}(t)$ and $u_{w,j}(t)$ are the absolute displacements of the lumped mass m_j and of the ideal point wheel, respectively.

The interaction force of the jth moving oscillator $f_j(t)$, will depend on both the spring-dashpot system and the weight of the oscillator and it can be expressed as:

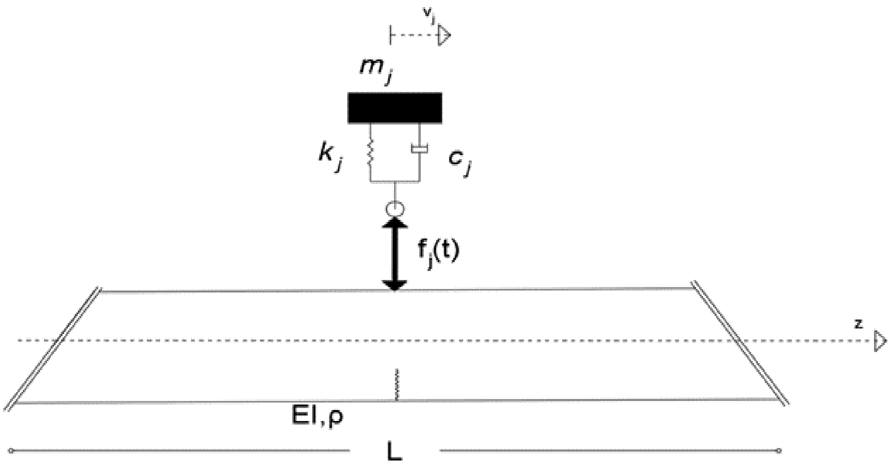

Figure 3. 2: Definition of the Reaction force

$$f_j(t) = m_j g + k_j\left[u_{v,j}(t) - u_{w,j}(t)\right] + c_j\left[\dot{u}_{v,j}(t) - \dot{u}_{w,j}(t)\right] \Rightarrow \qquad \text{Eq. 91}$$

$$f_j(t) = m_j\left[g - \ddot{u}_{v,j}(t)\right] \qquad \text{Eq. 92}$$

where g is the intensity of the surrounding gravitational field.

Assuming that there is no loss of contact between the moving oscillators and the surface of the bridge, the compatibility condition should hold at every instantaneous position $z_j(t)$ of every oscillator, according to the relationship:

$$u_{w,j}(t) = \left[U\left[L - \left(z_{j,0} + v_j t\right)\right]u(z,t)\right]\Big|_{z=z_j(t)} = U\left[L - \left(z_{j,0} + v_j t\right)\right]u\left(z_j(t), t\right)\right] \qquad \text{Eq. 93}$$

Moreover, the time derivative of the absolute displacement of the displacement of the wheel of the jth moving oscillator $u_{w,j}(t)$, is calculated as:

$$\dot{u}_{w,j}(t) = \left[\frac{d}{dt}\left(U\left[L - \left(z_{j,0} + v_j t\right)\right]u(z,t)\right)\right]\Big|_{z=z_j(t)} \Rightarrow \qquad \text{Eq. 94}$$

$$\dot{u}_{w,j}(t) = \left.\frac{\partial\left(U\left[L - \left(z_{j,0} + v_j t\right)\right]u(z,t)\right)}{\partial t}\right|_{z=z_j(t)} + \qquad \text{Eq. 95}$$

$$+\dot{z}_j(t)\left.\frac{\partial\left(U\left[L - \left(z_{j,0} + v_j t\right)\right]u(z,t)\right)}{\partial z}\right|_{z=z_j(t)} \Rightarrow$$

$$\dot{u}_{w,j}(t) = U\left[L - \left(z_{j,0} + v_j t\right)\right]\left[\left.\frac{\partial(u(z,t))}{\partial t}\right|_{z=z_j(t)} + \dot{z}_j(t)\left.\frac{\partial(u(z,t))}{\partial z}\right|_{z=z_j(t)}\right] \qquad \text{Eq. 96}$$

Now, modifying the expressions above in terms of the generalized coordinates in accordance with the mode superposition method, we obtain:

$$u_{w,j}(t) = \left[U\left[L - \left(z_{j,0} + v_j t\right)\right]\sum_{r=1}^{N} \Phi_r(z_j(t))q_r(t)\right]\Bigg|_{z=z_j(t)} \qquad \text{Eq. 97}$$

$$\dot{u}_{w,j}(t) = U[L - (z_{j,0} + v_j t)] \left[\sum_{r=1}^{N} \Phi_r(z_j(t)) \dot{q}_r(t) + \dot{z}_j(t) \sum_{r=1}^{N} \Phi_r{}'(z_j(t)) q_r(t) \right] \quad \text{Eq. 98}$$

where the prime means the total derivative with respect to z, as:

$$\Phi_r{}'(z_j(t)) = \left. \frac{\partial \Phi_r(z(t))}{\partial z} \right|_{z=z_j(t)} \quad \text{Eq. 99}$$

After the last calculations, the expression governing the motion of the oscillators, for every single mode r, can be rewritten as:

$$m_j \ddot{u}_{v,j}(t) + c_j \dot{u}_{v,j}(t) + k_j u_{v,j}(t) = [c_j b_{j,r}(t) + k_j a_{j,r}(t)] q_r(t) + c_j a_{j,r}(t) \dot{q}_r(t) \quad \text{Eq. 100}$$

where $b_j(t)$ and $a_j(t)$ are defined in order to simply the expression, as:

$$a_{j,r}(t) = U[L - (z_{j,0} + v_j t)] \Phi_r(z_j(t)) \quad \text{Eq. 101}$$

$$b_{j,r}(t) = U[L - (z_{j,0} + v_j t)] \dot{z}_j(t) \Phi_r{}'(z_j(t)) \quad \text{Eq. 102}$$

where $\dot{z}_j(t)$ is the velocity of the jth moving oscillator when in contact with the bridge at every time step t, equal with v_j when the oscillator's speed is constant.

In the same manner, upon substitution of the expression of the motion at the ideal wheel point we can rewrite the expression of the interaction force, in terms of beam's modal coordinates, as:

$$f_j(t) = m_j g + k_j [u_{v,j}(t) - a_{j,r}(t) q_r(t)] + c_j [\dot{u}_{v,j}(t) - a_{j,r}(t) \dot{q}_r(t) - b_{j,r}(t) q_r(t)] \quad \text{Eq. 103}$$

Finally, upon substitution of the expression of the interaction force in the equation of motion of the beam, we can also rewrite it in the modal space, as:

$$\widehat{\boldsymbol{M}}(t) \ddot{\boldsymbol{q}}(t) + \widehat{\boldsymbol{D}}(t) \dot{\boldsymbol{q}}(t) + \widehat{\boldsymbol{K}}(t) \boldsymbol{q}(t) = \widehat{\boldsymbol{F}}(t) \quad \text{Eq. 104}$$

where $q(t)$ is a N-dimensional array collecting the $q_r(t)$, while the modal damping $\widehat{\boldsymbol{D}}(t)$ and stiffness $\widehat{\boldsymbol{K}}(t)$ matrices are given by a constant term, arising from the beam plus a time-varying term due to the passage of the moving oscillators, as:

$$\widehat{\boldsymbol{D}}(t) = \overline{\boldsymbol{D}} + \Delta \boldsymbol{D}(t) \quad \text{Eq. 105}$$

$$\widehat{\boldsymbol{K}}(t) = \overline{\boldsymbol{K}} + \Delta \boldsymbol{K}(t) \quad \text{Eq. 106}$$

In this case, the modal mass is equal to:

$$\left| \widehat{\boldsymbol{M}}(t) \right|_{rs} = \delta_{rs} \quad \text{Eq. 107}$$

It can be easily shown that each entry of $\widehat{\boldsymbol{D}}(t)$ and $\widehat{\boldsymbol{K}}(t)$ matrices is given by:

$$\left|\widehat{\boldsymbol{D}}(t)\right|_{rs} = 2\zeta_r \omega_r \delta_{rs} + \sum_{j=1}^{n} \left[\Phi_r(vt)\ c_j\ U\left[L - \left(z_{j,0} + v_j t\right)\right] \Phi_r(vt)\right]$$ *Eq. 108*

$$\left|\widehat{\boldsymbol{K}}(t)\right|_{rs} = \omega_r^2 \delta_{rs} + \\ + \sum_{j=1}^{n} \Phi_r(vt)\ \left[k_j\ U\left[L - \left(z_{j,0} + v_j t\right)\right] \Phi_r(vt) +\ c_j\ U\left[L - \left(z_{j,0} + v_j t\right)\right] \dot{z}_j(t) \Phi_r{}'(v_j t)\right]$$ *Eq. 109*

Lastly, the right hand side of the equation of motion is equal to:

$$\widehat{\boldsymbol{F}}(t) = U\left[L - \left(z_{j,0} + v_j t\right)\right] \Phi_r(vt)\left[m_j\ g\ + c_j \dot{u}_{v,j}(t) + k_j u_{v,j}(t)\right]$$ *Eq. 110*

Notice, of course, that the motion of the bridge and the vehicles (moving oscillators) are coupled. The solution of their expressions can be found with the help of any suitable step-by-step algorithm, in our case with the unconditionally stable Newmark's β-method integration scheme which is described with the equations below:

$$\boldsymbol{M}\ddot{u} + \boldsymbol{C}\dot{u} + \boldsymbol{K}u = F_{external}$$ *Eq. 111*

Using the extended mean value theorem:

$$\dot{u}_{n+1} = \dot{u}_n + \Delta t\ \ddot{u}_\gamma$$ *Eq. 112*

$$\ddot{u}_\gamma = (1-\gamma)\ddot{u}_n + \gamma \ddot{u}_{n+1}, \qquad 0 \le \gamma \le 1$$ *Eq. 113*

$$u_{n+1} = u_n + \Delta t\ \dot{u} + 0.5\ \Delta t^2\ \ddot{u}_\beta$$ *Eq. 114*

$$\ddot{u}_\beta = (1-2\beta)\ddot{u}_n + 2\beta \ddot{u}_{n+1}, \qquad 0 \le 2\beta \le 1$$ *Eq. 115*

For the unconditionally stable Newmark integration scheme, $\gamma = 0.5$ and $\beta = 0.25$

3.2 Which is the optimal measured quantity to detect a crack? What would be the minimum depth of a crack to be identifiable?

In order to answer which is the optimal measured quantity to detect a crack, a sensitivity analysis is needed investigating the results of:

- Oscillator's Response - $u_{v,j}(t), \ddot{u}_{v,j}(t)$
- Beam's Response - $u(z,t)$
- Reaction force - $f_j(t)$
- Eigenfrequencies - $\omega_{i,r}$

Meaning that the optimal measurement will be found by looking at the changes of the Undamaged and Damaged cases of the bridge, specifically at the moving oscillator's response (displacement, acceleration) , at the beam's response and its modal characteristics and at the reaction force acting from the ideal point wheel of the moving oscillator to the surface of the bridge.

Numerical application (3.1) – Investigation of different damage scenarios:

Without further delay the numerical application is presented, where its results will be discussed in detail in order to draw conclusions about crack(s) identification. It concerns a simply-supported damaged bridge with one crack at the middle, located at the bottom side of the cross-section. The values of the moving oscillator, of the bridge and of the crack are presented on the tables below.

As far as the crack is concerned, 6 different crack's depth were considered ranging from 2% to 20% of the beam's height, to be able to recognize the starting value, or equally the minimum intensity, where the crack will be identifiable. For each case the damage parameter (α) as well as the value of the stiffness of the rotational spring (representing the crack) are mentioned on the table below.

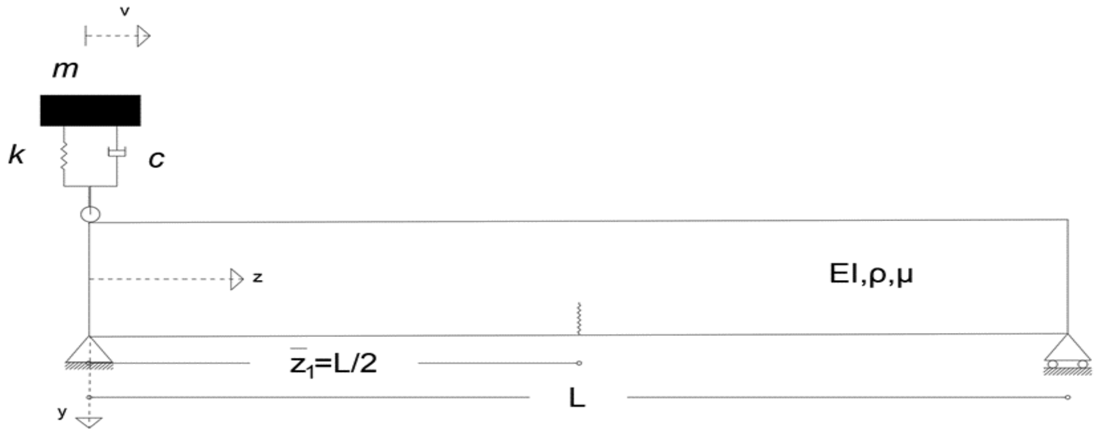

Figure 3. 3: Numerical application (3.1) - Model

.

Table 3. 1: Numerical application (3.1) - Properties of the beam

Properties	Length - L (m)	Density - ρ [kg/m^3]	Cross-sectional area – A (m^2)	Young's modulus - E (GPa)	damping ratio - ζ	Second moment of inertia – I (m^4)
Beam	100	13842.7	1.44	207	0.025	0.174

Table 3. 2: Numerical application (3.1) - Properties of the moving oscillator

Properties	Mass -m (kg)	Damping – c (Ns/m)	Stiffness -k (N/m)	Speed – v (m/s)
Oscillator	1000	25130	3.96x10^6	11.1

Table 3. 3: Numerical application (3.1) - Properties of the crack

Properties	Location - $\bar{z}$ (m)	Depth d (m) – All cases	Equivalent stiffness - K (kN/m) x10^{-6} – All cases	Damage parameter – α (m^{-1}) – All cases
Crack	50	0.024 / 0.06 / 0.096 / 0.132 / 0.18 / 0.24	655.18 / 250.08 / 148.88 / 102.95 / 70.36 / 48.05	0.055 / 0.144 / 0.242 / 0.350 / 0.512 / 0.749

As the conclusions of this project need to be as accurate as possible, a fairly large bridge was considered ($L = 100\ m$), then the mass of the moving oscillator ($m = 1000\ kg$) is less than the average mass of a car ($m \cong 1500\ kg$) and its velocity $v = 11.1 \frac{m}{s} \approx 40 \frac{km}{hr}$ is less than the average speed of a car and also the one that cause smaller displacements at the bridge.

This is also indicated in the next figure where at the vertical axis the maximum deflection of the bridge at the midpoint was calculated for 3 different values of the moving oscillator's speed, $v = 11.1 \frac{m}{s}$, $v = 22.2 \frac{m}{s} \approx 80 \frac{km}{hr}$ and $v = 33.3 \frac{m}{s} \approx 120 \frac{km}{hr}$ and at the horizontal axis the position of the moving oscillator is plotted until it reaches the end of the bridge.

From figure [3.4] the effect of using a different speed for the moving vehicle is observed, as far as the midpoint displacement of the bridge is concerned at least, when increasing the velocity the displacement increases as well until a threshold value where the vehicle is going so fast , reaching the end of the bridge much quicker, that there is no time for the bridge to deform. That is the reason that for $v = 33.3 \frac{m}{s}$ the maximum midpoint deflection is less than the one when using $v = 33.3 \frac{m}{s}$. Another way to explain it is that for $v = 22.2 \frac{m}{s}$ the vehicle is present for 50% more time ($\approx 4.5\ sec$) at the bridge than for the case of $v = 33.3 \frac{m}{s}$ ($\approx 3.0\ sec$).

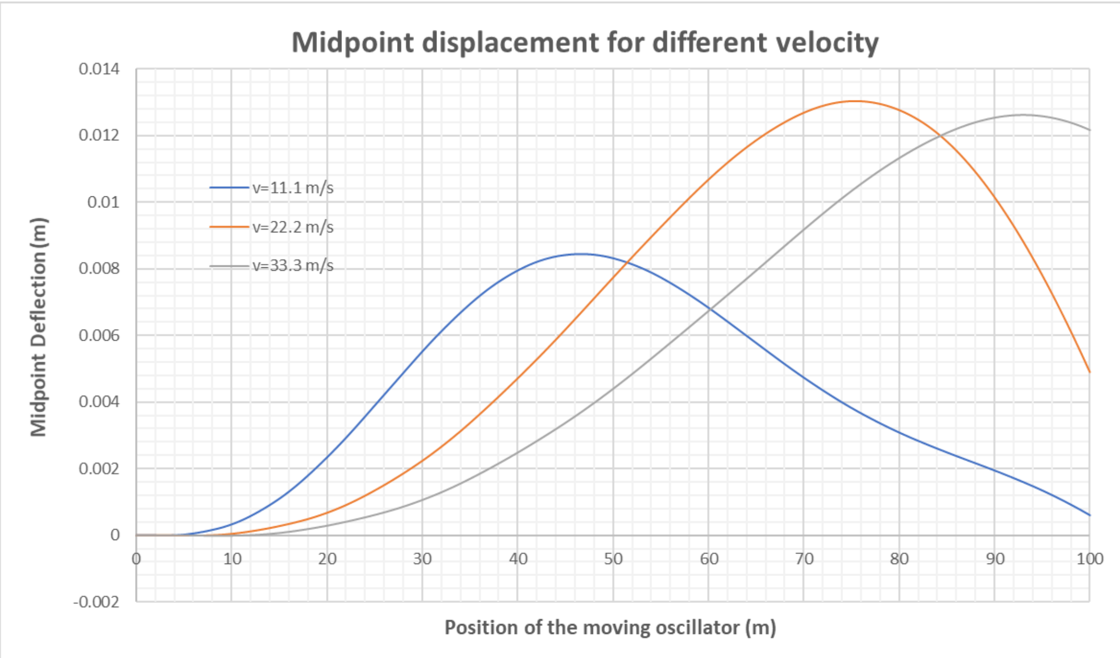

Figure 3. 4: Numerical application (3.1) - Midpoint Deflection versus Position of the moving oscillator - Sensitivity analysis for the speed of the moving oscillator

Knowing now all the values of the properties of the damage, the bridge and the vehicle all the results will be discussed in order to find the optimal quantity to detect crack(s).

Starting with the eigenfrequencies of the bridge, the values for the 5 first modes are presented, for the Undamaged and all the Damaged cases (different crack depth), calculated by solving the expressions of the free vibrations problem and verified with a corresponding model in SAP2000.

Mode number	*Undamaged*	*Damaged d/h=2%*	*Damaged d/h=5%*	*Damaged d/h=8%*	*Damaged d/h=11%*	*Damaged d/h=15%*	*Damaged d/h=20%*
1	***1.3243***	***1.3235***	***1.3224***	***1.3211***	***1.3196***	***1.3175***	***1.3145***
2	5.2972	5.2972	5.2972	5.2972	5.2972	5.2972	5.2972
3	***11.9187***	***11.9122***	***11.9016***	***11.8901***	***11.8775***	***11.8587***	***11.8314***
4	21.1889	21.1889	21.1889	21.1889	21.1889	21.1889	21.1889
5	***33.1076***	***33.0895***	***33.0603***	***33.0284***	***32.9937***	***32.9421***	***32.8679***

Table 3. 4: Numerical application (3.1) - Eigenfrequencies for different Damage cases

By looking at the results, a reduction of the 1st , the 3rd and the 5th value is presented for each damaged case and as expected that reduction increases proportionally with the increase of the crack's depth or equally with the increase of the intensity of the crack. Because of the location of the crack, exactly at the midpoint of the bridge, the values of the 2nd and the 4th eigenfrequency remain the same for each and every case.

Looking at the maximum value for the crack dept, equal to 20% of the beam's height, the differences $\left(\frac{Damaged-Undamaged}{Undamaged} * 100\right)$ for the 1st , the 3rd and the 5th eigenfrequency are -0.74% , -0.73% and , -0.72% respectively.

On the other hand, these differences could not really be used to indicate that a crack is present or not as they are so small that any other possible reason can also be the cause for the same reduction. These causes were discussed in the introduction of this project and they are the reason why such small reductions could not be the optimal quantity for crack identification that this project is aiming to find.

Moving now to the dynamic response of the beam, the midpoint displacement will be plotted for every time moment, until the moving oscillator reaches the end of the bridge.

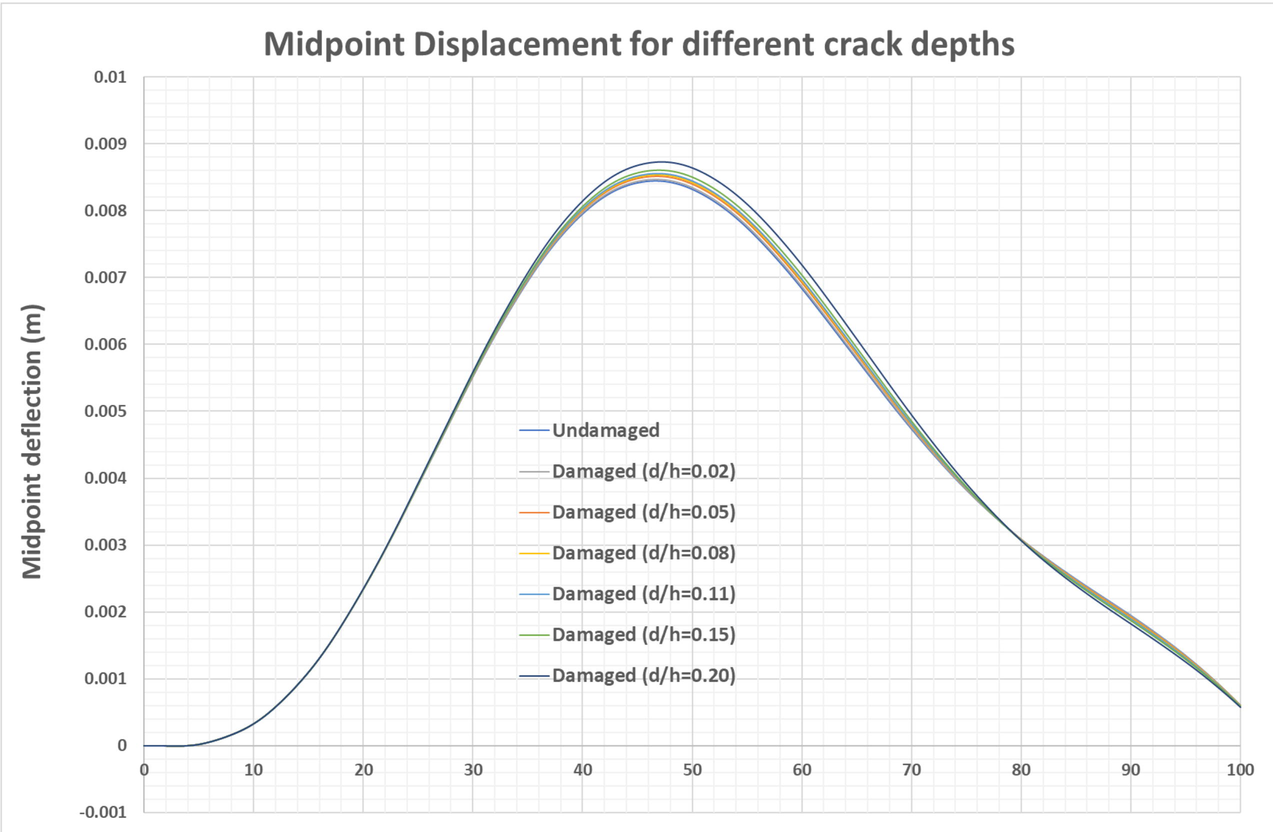

Figure 3. 5: Numerical application (3.1) - Midpoint Deflection versus Position of the moving oscillator - Damage cases

As expected, the values of the midpoint displacement increase as the crack's depth increases varying, but not so much, from the Undamaged case. While the maximum value is present close to the time-moment that the moving oscillator reach the crack ($z = 50m$), that observation depends mainly, as presented before, on the velocity of the vehicle and not so much on the location of the crack. Another way to see this, is by plotting the difference of the midpoint displacement of each Damaged case with the Undamaged one ($Damaged - Unamaged$).

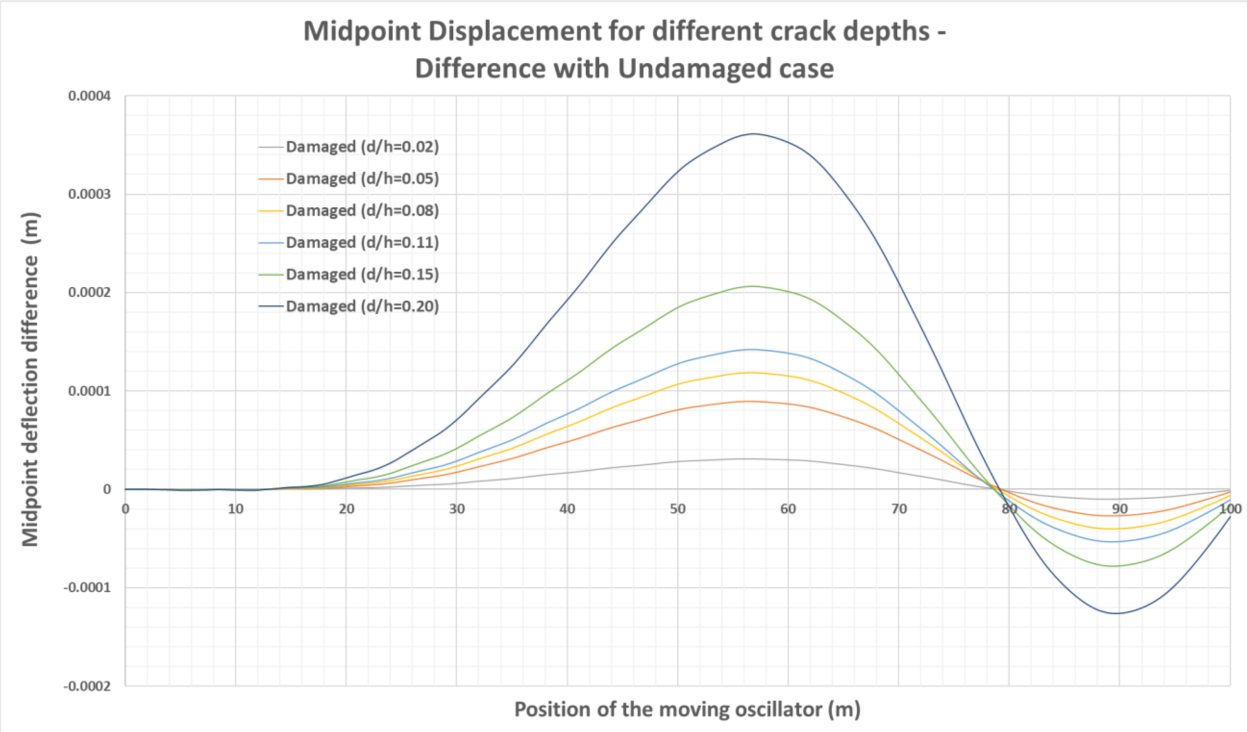

Figure 3. 7: Numerical application (3.1) - Midpoint deflection (Difference with Undamaged case) versus Position of the moving oscillator – Damage cases

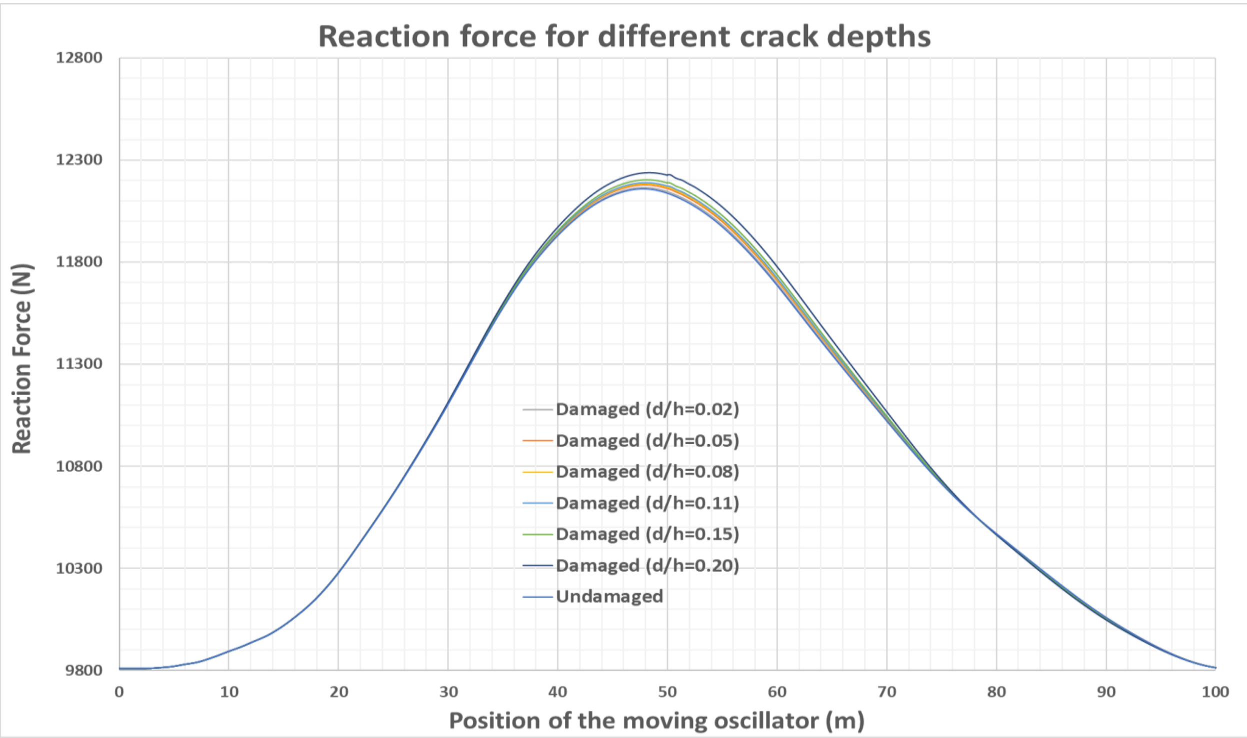

Figure 3. 6: Numerical application (3.1) - Reaction force versus Position of the moving oscillator- Damage cases

Again, in figure [3.6] there is not a clear indication that the crack is located at the midpoint of the bridge, thus the beam's dynamic deflection could not be the optimal quantity for crack identification that this project is aiming to find.

Moving now to the next measurement which is the reaction force, as presented in figure [3.7] and with the equation [92] that defines it, figure [3.7] is a plot showing the variation of the reaction force when the jth vehicle moves along the beam from the static force of the same vehicle $\left(f_{j,static} = m * g = 1000 * 9.81 = 9810\ N\right)$ for the Undamaged and every Damaged case.

Figure [3.7] follows the same notion as the beam's displacement with the larger values located close to the midpoint, but in order to draw conclusions about what is happening at the location of the crack, another plot with the difference of the reaction force of each Damaged case with the Undamaged one $(Damaged - Unamaged)$ is presented.

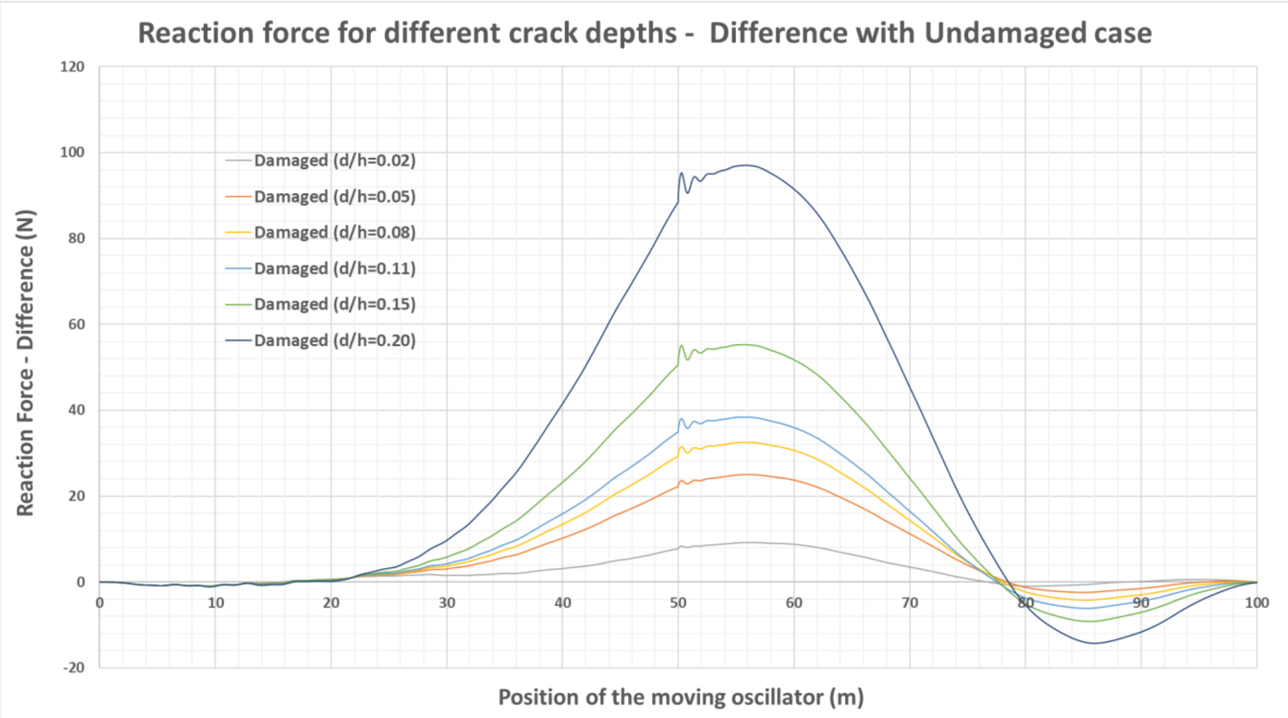

Figure 3. 8: Numerical application (3.1) - Reaction Force (Difference with Undamaged case) - versus the Position of the moving oscillator – Damage cases

Looking at Figure [3.8] it seems that the reaction force is a valuable quantity for crack identification as there are clear fluctuations of its values, starting exactly when the moving vehicle reach the location of the crack $(z = 50m)$, and lasting for a small period of time until the curve becomes again as smooth as it was before. These fluctuations depend on the intensity of the crack or equally on the value of the stiffness of the rotational spring (representative of the crack) and are more observable, of course, as the crack's depth increases. It seems that for the specific properties of the bridge and the oscillator, the cracks with a depth/height $\geq 5\%$ could be identified having the measurements of the reaction force, where height is the one of the cross-section of the bridge.

Moving to the moving oscillator's dynamic response, the displacement $u_{v,j}(t)$ will be first presented for the Undamaged and all the Damaged cases (different crack depths).

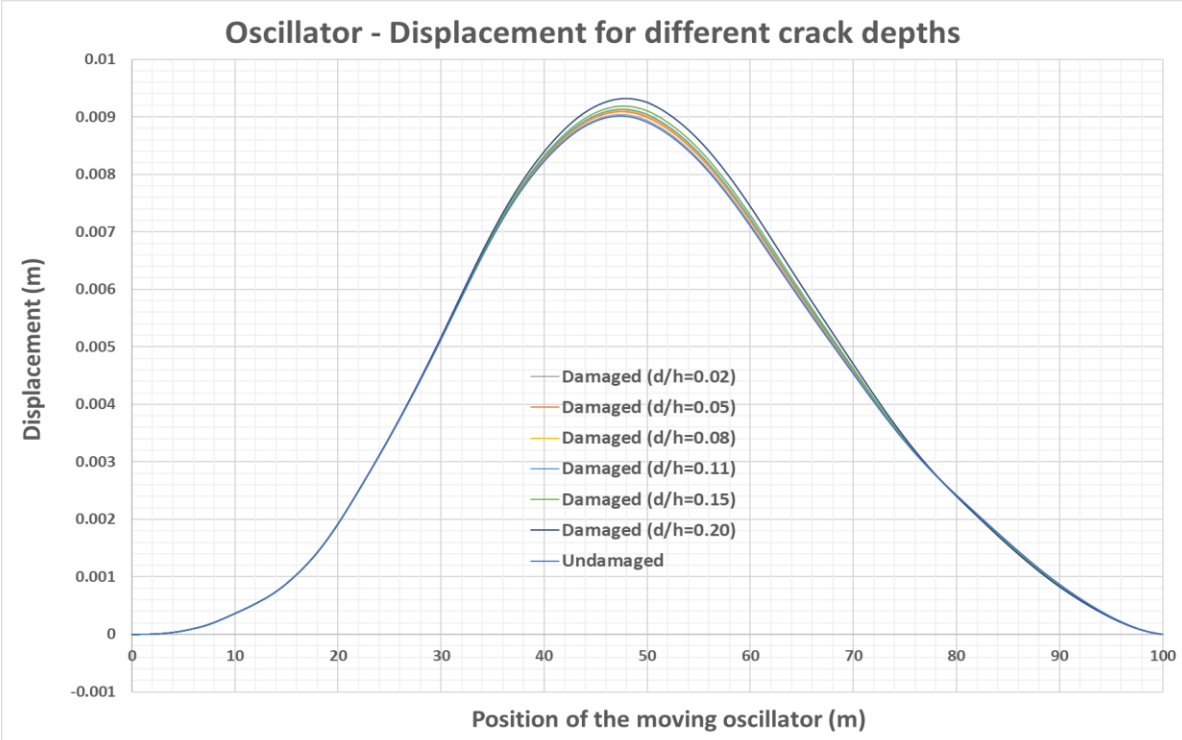

Figure 3. 9: Numerical application (3.1) - Oscillator's Displacement versus Position of the moving oscillator - Damage cases

Again, the displacement of the vehicle follows the same notion as the midpoint displacement curve but with a slightly higher values and going back almost to zero when the vehicle reach the end of the bridge in contrast with the beam that still vibrates. Now, the difference of the oscillator's displacement of each Damaged case with the Undamaged one $(Damaged - Unamaged)$ is presented.

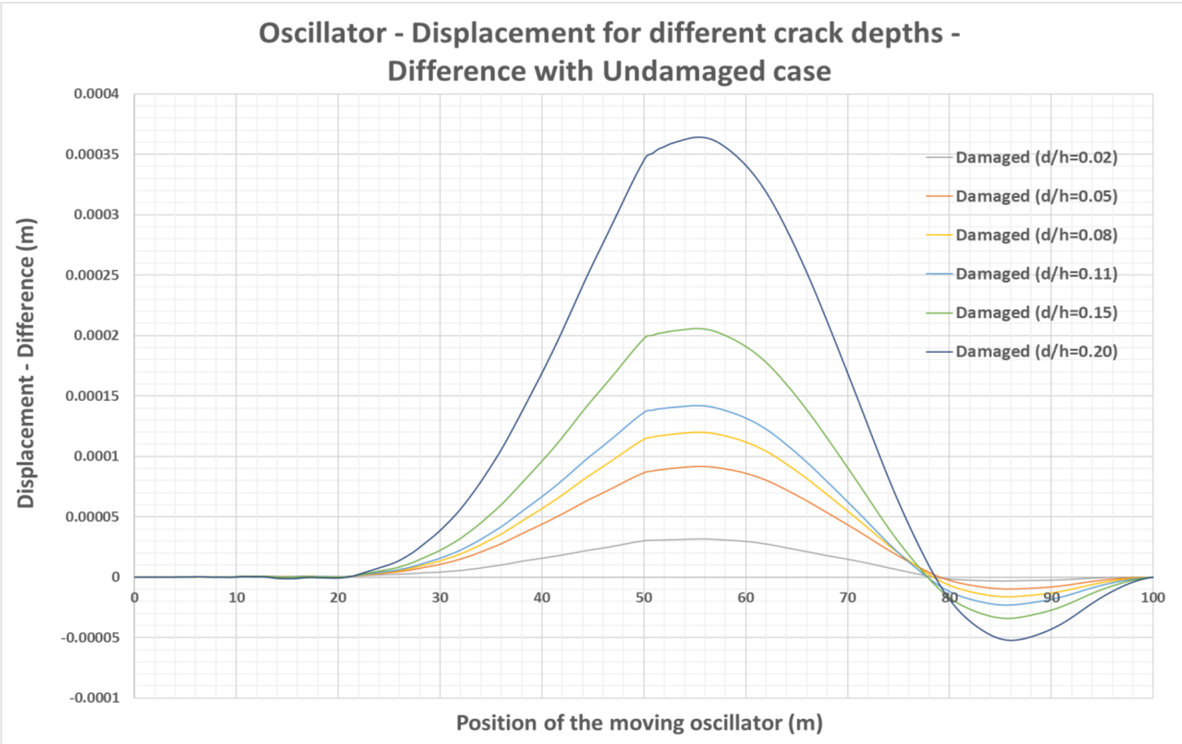

Figure 3. 10: Numerical application (3.1) - Oscillator's Displacement (Difference with Undamaged case) versus the Position of the moving oscillator - Damage cases

In figure [3.10] looking at each curve for each Damaged case, a kink is observed exactly at the middle of the bridge ($z = 50m$) where the crack is located. That sudden change of curvature was expected by modelling the crack as a rotational spring where a drop of flexural rigidity is present. Like before, that kink is more and more observable and can easier be a sign of crack identification when the depth of the crack increases, and in this case for a depth/height $\geq 8\%$, the measurements could be used to identify the crack(s), where height is the one of the cross-section of the bridge.

Finally, the last quantity that will be discussed in this project to find the optimal measurement to detect crack(s) is the moving oscillator's acceleration $\ddot{u}_{v,j}(t)$. Figure [3.11] shows the Undamaged as well as all the Damaged cases (different crack depth) for the vehicle's acceleration until it reaches the end of the bridge.

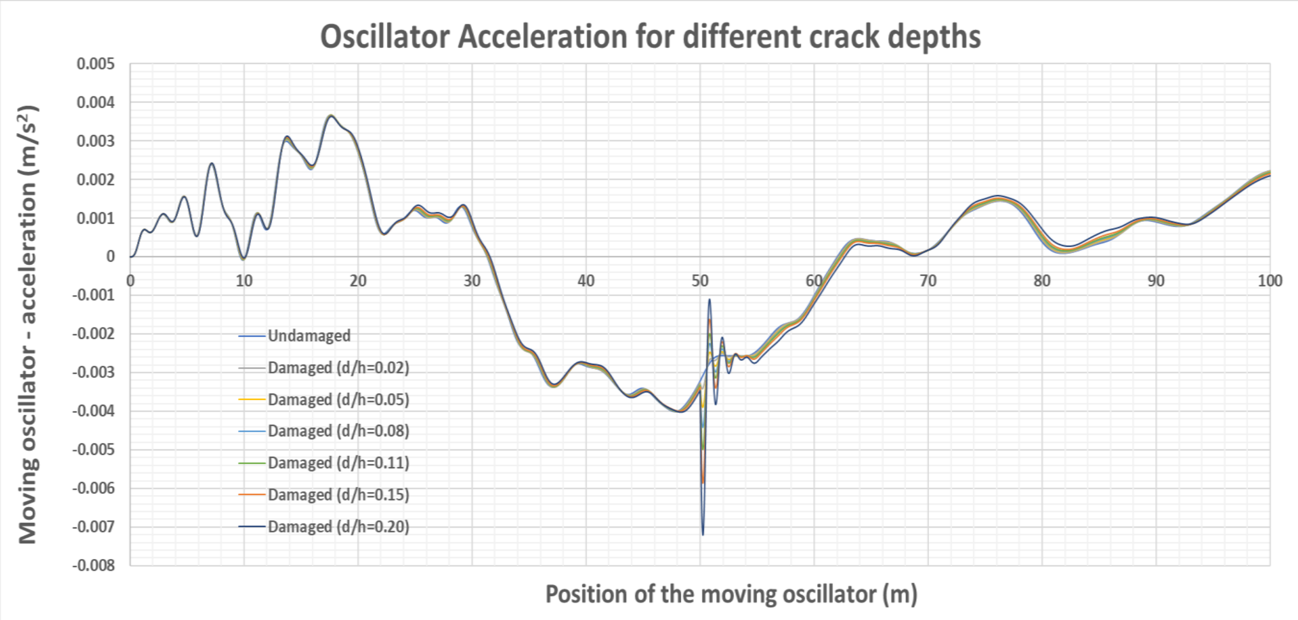

Figure 3. 11: Numerical application (3.1) - Oscillator's Acceleration versus the Position of the moving oscillator – Damage cases

For the first time the graphs with the total values and not with the difference with the Undamaged case, already make clear where the crack is located. It is observed that there is a clear high increase of the values exactly at the location of the crack ($z = 50m$), and the fluctuations last for approximately $0.5\ sec$, given the fact that the speed of the vehicle is $v = 11.1\frac{m}{s}$. These changes will be more clear in the next figure where the difference of the oscillator's acceleration of each Damaged case with the Undamaged one ($Damaged - Unamaged$) is presented.

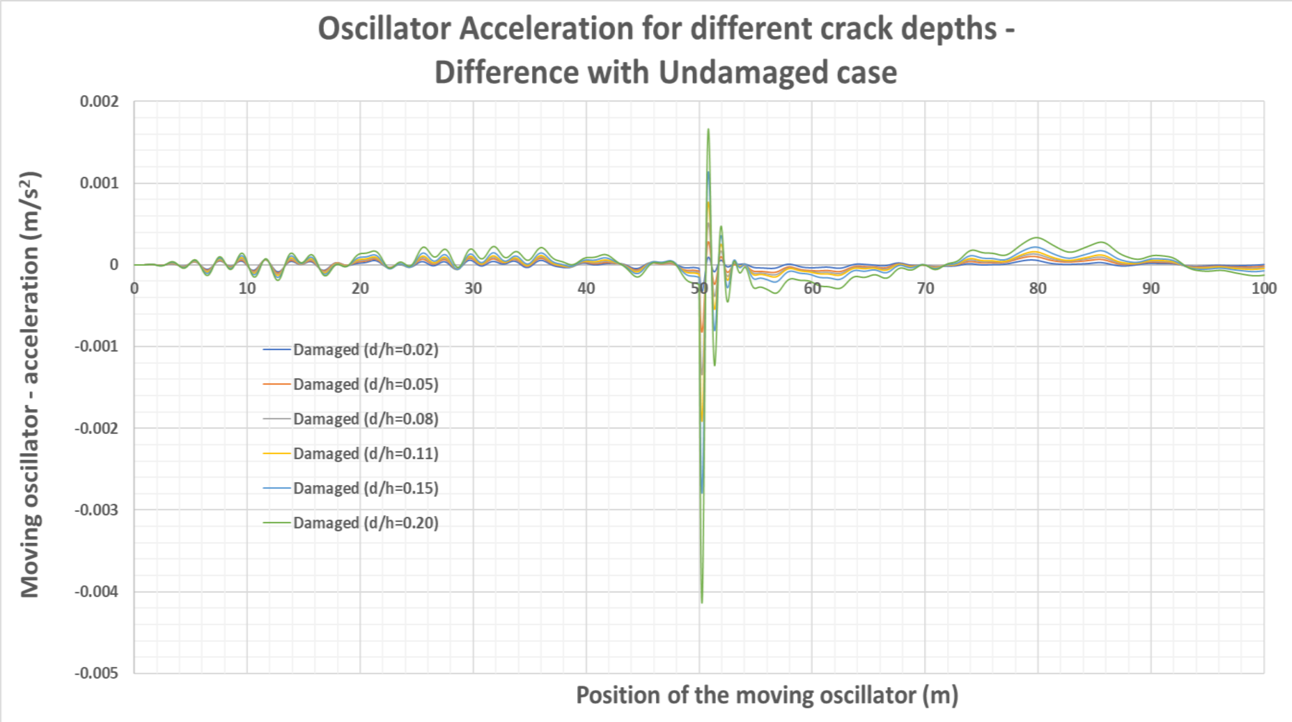

Figure 3. 12: Numerical application (3.1) - Oscillator's Acceleration (Difference with undamaged case) versus Position of the moving oscillator – Damage cases

As expected, in figure [3.12] it becomes even more obvious that there is a sudden increase of flexibility at the middle of the bridge, indicating the presence of a crack. It also seems that the vehicle's acceleration is the most sensitive quantity considering that the values calculated at the location of the crack for the Damaged cases are multiple times the value of the Undamaged case being much more clear than any other observation in all the other results. The value of the intensity of the crack, in this case, that could be identified given that the real measurements are known, is for a ratio of crack's depth/height $\geq 2\%$, where height is the one of the cross-section of the bridge.

- Which is the optimal measured quantity to detect a crack?

By performing a sensitivity analysis for a simply-supported beam-type damaged bridge with one crack at the midpoint, different measurements were examined in order to answer which one will be the most sensitive for crack identification. After comparing the results for 6 different crack intensities the optimal measured quantity to detect a crack found to be the acceleration of the moving oscillator. The values of the minimum depth of a crack found to be identifiable by each one of the measurements, are mentioned below showing which are the most valuable to use.

- What would be the value of the depth of a crack to be identifiable?

The values mentioned here were calculated carefully and presented above with figures. It is important to say that even that these values were found for the specific problem and the specific properties of the bridge, vehicle and damage, the main conclusions about the optimal measured quantity and which would be the approximate minimum depth of the crack to be identifiable, are still valid for other models with different properties.

The calculated ratio d/h, namely crack depth over the height of the cross-section of the bridge, for each measurement so that the crack will be identifiable is:

- Eigenfrequencies ≈ d/h> 15%
- Reaction force: ≈ d/h=5%
- Oscillator's Displacement ≈ d/h=8%
- Oscillator's Acceleration ≈ d/h=2%

3.3 Would the model of the crack affect the identification?

In this section a different way of modelling the crack will be discussed in order to examine if the main conclusions found before are still valid and that the findings of this thesis project about crack identification hold for different ways of considering the damage in a bridge. In this way all the suggestions and recommendations of this project will be more valuable and could be used for other investigations without the dependence of the modelling of the damage.

All the results calculated before concerned modelling the damage as a rotational spring at the location of the crack with a stiffness K_r calculated with an empirical formula. The new way of modelling the damage is with a zone with a specific length (t) with reduced flexural rigidity (EI) due to the presence of the crack. The two methods of modelling the crack are presented in figure [3.13], rotational spring (top) and a zone with reduced flexural rigidity (bottom).

As it has also been done considering the crack as a rotational spring, the analytical expressions of the mode shapes derived in the first part of this thesis will also be used for the new way of modelling the crack. In this case, only the expressions for the Undamaged case are important, solving the model in a stepwise manner. In fact, the same way of solving that was used for the bridge with step changes in material will also be used here, by considering now separately a beam segment with a different flexural rigidity than the rest of the bridge (a reduced one to be precise) with a length equal to (t), representative of the zone influenced by the presence of the crack. The fact that this approach could be used makes even more important and helpful the analytical expressions for the mode shapes derived in the first part, as they are able to consider accurately any number of these step changes in material in bridges.

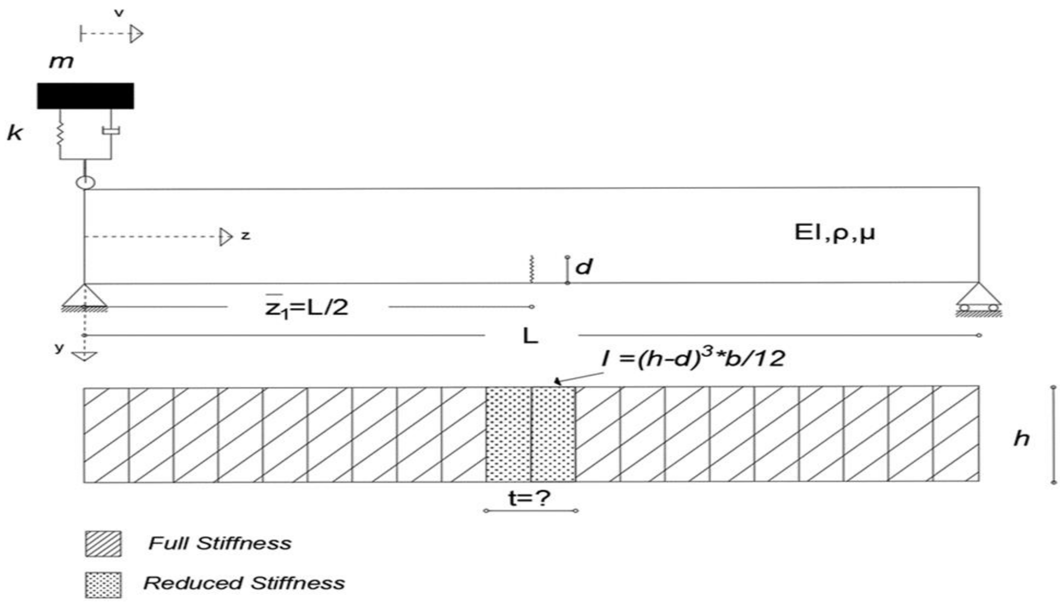

Figure 3. 13: Different ways of modelling a crack: Translational spring (top) - Influenced zone (bottom)

3.3.1 How could we obtain the same changes at the eigenfrequencies from the 2 methods? Influence zone (t) equal to?

The value of the influence zone (t) is, indeed, a matter of discussion as it is really difficult to measure precisely the part (the length) of the bridge that is affected by one and only crack. Before using an empirical value and in order to get a first impression about the differences of the two ways of modelling the crack, the value of the influence zone (t) needed to achieve almost the same changes at the eigenfrequencies, will be measured. Specifically, the ratio of the influence zone over the beam's height (t/h) will be calculated to get a sense of the physical model.

As far as the numerical example of the simple supported beam with one crack located at the midpoint is concerned, using the analytical expressions derived in the beginning of this thesis project, after a number of repetitions for the value (t), almost identical eigenfrequencies were found for the 2 different ways of modelling the crack for 6 different crack's depth scenarios (from 2% to 20% of the beam's height).

Table 3. 5: Eigenfrequencies for different Damage cases - Comparison of different ways of modeling the crack

Mode number	*Undamaged*	*Damaged d/h=2% => t/h=75%*	*Damaged d/h=5%=> t/h=75%*	*Damaged d/h=8%=> t/h=75%*	*Damaged d/h=11%=> t/h=75%*	*Damaged d/h=15%=> t/h=75%*	*Damaged d/h=20%=> t/h=75%*
1	*1.3243*	*1.3235*	*1.3224*	*1.3212*	*1.3198*	*1.3175*	*1.3145*
2	5.2972	5.2972	5.2972	5.2972	5.2972	5.2972	5.2972
3	*11.9187*	*11.9120*	*11.9020*	*11.8912*	*11.8783*	*11.8585*	*11.8324*
4	21.1889	21.1889	21.1889	21.1889	21.1889	21.1889	21.1889
5	*33.1076*	*33.0891*	*33.0613*	*33.0305*	*32.9962*	*32.9417*	*32.8707*

The conclusion is that the influence zone was calculated equal to 65%-75% of the beam's height, depending on the damaged case considered, meaning that for d/h=2% the influence zone (t) over the crack's depth (d) is equal to 37.5 and for d/h=20% it is equal to 3.25. Knowing that it is not realistic that a length of 37.5 times the depth of the crack will be affected by such a small crack, the new method of modelling the crack (namely with a the zone of reduced rigidity - EI) will lead to less sensitive identification results for the same measured quantities found before (reaction force, vehicle's acceleration etc.). This conclusion will be, of course, verified in the next pages where for the same model the results of the measurements for the 2 ways of modelling the crack will be compared and discussed.

3.3.2 Numerical application (3.2) - Comparison of different ways of modelling the crack

The first step will be to verify the computational strategy followed for the two different methods of modelling the crack, namely as a rotational spring placed at the crack's location or as an influenced length of the beam with decreased rigidity. This will be achieved by comparing the results of the Undamaged case that should coincide, as they describe the same physical model without the presence of any crack or a part with reduced rigidity.

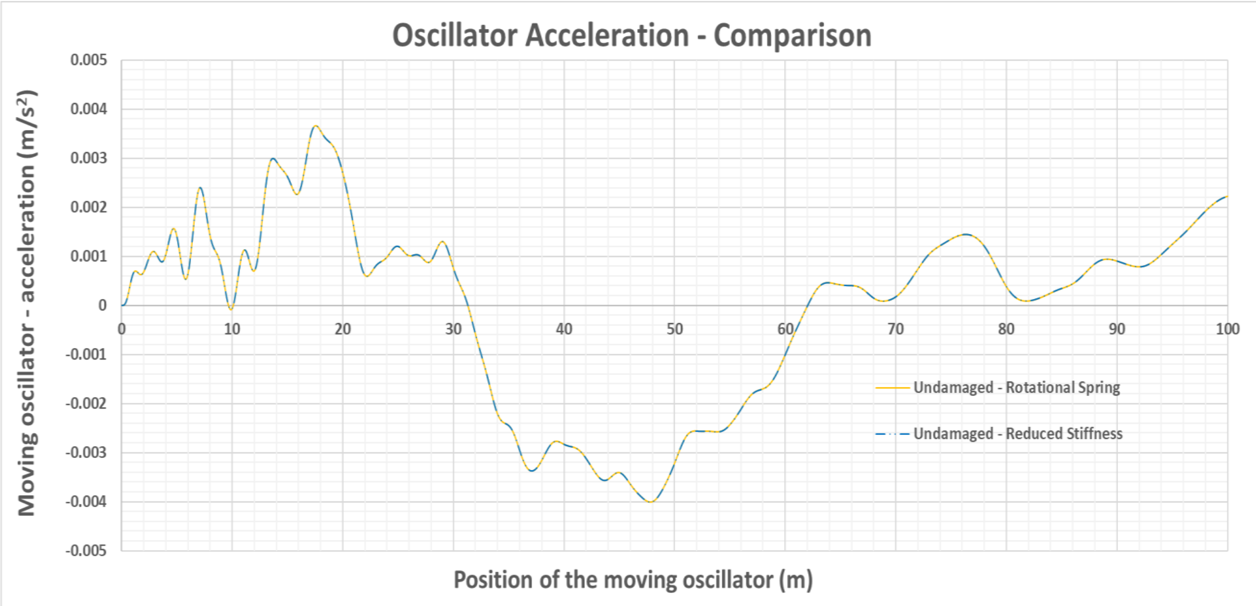

Figure 3. 15: Numerical application (3.2) - Verification of the models with a different way of modelling the crack – Oscillator's Acceleration Undamaged case

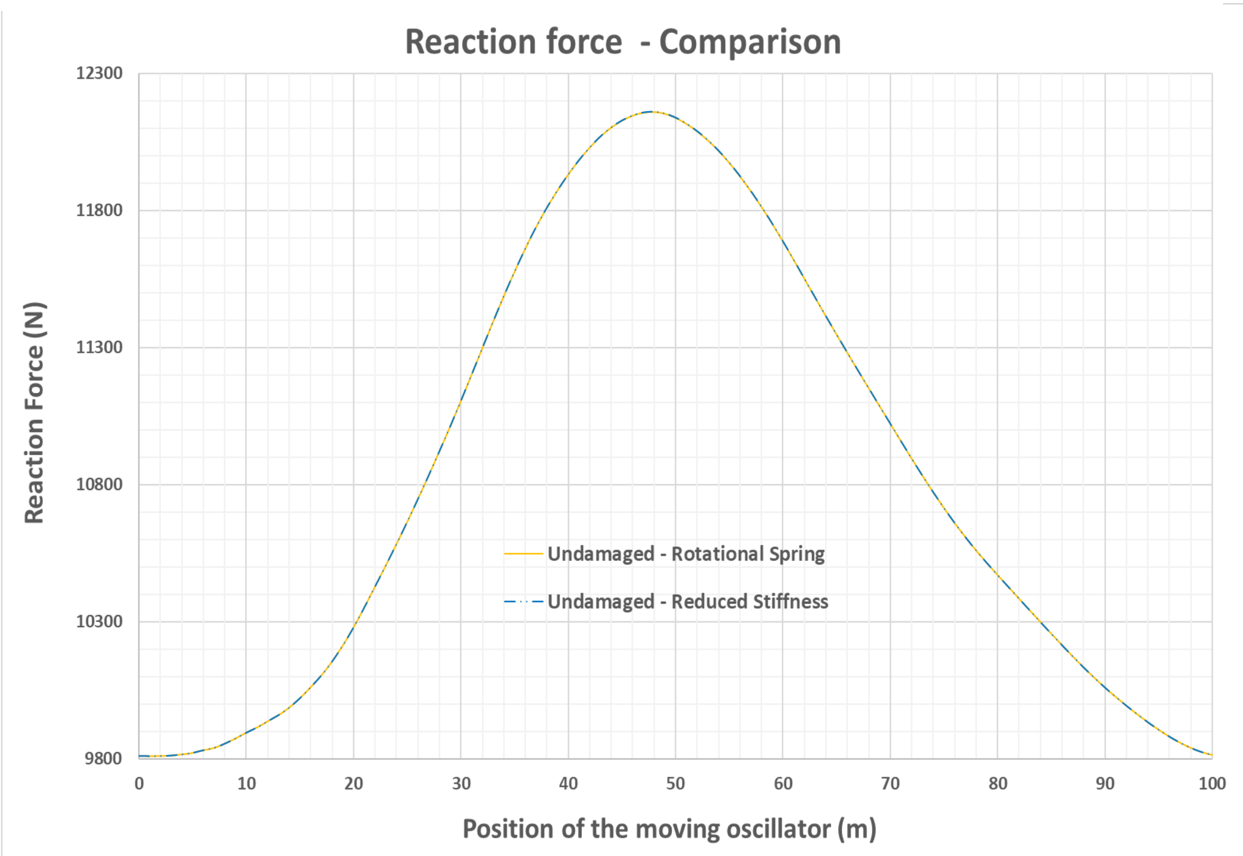

Figure 3. 14: Numerical application (3.2) - Verification of the models with a different way of modelling the crack - Reaction Force – Undamaged case

.

Indeed, the figures [3.14] , [3.15] showing the moving vehicle's acceleration (modelled as spring-mass system) and the reaction force acting on top of the beam, verify that the plots for the two cases coincide.

Now, that the computational strategy followed is verified for both cases, the Damaged scenario should be compared in order to draw conclusions about the sensitivity of the identification techniques used in the previous numerical examples, about the new way of modelling the crack. The next three figures [] , [] indicate the most sensitive measurements derived from the motion of the vehicle (acceleration and displacement) and the reaction force, only for the case of $d/h = 15\%$, so that it will be more easy to compare the new method for a specific Damage scenario. Important to mention, that for all the numerical examples to follow the value of the influence zone will be equal to 3 times the crack's depth $(t = 3d)$, meaning that the length influenced by the crack will be 1.5 times its depth for each of its side.

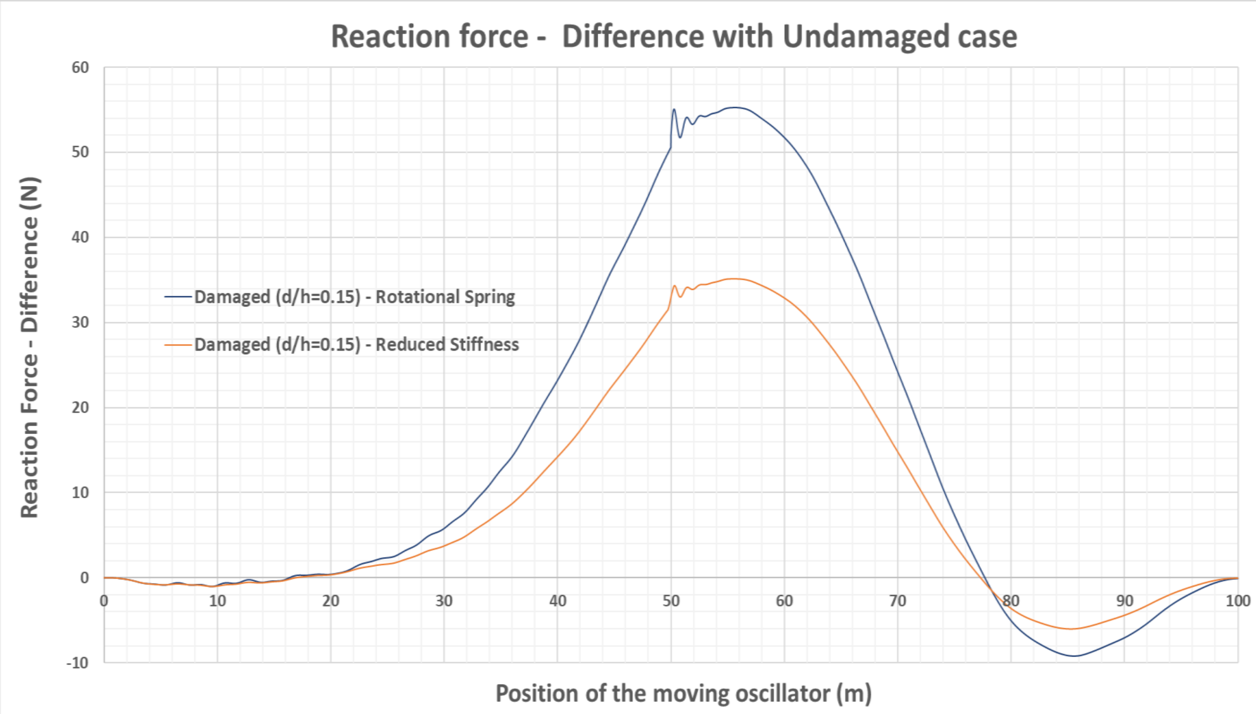

Figure 3. 16: Numerical application (3.2) - Reaction Force (Difference with Undamaged case) versus Position of the moving oscillator – d/h=0.15

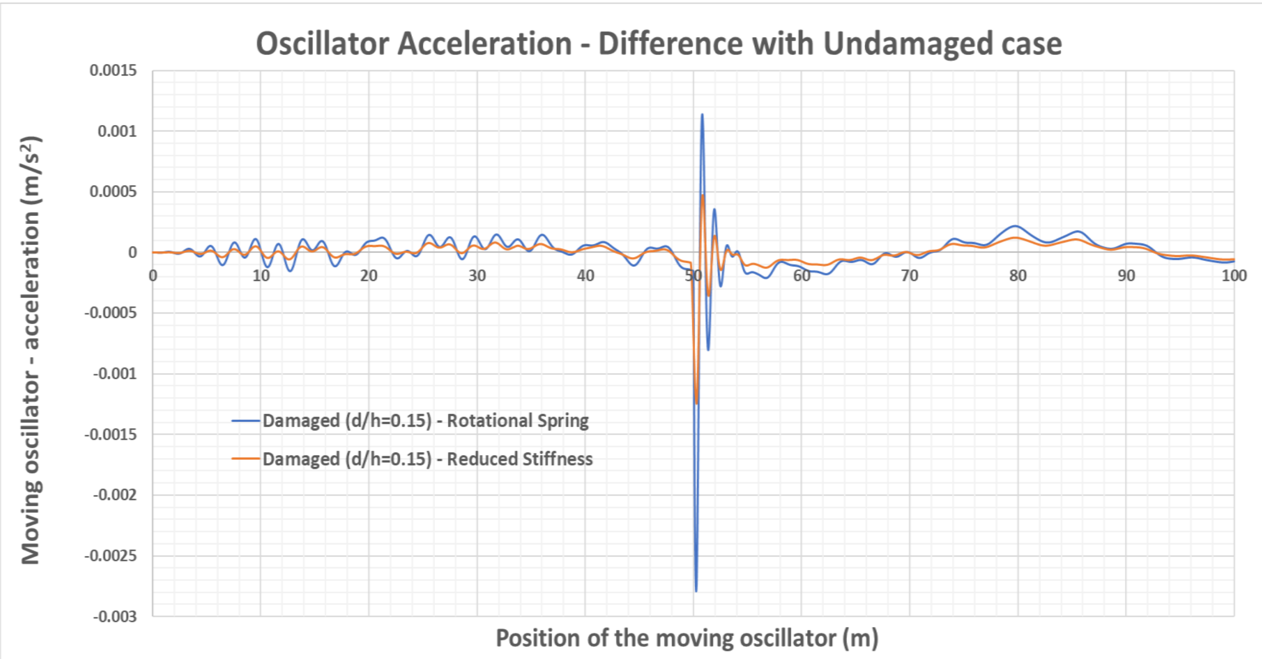

Figure 3. 17: Numerical application (3.2) - Oscillator's Displacement (Difference with undamaged case) versus Position of the moving oscillator – d/h=0.15

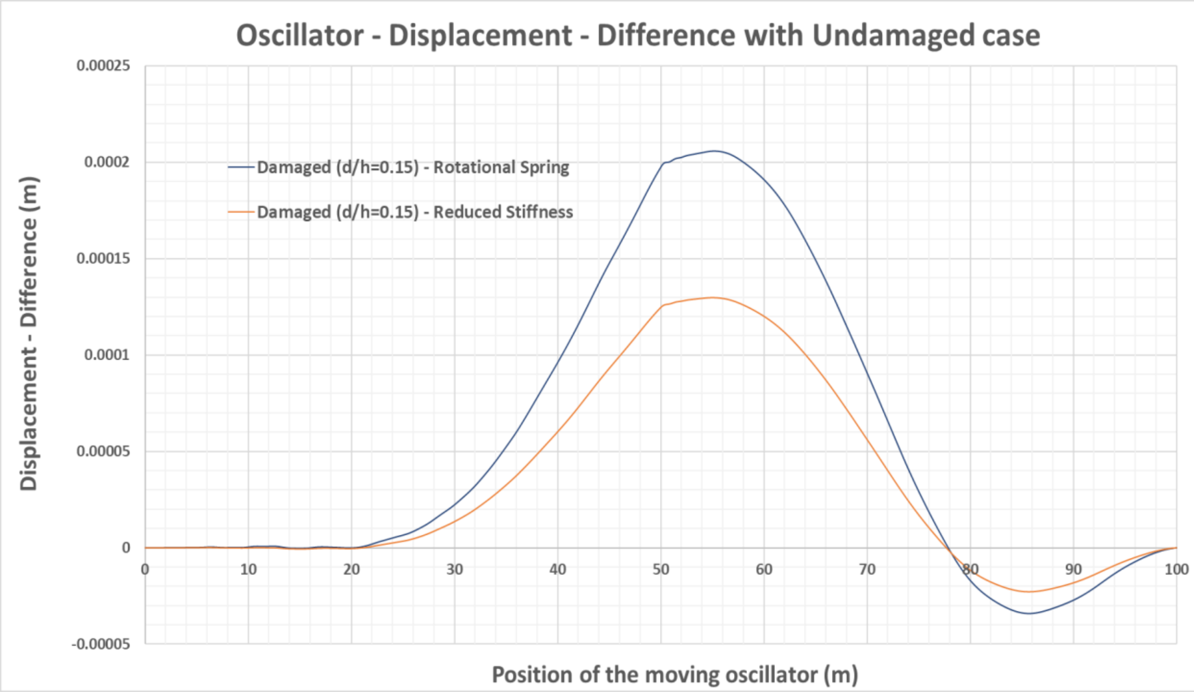

Figure 3. 18: Numerical application (3.2) - Oscillator's Displacement (Difference with undamaged case) versus Position of the moving oscillator – d/h=0.15

Looking at the figures [3.16] , [3.17], [3.18] the assumption that was mentioned above, meaning that with the new way of modelling the crack the identification is less sensitive, is verified. The figures indicate the values of these quantities when calculating their difference with the Undamaged case in order to be able to distinguish the location of the crack. For each plot with the "orange" color, that represents the method of modelling the crack as a length with reduced rigidity, all the values are smaller than the ones of the first method (when the crack is modelled as a rotational spring). In addition, all the signs that were mentioned before for identification purposes, namely the fluctuations of the reaction force and the vehicle's acceleration or the abrupt change of curvature at the graph of the vehicle's displacement, are all now less sensitive when reaching the location of the crack.

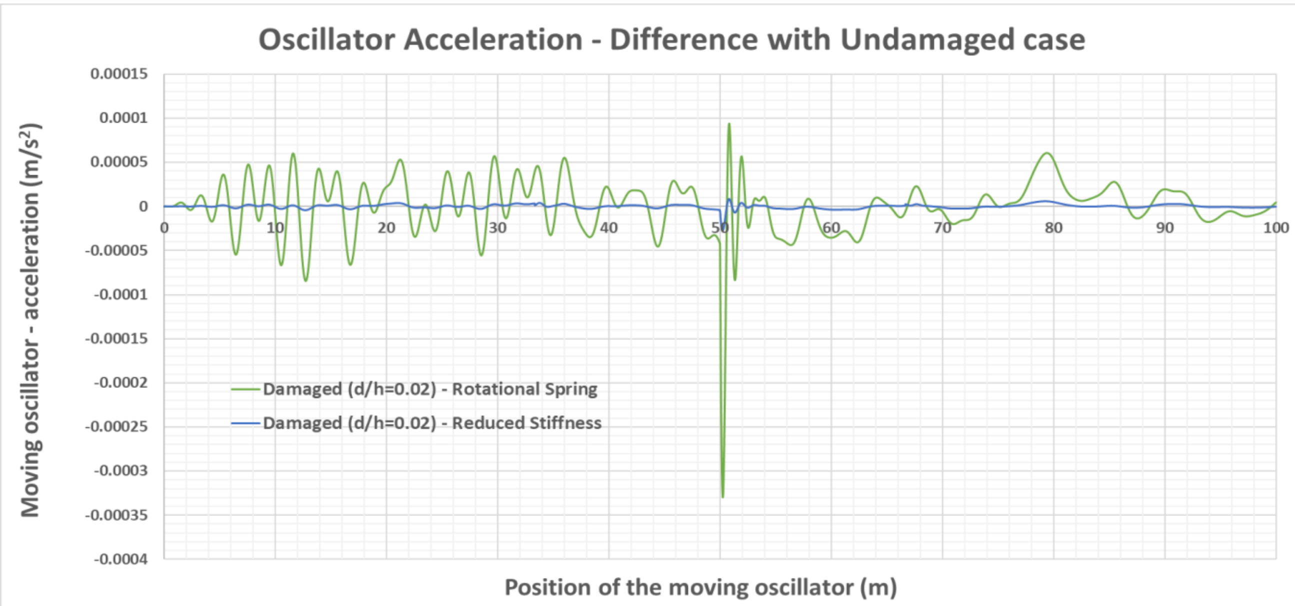

Figure 3. 19: Numerical application (3.2) - Oscillator's Acceleration (difference with undamaged case) versus Position of the moving oscillator - d/h=0.02

It seems that by representing the crack just as a length of reduced rigidity, can be used again for identification purposes but the sensitivity of the results would be more dependent on the intensity of the damage, meaning that smaller cracks might be less or, worse, not at all identifiable. On the other hand, modelling the crack as a rotational spring exactly placed at the location of the crack will cause such a change of the momentum that could be even visible for really small cracks, as proved before for the case of the vehicle's acceleration. Exactly this, is visible in figure [3.19] where the Damaged case of the minimum crack depth under investigation is considered $(d/h = 2\%)$. Even in this case, as far as the rotational spring is concerned there is a noticeable disruption the time-moment the moving vehicle reach the location of the crack in contrast with the new method where these fluctuations are so small that could not be used for crack(s) identification anymore.

What would be the value of the depth of a crack to be identifiable?

As the new way of modelling the crack leads to less sensitive identification measurements, a new minimum intensity for each quantity after a number of repetitions, thanks to the analytical expressions derived in this project. The new calculated ratio d/h, namely crack depth over the height of the cross-section of the bridge, for each measurement so that the crack will be identifiable is:

- Eigenfrequencies ≈ d/h> 35%
- Reaction force: ≈ d/h=8%
- Oscillator's Displacement ≈ d/h=10%
- Oscillator's Acceleration ≈ d/h=5%

As it has already been proved, all these values are higher than the ones found for the case of modelling the crack with a rotational spring.

3.4 Would the number of cracks affect the identification?

<u>Numerical application (3.3) – Two cracks present:</u>

This numerical application is about the same physical model (same properties of the beam and the moving vehicle) of the numerical application [3.1] but with the important change of adding another crack in order to test if the identification will be affected by the number of cracks present along the beam. Specifically, one crack is located at $L/3$ with a ratio $d/h = 15\%$, and one more is located at $2L/3$ with a ratio $d/h = 10\%$. All the values needed for the 2 ways of modelling the cracks are presented in Table [3.6], namely the value of the stiffness of the rotational spring and the damage parameter for the first method and the value of the influence zone for the second one.

Table 3. 6: Numerical application (3.3) - Properties of the cracks

Properties <u>Crack</u>	Location - $\bar{z}$ (m)	Depth - *d* (m)	Equivalent stiffness - *K* x10^{-6} (kN/m)	Damage parameter – α (m^{-1})	Influence zone – t (m)
<u>1</u>	33.3	0.18	48.05	0.749	0.54
<u>2</u>	66.6	0.132	70.36	0.512	0.396

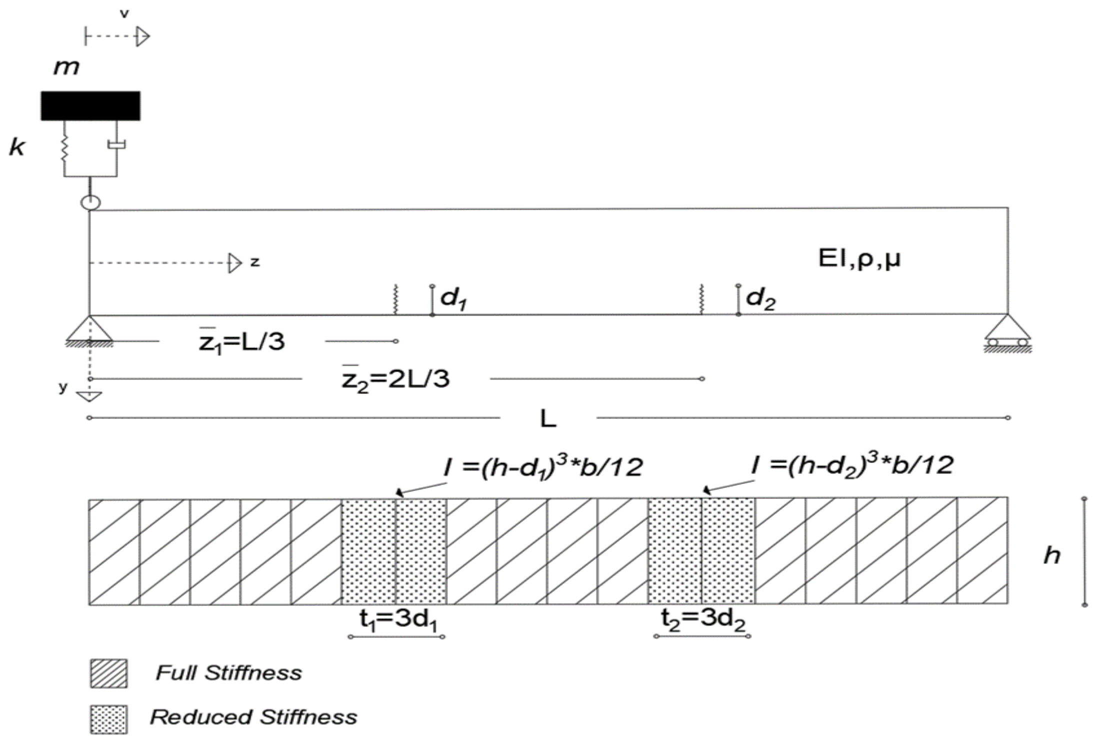

Figure 3. 20: Numerical application (3.3) – Model definition

For this model, only the results coming from the moving vehicle's acceleration will be plotted, being the most sensitive measurement as it was found before, but also because it is now important to prove if the identification methods still hold and not which is the optimal measurement for it.

In figure [3.21] and [3.22] the total values of the oscillator's acceleration and their difference with the Undamaged case are plotted, respectively. Both figures contain the graphs of both ways of modelling the crack in the analysis, to compare them.

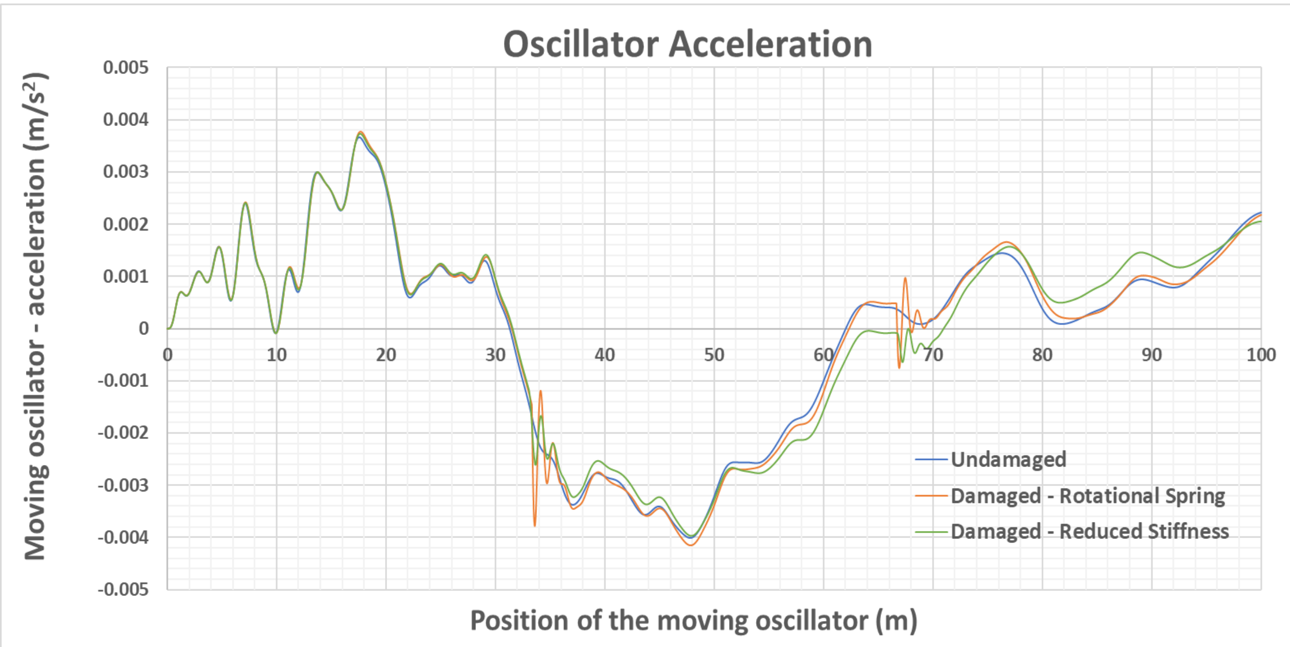

Figure 3. 21: Numerical application (3.3) - Oscillator's Acceleration versus Position of the moving oscillator - 2 cracks

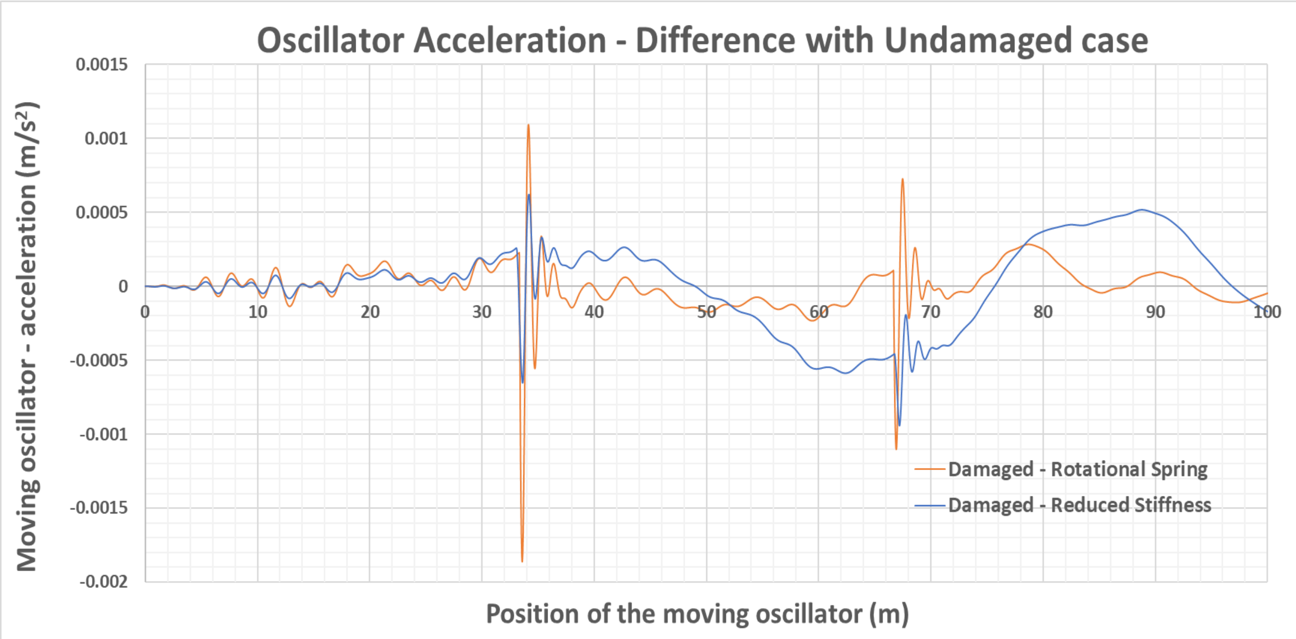

Figure 3. 22: Numerical application (3.3) - Oscillator's Acceleration (Difference with undamaged case) versus Position of the moving oscillator - 2 cracks

Looking at the results, when the moving vehicle reach each one of the crack, there are large fluctuations present at the graphs, indicating the location of the damage for both methods. Again, the difference of the 2 methods is that the one concerning a length of reduced rigidity close to each crack, is less sensitive than the one of a rotational spring representing each crack. Another difference is that, even if the location of the crack(s) is more clear for the method with the rotational spring, the differences with the Undamaged case after passing the first crack are smaller than the other method, because of the fact that the rotational spring concerns a specific point of the beam and after a while the values always tend to return to the values of the Undamaged case.

All in all, it is noticed that the validity of the identification still holds for more than one crack present along the beam and all the conclusions already mentioned before about the measurements could be used for any number of cracks.

3.5 Would the complexity of the beam-type bridge (varying rigidity) affect the identification?

<u>Numerical application (3.4):</u>

In this numerical application the identification of the crack will be tested for the case of increased complexity as far as the bridge is concerned. Specifically, as it was also done before in this project, the case of a beam-type bridge with step changes in material will be considered, for the model of a simply-supported bridge with one crack at the midpoint. The values of the measurements will be found for both methods in order to validate the identification without the dependence of the way of modelling the crack.

Note that for the case of the "reduced stiffness" method, 5 different beam segments are considered, and the solution will come from a stepwise use of the analytical expressions of the mode shapes derived for the

Undamaged case, just with a different value of length and rigidity. Again the influence zone (t) will be equal to 3 times the depth of the crack. The properties of the model are presented below.

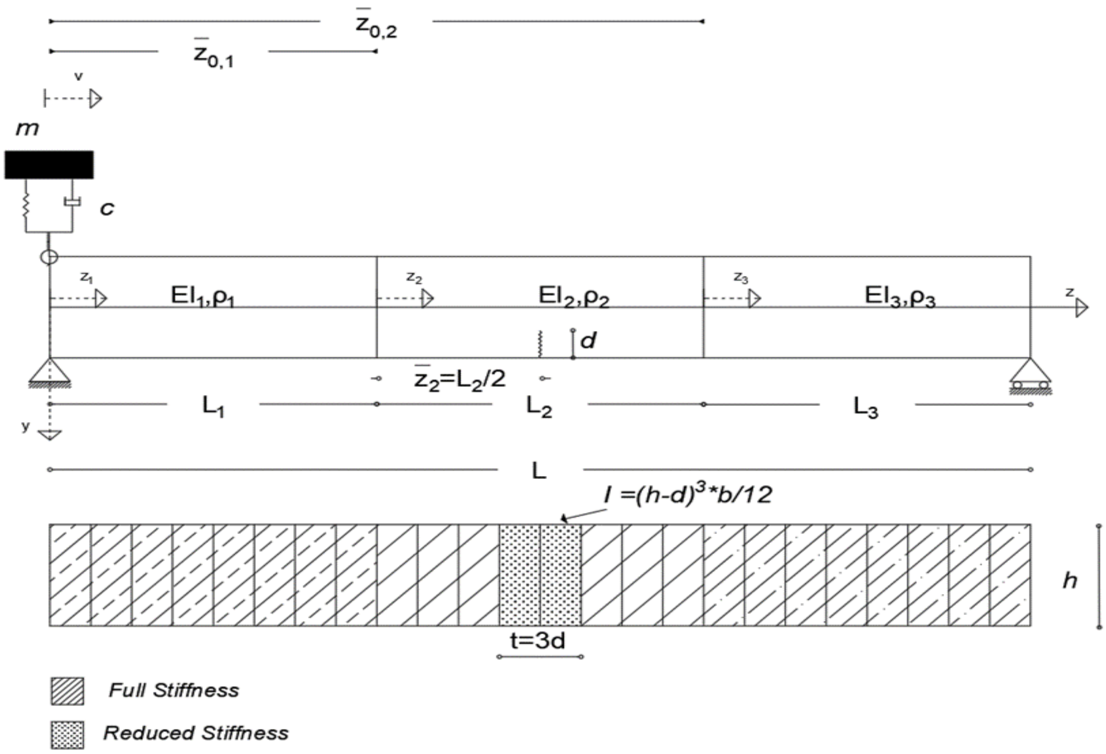

Figure 3. 23: Numerical application (3.4) - Model definition

Table 3. 7: Numerical application (3.4) - Properties of the Beams

Properties	*Beam 1*	*Beam 2*	*Beam 3*
Length [m]	100/3	100/3	100/3
Density [kg/m^3]	7800	7400	7000
Young's modulus [kN/m^2]	2.10x10^8	2.00x10^8	1.90x10^8

Table 3. 8: Numerical application (3.4) - Properties of the moving oscillator

Properties	Mass -*m* (kg)	Damping – *c* (Ns/m)	Stiffness -*k* (N/m)	Speed – *v* (m/s)
Oscillator	1000	25130	3.96x10^6	11.1

Table 3. 9: Numerical application (3.4) - Properties of the crack

Properties	Location - $\bar{z}$ (m)	Depth - *d* (m)	Equivalent stiffness - *K* x10^{-6} (kN/m)	Damage parameter – α (m^{-1})	Influence zone – t (m)
Crack	50	0.132	70.36	0.512	0.396

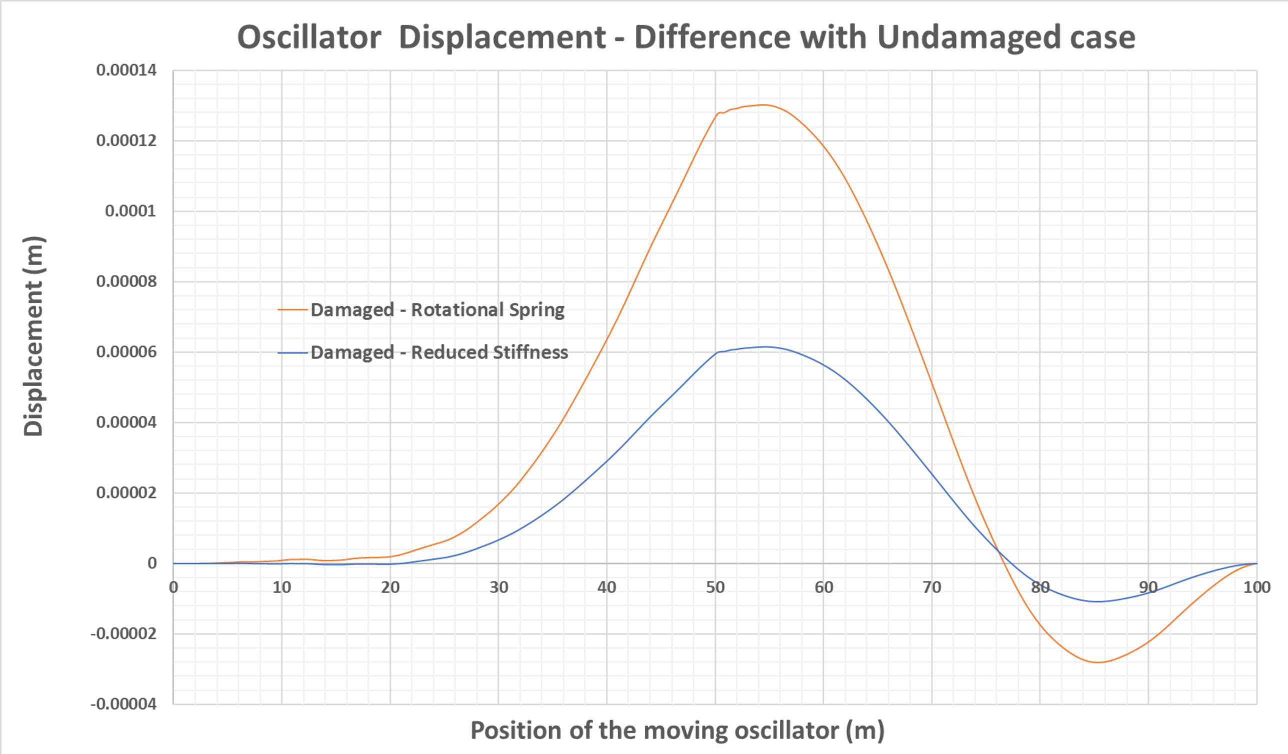

Figure 3. 24: Numerical application (3.4) - Oscillator's Displacement (Difference with undamaged case) versus Position of the moving oscillator – d/h=0.10

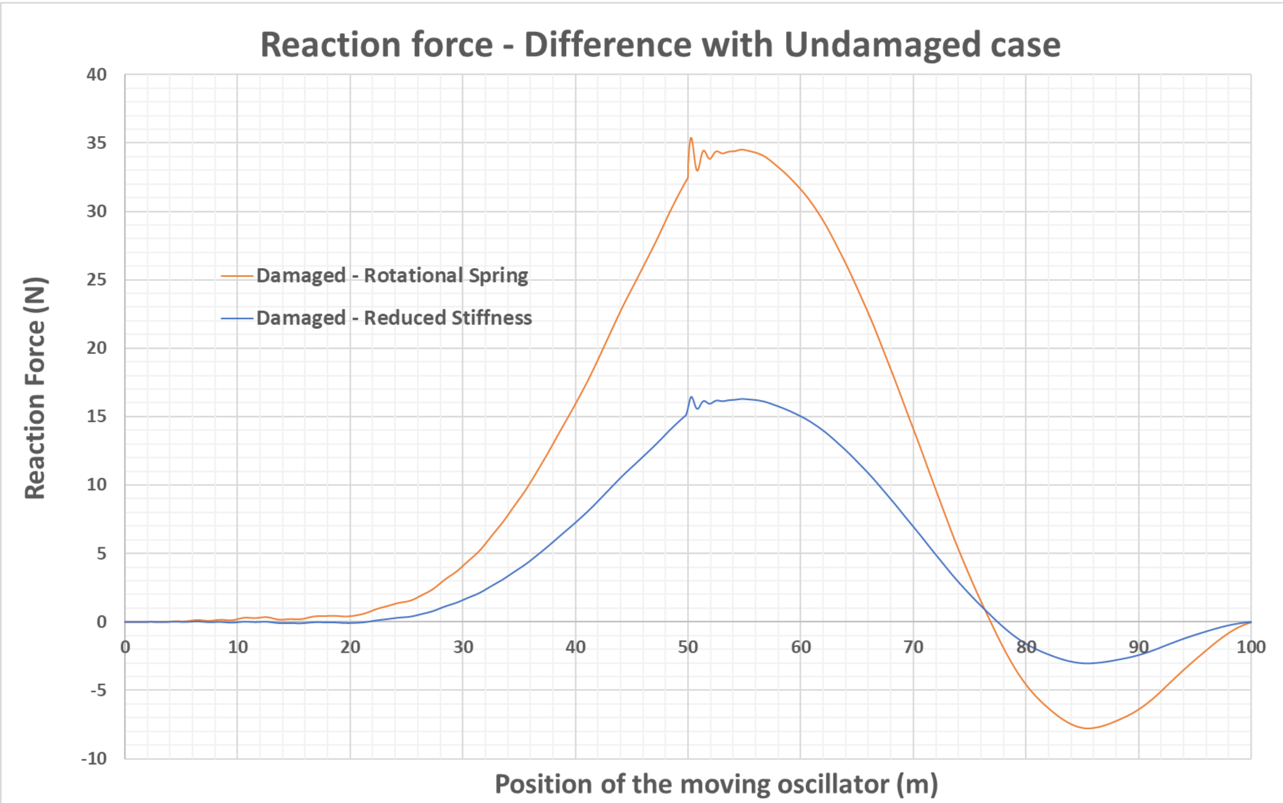

Figure 3. 25: Numerical application (3.4) – Reaction Force (Difference with undamaged case) versus Position of the moving oscillator – d/h=0.10

Figures [3.24], [3.25] indicate that the identification of the location of the crack still holds for a beam-type bridge with increased complexity, namely three different beam segments with different properties. Again, using the "reduced stiffness" method the values are smaller when comparing the difference with the Undamaged case, and the results are generally less sensitive when the moving vehicle passes on top of the location of the crack.

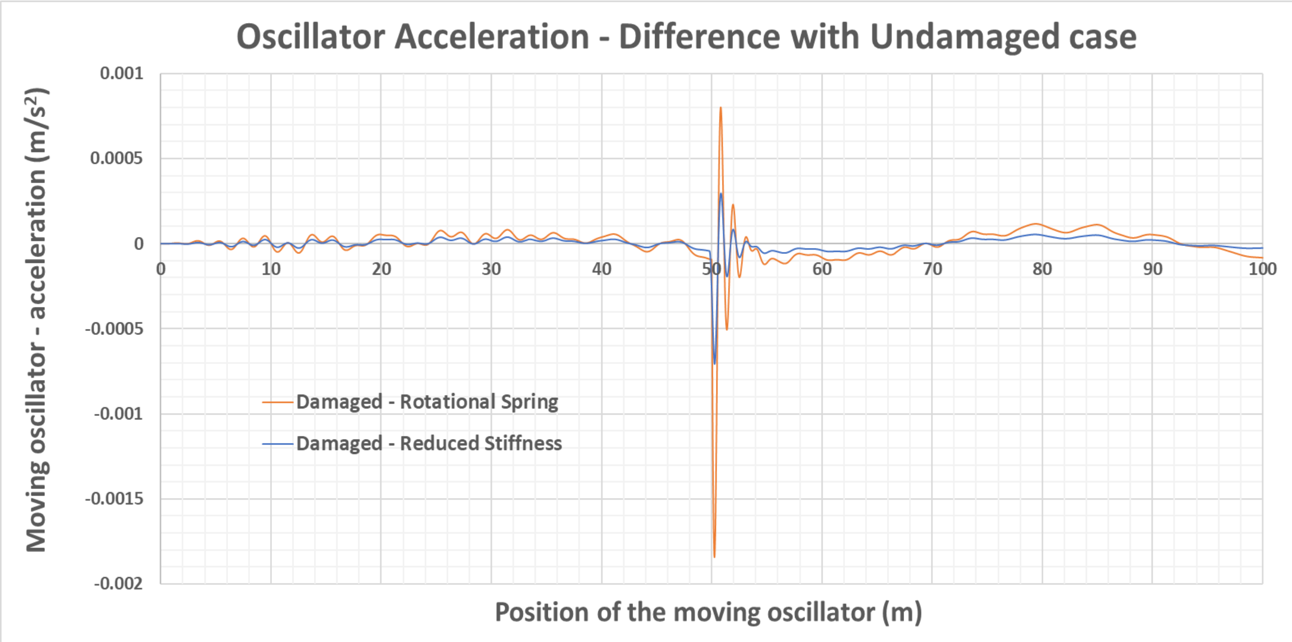

Figure 3. 26: Numerical application (3.4) - Oscillator's Acceleration (Difference with undamaged case) versus Position of the moving oscillator – d/h=0.10

The same applies for the vehicle's acceleration in Figure [3.26], the one that found to be the most sensitive measurement, where an abrupt disruption of the values is present exactly at the location of the crack, indicating the loss of rigidity due to the damaged material.

To sum up, using the governing equations derived in this thesis project and the novel analytical expressions for the mode shapes combined with the knowledge of the optimal measurement for identification purposes and the minimum crack depth that is identifiable, it is possible to deal with any beam-type bridge with any number of step changes in material and/or any number of cracks. This makes the findings of this research extremely useful for crack(s) identification and could be used for the structural health monitoring of existing bridges, with the proper knowledge and judgement of the people involved.

Chapter 4

4. Dynamic response of beams with switching cracks under moving vehicle loads

In this chapter, the dynamic response of beam-type bridges with switching cracks under moving vehicle loads will be discussed in order to investigate models with crack(s) with time-variant properties. To do that, the new analytical expressions derived in Chapter 2 will be modified, by introducing a Boolean variable, to be able to account for the opening/closing of one or more cracks along the bridge. Then, a computational strategy is presented which describes the procedure to calculate the dynamic response of such models, incorporating new terms as “transition instant” and “open cracks distribution” that are explained thoroughly in this chapter.

Furthermore, the computational strategy is verified by comparing the results from MATLAB, where the new analytical expressions were used, with the results from a finite element model in SAP2000. The outcomes of these analyses agree with the existing research in literature and at the same time improve the capabilities of the model because of the nature of the analytical expressions to be able to deal with any type of beam bridge. Finally, as predicting the dynamic response of damages with time-varying properties is now possible, it is calculated and compared with the response coming from the widely adopted always-open crack model and with the undamaged model to draw conclusions about the main differences between crack(s) with time-variant or time-invariant properties and how these affect the damage identification techniques examined in the previous chapter.

All in all, the research sub-questions to be discussed in this chapter, are:

- How to model the switching crack in the Euler-Bernoulli beam?
- How to exploit closed-form solutions of the mode shapes to account for the switching cracks?
- How to evaluate the open cracks distribution at a time instant?
- Are the always-open or always-closed crack distributions the boundaries for the switching crack model?
- What would be the differences in damage identification when using the switching crack model instead of the widely adopted always-open crack model?

4.1 How to model the switching crack in the Euler-Bernoulli beam?

In this part, the way that the switching crack will be incorporated in the governing equations of an Euler-Bernoulli beam, will be discussed.

Consider first the case of a damaged beam, with cracks specified by a vector $\boldsymbol{\Lambda}_i$ with entries $\lambda_{i,j}$ equal to 1 if the jth crack is open, or 0 if the jth crack is closed (undamaged), so that the transversal deflection of the ith beam is indicated with $u(z_i, t, \boldsymbol{\Lambda}_i)$.

Now, the mode superposition method can be applied by considering the mode shapes of the ith beam damaged beam as:

$$u(z_i, t, \boldsymbol{\Lambda}_i) = \sum_{r=1}^{\infty} \Phi_{i,r}(z_i, \boldsymbol{\Lambda}_i) q_{i,r}(t) \qquad \textit{Eq. 116}$$

where $\Phi_{i,r}(z_i, \boldsymbol{\Lambda}_i)$ is the rth mode shape of the ith damaged beam with open cracks specified by the vector $\boldsymbol{\Lambda}_i$ and $q_{i,r}(t)$ is the rth generalized coordinate. Considering a modal truncation:

$$u(z_i, t, \boldsymbol{\Lambda}_i) \cong \sum_{r=1}^{N} \Phi_{i,r}(z_i, \boldsymbol{\Lambda}_i) q_{i,r}(t) \qquad \textit{Eq. 117}$$

Where N is the number of modes which are included in the modal expansion and a sufficient number should be included to minimize the error in the response calculation.

Substituting in the governing equation:

$$\sum_{r=1}^{N} \left[EI(z_i)\Phi''_{i,r}(z_i, \boldsymbol{\Lambda}_i) q_{i,r}(t)\right]'' + \rho_i A_i \sum_{r=1}^{N} \Phi_{i,r}(z_i, \boldsymbol{\Lambda}_i) \ddot{q}_{i,r}(t) = 0 \qquad \textit{Eq. 118}$$

The flexibility model is now modified for switching cracks which considers a crack as open or closed depending on the sign of the elastic axial strain calculated at the crack center and the side where the crack is located. The dimensionless bending flexibility of the beam, is now defined as:

$$\widetilde{EI}(z_i)^{-1} = 1 + \sum_{j=1}^{n} \alpha_{i,j} \lambda_{i,j} \delta(z_i - \bar{z}_{i,j}) \qquad \textit{Eq. 119}$$

where n is the number of cracks, the jth one occurring at the abscissa $\bar{z}_{i,j}$, $\delta(z_i - \bar{z}_{i,j})$ is the Dirac delta function centered at the jth crack position; $\lambda_{i,j}$ is the so-called switching crack variable that is a Boolean variable which takes the values of 1 if the crack is open and 0 if the crack is closed; $\alpha_{i,j}$ is a parameter related to the severity of the damage at $z_i = \bar{z}_{i,j}$.

The transition from open to closed in the static analysis of jointed damaged Euler-Bernoulli beams is expressed as:

$$\lambda_{i,j} = \begin{cases} 0, & \tilde{\varepsilon}_{i,j} \leq 0 \\ 1, & \tilde{\varepsilon}_{i,j} > 0 \end{cases} \qquad \textit{Eq. 120}$$

where $\tilde{\varepsilon}_{i,j}$ is the elastic axial strain at the jth crack of the ith beam (positive if the fibre at the center of the crack is stretching; negative if it is compressing), which is given by:

$$\tilde{\varepsilon}_{i,j} = \frac{N(\bar{z}_{i,j})}{EA_{i,0}} + \frac{M(\bar{z}_{i,j})}{EI_{i,0}} \bar{y}_{i,j} \qquad \textit{Eq. 121}$$

where $N(\bar{z}_{i,j})$ is the axial force at $z_i = \bar{z}_{i,j}$ (which is positive in tension and negative in compression); EA_0 is the axial rigidity (where A_0 is the undamaged cross-sectional area); $M(\bar{z}_{i,j})$ is the bending moment about the neutral axis; $\bar{y}_{i,j}$ is the distance between the neutral axis and the jth crack at the ith beam: When $\bar{y}_{i,j} > 0$, the jth crack occurs at the bottom side of the ith beam and it tends to open when the ith beam is sagging, while the opposite happens when $\bar{y}_{i,j} < 0$. When all $\lambda_{i,j}$ parameters are equal to 0, then an assembly of uncracked Euler-Bernoulli beams is considered and when all the parameters are set to 1, the always open cracks model is considered.

In the absence of axial loading, the elastic axial strain can be written as:

$$\tilde{\varepsilon}_{i,j} = \frac{M(\bar{z}_{i,j})}{EI_{i,0}} \bar{y}_{i,j} \tag{Eq. 122}$$

where $M(\bar{z}_{i,j}) = -EI(z_{i,j})u''(z_{i,j}) = -EI(z_{i,j}) \sum_{r=1}^{N} \Phi''_{i,r}(\bar{z}_{i,j}, \boldsymbol{\Lambda}_i) q_{i,r}(t)$

4.2 How to exploit closed-form solutions of the mode shapes to account for the switching cracks?

In order to produce the closed-form expressions for the mode shapes in the case of the switching crack model, the expressions derived in the first part can be modified including now the Boolean variable $\lambda_{i,j}$.

This means that for the damaged case with the switching crack model the analytical expressions for the mode shapes are given as:

$$\begin{aligned}\widetilde{\Phi}_i(z_i, \boldsymbol{\Lambda}_i) = \frac{1}{2\beta_i} & [\beta_i(C_3 - C_1\beta_i^2)\cos(\beta_i z_i) + \beta_i(C_1\beta_i^2 + C_3)\cosh(\beta_i z_i) + (C_2\beta_i^2 + C_4)\sinh(\beta_i z_i) \\ & + (C_4 - C_2\beta_i^2)\sin(\beta_i z_i)] \\ & + \frac{\beta_i^3}{2}\sum_{j=1}^{n} \alpha_{i,j}\lambda_{i,j}\widetilde{W}_i(\bar{z}_{i,j})[\sinh(\beta_i(z_i - \bar{z}_{i,j})) - \sin(\beta_i(z_i - \bar{z}_{i,j}))]\mathcal{H}(z_i - \bar{z}_{i,j})\end{aligned} \tag{Eq. 123}$$

where,

$$\begin{aligned}\widetilde{W}_i(\bar{z}_{i,j}) = \frac{1}{2\beta_i^3} & [\beta_i(C_1\beta_i^2 - C_3)\cos(\beta_i\bar{z}_{i,j}) + \beta_i(C_1\beta_i^2 + C_3)\cosh(\beta_i\bar{z}_{i,j}) + (C_2\beta_i^2 + C_4)\sinh(\beta_i\bar{z}_{i,j}) \\ & + (C_2\beta_i^2 - C_4)\sin(\beta_i\bar{z}_{i,j})] \\ & + \frac{\beta_i}{2}\sum_{k=1}^{j-1} \alpha_{i,k}\lambda_{i,k}\widetilde{W}_i(\bar{z}_{i,k})[\sinh(\beta_i(\bar{z}_{i,j} - \bar{z}_{i,k})) - \sin(\beta_i(\bar{z}_{i,j} - \bar{z}_{i,k}))]\mathcal{H}(\bar{z}_{i,j} - \bar{z}_{i,k})\end{aligned} \tag{Eq. 124}$$

The same applies for the analytical expressions derived for the unknown integration constants, found by enforcing the continuity conditions at each interface point. The only differences, that indicate the presence of switching cracks and not the always-open cracks, are the functions $\Pi_{i,r}^{(1)}$, $\Pi_{i,r}^{(2)}$, $\Pi_{i,r}^{(3)}$ and $\Pi_{i,r}^{(4)}$, which are now given as:

$$\begin{aligned}\Pi_{i,r}^{(1)} = \frac{1}{2\tilde{\gamma}_{i,r}\delta_{i,r}^4} & \left[\sum_{j=1}^{n_i}\left\{\alpha_{i,j}\lambda_{i,j}\widetilde{W}_i(\bar{z}_{i,j})\beta_i\left[\sinh\left(\beta_i(L_i - \bar{z}_{i,j})\right) - \sin(\beta_i(L_i - \bar{z}_{i,j}))\right]\right\}\right] \\ & - \frac{\beta_{i+1}}{2}\sum_{j=1}^{n_{i+1}}\left\{\alpha_{i+1,j}\lambda_{i+1,j}\widetilde{W}_{i+1}(\bar{z}_{i+1,j})\left[\sinh\left(\beta_{i+1}(\bar{z}_{i+1,j})\right) - \sin(\beta_{i+1}(\bar{z}_{i+1,j}))\right]\right\}\end{aligned} \tag{Eq. 125}$$

$$\Pi_{i,r}^{(2)} = \frac{1}{2\tilde{\gamma}_{i,r}\delta_{i,r}^{4}}\left[\sum_{j=1}^{n_i}\left\{\alpha_{i,j}\lambda_{i,j}\widetilde{W}_i(\bar{z}_{i,j})\beta_i^2\left[cosh\left(\beta_i(L_i - \bar{z}_{i,j})\right) - cos(\beta_i(L_i - \bar{z}_{i,j}))\right]\right\}\right. \\ \left. - \frac{\beta_{i+1}^2}{2}\sum_{j=1}^{n_{i+1}}\left\{\alpha_{i+1,j}\lambda_{i+1,j}\widetilde{W}_{i+1}(\bar{z}_{i+1,j})\left[cosh\left(\beta_{i+1}(\bar{z}_{i+1,j})\right) - cos(\beta_{i+1}(\bar{z}_{i+1,j}))\right]\right\}\right] \quad \text{Eq. 126}$$

$$\Pi_{i,r}^{(3)} = \frac{1}{2}\left[\sum_{j=1}^{n_i}\left\{\alpha_{i,j}\lambda_{i,j}\widetilde{W}_i(\bar{z}_{i,j})\beta_i^3\left[sinh\left(\beta_i(L_i - \bar{z}_{i,j})\right) + sin(\beta_i(L_i - \bar{z}_{i,j}))\right]\right\}\right. \\ \left. - \frac{\beta_{i+1}^3}{2}\sum_{j=1}^{n_{i+1}}\left\{\alpha_{i+1,j}\lambda_{i+1,j}\widetilde{W}_{i+1}(\bar{z}_{i+1,j})\left[sinh\left(\beta_{i+1}(\bar{z}_{i+1,j})\right) + sin(\beta_{i+1}(\bar{z}_{i+1,j}))\right]\right\}\right] \quad \text{Eq. 127}$$

$$\Pi_{i,r}^{(4)} = \frac{1}{2}\left[\sum_{j=1}^{n_i}\left\{\alpha_{i,j}\lambda_{i,j}\widetilde{W}_i(\bar{z}_{i,j})\beta_i^4\left[cosh\left(\beta_i(L_i - \bar{z}_{i,j})\right) + cos(\beta_i(L_i - \bar{z}_{i,j}))\right]\right\}\right. \\ \left. - \frac{\beta_{i+1}^4}{2}\sum_{j=1}^{n_{i+1}}\left\{\alpha_{i+1,j}\lambda_{i+1,j}\widetilde{W}_{i+1}(\bar{z}_{i+1,j})\left[cosh\left(\beta_{i+1}(\bar{z}_{i+1,j})\right) + cos(\beta_{i+1}(\bar{z}_{i+1,j}))\right]\right\}\right] \quad \text{Eq. 128}$$

where n_i and n_{i+1}, are the number of cracks for the ith and $(i+1)$th beam respectively.

4.3 Dynamic response of beam-type bridges with switching cracks under moving vehicle loads

4.3.1 Governing equations

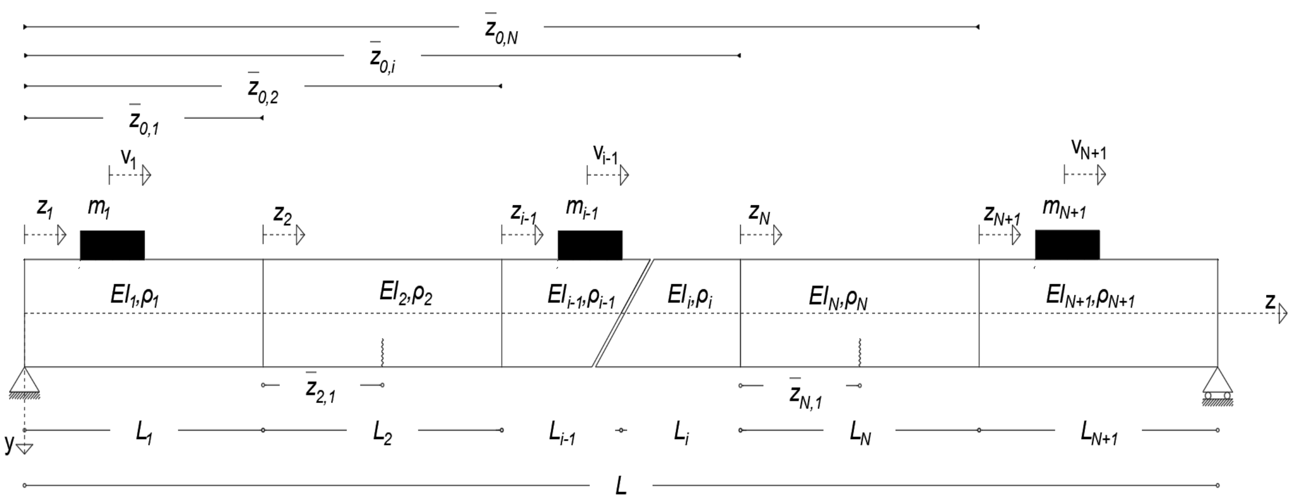

Figure 4. 1: Euler-Bernoulli beam with step changes in material and multiple cracks, subjected to moving vehicle loads modelled as moving masses

Equation of motion for an Euler-Bernoulli beam:

$$\frac{\partial^2}{\partial z_i^2}\left[EI(z_i)\frac{\partial^2 u(z_i,t)}{\partial z_i^2}\right] + \rho_i A_i \frac{\partial^2 u(z_i,t)}{\partial t^2} = F(z_i,t) \quad \text{Eq. 129}$$

where the loading is equal to:

$$F(z_i,t) = m\big(g - a_{i,t}\big)\delta(z_i - vt) \quad \text{Eq. 130}$$

where the Dirac delta function $\delta(z_i - vt)$ accounts for the position of the mass on the ith beam and therefore it specifies the excitation point, mg is a constant force corresponding to the weight of the moving mass, $ma_{i,t}$ is a dynamic force due to the moving mass where $a_{i,t}$ is the transverse acceleration of the moving mass which is given by:

$$a_{i,t} = \left(\frac{\partial^2}{\partial t^2}u(z_i,t) + 2v\frac{\partial^2}{\partial z_i \partial t}u(z_i,t) + v^2\frac{\partial^2}{\partial {z_i}^2}u(z_i,t)\right) \quad \text{Eq. 131}$$

The first term on the right hand side is the vertical component of the acceleration, the second term is the Coriolis acceleration and the last term corresponds to the centripetal acceleration of the moving mass.

The solution was obtained, considering a modal truncation, as:

$$u(z_i,t,\boldsymbol{\Lambda}_i) \cong \sum_{r=1}^{N} \Phi_{i,r}(z_i,\boldsymbol{\Lambda}_i)q_{i,r}(t) \quad \text{Eq. 132}$$

where the deflection of the beam is given as a linear combination of time-dependent modal amplitudes and spatially-dependent mode shapes. The mode shapes calculated above were found considering an assembly of undamped beams, ignoring the presence of the moving object, since its mass is usually much lower than that of the beam. If that was not the case, it would result to time-dependent mode shapes varying as the mass position is changing and therefore not allowing the application of the mode superposition method.

Substituting the solution in the governing equation we obtain:

$$\sum_{r=1}^{N}\left[EI(z_i)\Phi_{i,r}''(z_i,\boldsymbol{\Lambda}_i)q_{i,r}(t)\right]''+\rho_iA_i\sum_{r=1}^{N}\Phi_{i,r}(z_i,\boldsymbol{\Lambda}_i)\ddot{q}_{i,r}(t)=F(z_i,t) \qquad \text{Eq. } 133$$

where the loading term is rewritten as:

$$F(z_i,t)=m\left[g-\sum_{r=1}^{N}\Phi_{i,r}(z_i,\boldsymbol{\Lambda}_i)\ddot{q}_{i,r}(t)-v^2\sum_{r=1}^{N}\Phi_{i,r}''(z_i,\boldsymbol{\Lambda}_i)q_{i,r}(t)-2v\sum_{r=1}^{N}\Phi_{i,r}'(z_i,\boldsymbol{\Lambda}_i)\dot{q}_{i,r}(t)\right]\delta(z_i-vt) \qquad \text{Eq. } 134$$

Next step will be multiplying each term with $\Phi_{i,s}(z_i,\boldsymbol{\Lambda}_i)$ and integrating along the length of the ith beam:

$$\sum_{r=1}^{N}\int_0^{L_i}\Phi_{i,s}(z_i,\boldsymbol{\Lambda}_i)\left[EI(z_i)\Phi_{i,r}''(z_i,\boldsymbol{\Lambda}_i)q_{i,r}(t)\right]''dz_i+\rho_iA_i\sum_{r=1}^{N}\int_0^{L_i}\Phi_{i,s}(z_i,\boldsymbol{\Lambda}_i)\Phi_{i,r}(z_i,\boldsymbol{\Lambda}_i)\ddot{q}_{i,r}(t)dz_i$$
$$=\int_0^{L_i}\Phi_{i,s}(z_i,\boldsymbol{\Lambda}_i)F(z_i,t)dz_i \qquad \text{Eq. } 135$$

As the mode shape between two successive cracks can be described as that of the undamaged beam, the mode shape of a damaged beam can be considered as a superposition of the mode shapes of undamaged beams. Meaning, the orthogonality properties of the damaged beam mode shapes with respect to the mass and the stiffness hold, so that:

$$\rho_iA_i\int_0^{L_i}\Phi_{i,s}(z_i,\boldsymbol{\Lambda}_i)\Phi_{i,r}(z_i,\boldsymbol{\Lambda}_i)dz_i=\boldsymbol{M}_{i,r}\delta_{rs} \qquad \text{Eq. } 136$$

$$\int_0^{L_i}\Phi_{i,s}(z_i,\boldsymbol{\Lambda}_i)\left[EI(z_i)\Phi_{i,r}''(z_i,\boldsymbol{\Lambda}_i)\right]''dz_i=\boldsymbol{K}_{i,r}\delta_{rs} \qquad \text{Eq. } 137$$

where δ_{rs} is the Kronecker delta which is defined as:

$$\delta_{rs}=\begin{cases}0, & if\ r\neq s\\ 1, & if\ r=s\end{cases} \qquad \text{Eq. } 138$$

and $\boldsymbol{M}_{i,r}$, $\boldsymbol{K}_{i,r}$ are respectively the modal mass and stiffness of the ith damaged beam and its rth damaged beam mode. These matrices are related as:

$$\boldsymbol{K}_{i,r}=\omega_{i,r}^2\boldsymbol{M}_{i,r} \qquad \text{Eq. } 139$$

where $\omega_{i,r}$ is the rth natural frequency of the ith damaged beam. After calculations we obtain for the rth beam mode of each ith damaged beam :

$$\ddot{q}_{i,r}(t)+\omega_{i,r}^2q_{i,r}(t)=\frac{1}{M_{i,r}}\int_0^{L_i}\Phi_{i,s}(z_i,\boldsymbol{\Lambda}_i)F(z_i,t)dz_i \qquad \text{Eq. } 140$$

which represents a set of coupled second order differential equations.

Considering a jointed EB beam with step changes in flexural stiffness, cross-section and density, these variations could be expressed with the generalized functions:

$$EI(z) = EI_1(z) + \sum_{r=2}^{N+1} \left[EI_i\left(z - \bar{z}_{0,i-1}\right) - EI_{i-1}\left(z - \bar{z}_{0,i-2}\right) \right] H\left(z - \bar{z}_{0,i-1}\right) \quad \text{Eq. 141}$$

$$A(z) = A_1(z) + \sum_{r=2}^{N+1} \left[A_i\left(z - \bar{z}_{0,i-1}\right) - A_{i-1}\left(z - \bar{z}_{0,i-2}\right) \right] H\left(z - \bar{z}_{0,i-1}\right) \quad \text{Eq. 142}$$

$$\rho(z) = \rho_1(z) + \sum_{r=2}^{N+1} \left[\rho_i\left(z - \bar{z}_{0,i-1}\right) - \rho_{i-1}\left(z - \bar{z}_{0,i-2}\right) \right] H\left(z - \bar{z}_{0,i-1}\right) \quad \text{Eq. 143}$$

These formulas are expressed the same way as the time-dependent deflection of the jointed beam $W(z,t)$ and the rth mode shape $\widetilde{\Phi}_r(z)$. Moreover, because of expressing each of the 4 constants and frequency parameters of the mode shape of each ith beam as a function of the preceding beam by explicitly enforcing the continuity conditions at each interface, the mode shape of the entire jointed EB beam depends only on 4 constants. Lastly, each frequency parameter $\beta_{i,r}$ will be expressed as a function of the natural frequencies ω_r of the entire EB beam.

Consequently, all the expressions above as well as the orthogonality properties hold and the subscript i can be disregarded, like:

$$\ddot{q}_r(t) + \omega_r^2 q_r(t) = \frac{1}{M_r} \int_0^L \Phi_s(z, \boldsymbol{\Lambda}) F(z,t) dz \quad \text{Eq. 144}$$

and of course the solution is given as:

$$u(z,t,\boldsymbol{\Lambda}) \cong \sum_{r=1}^{N} \Phi_r(z,\boldsymbol{\Lambda}) q_r(t) \quad \text{Eq. 145}$$

where the right hand side can be obtained using the Dirac delta properties with the following expressions:

$$\begin{aligned} &\frac{1}{M_r} \int_0^L \Phi_s(z,\boldsymbol{\Lambda}) F(z,t) dz = \\ &= \frac{m}{M_r} \Phi_s(vt,\boldsymbol{\Lambda}) \left[g - \sum_{r=1}^{N} \Phi_r(vt,\boldsymbol{\Lambda}) \ddot{q}_r(t) - v^2 \sum_{r=1}^{N} \Phi_r''(vt,\boldsymbol{\Lambda}) q_r(t) \right. \\ &\left. - 2v \sum_{r=1}^{N} \Phi_r'(vt,\boldsymbol{\Lambda}) \dot{q}_r(t) \right] \end{aligned} \quad \text{Eq. 146}$$

Re-arranging the terms, the governing equations of motion can written as:

$$\widehat{\boldsymbol{M}}(t)\ddot{\boldsymbol{q}}(t) + \widehat{\boldsymbol{D}}(t)\dot{\boldsymbol{q}}(t) + \widehat{\boldsymbol{K}}(t)\boldsymbol{q}(t) = \widehat{\boldsymbol{F}}(t) \quad \text{Eq. 147}$$

where $q(t)$ is a N-dimensional array collecting the $q_r(t)$, while the modal mass $\widehat{\boldsymbol{M}}(t)$, damping $\widehat{\boldsymbol{D}}(t)$ and stiffness $\widehat{\boldsymbol{K}}(t)$ matrices are given by a constant term, arising from the beam plus a time-varying term due to the moving mass, as:

$$\widehat{\boldsymbol{M}}(t) = \overline{\boldsymbol{M}} + \Delta\boldsymbol{M}(t) \quad \text{Eq. 148}$$

$$\widehat{\boldsymbol{D}}(t) = \overline{\boldsymbol{D}} + \Delta\boldsymbol{D}(t) \quad \text{Eq. 149}$$

$$\widehat{\boldsymbol{K}}(t) = \overline{\boldsymbol{K}} + \Delta\boldsymbol{K}(t)$$ *Eq. 150*

It can be easily shown that each entry of $\widehat{\boldsymbol{M}}(t)$, $\widehat{\boldsymbol{D}}(t)$ and $\widehat{\boldsymbol{K}}(t)$ matrices is given by:

$$\left|\widehat{\boldsymbol{M}}(t)\right|_{rs} = \delta_{rs} + \frac{m}{M_r}\Phi_s(vt,\boldsymbol{\Lambda})\Phi_r(vt,\boldsymbol{\Lambda})$$ *Eq. 151*

$$\left|\widehat{\boldsymbol{D}}(t)\right|_{rs} = 0 + \frac{2vm}{M_r}\Phi_s{}'(vt,\boldsymbol{\Lambda})\Phi_r(vt,\boldsymbol{\Lambda})$$ *Eq. 152*

$$\left|\widehat{\boldsymbol{K}}(t)\right|_{rs} = \omega_r^2\delta_{rs} + \frac{v^2 m}{M_r}\Phi_s{}''(vt,\boldsymbol{\Lambda})\Phi_r(vt,\boldsymbol{\Lambda})$$ *Eq. 153*

and for the time-varying force vector

$$\left|\widehat{\boldsymbol{F}}(t)\right|_{r} = \frac{mg}{M_r}\Phi_r(vt,\boldsymbol{\Lambda})$$ *Eq. 154*

Finally the equation of motion of the rth mode is given by:

$$\left[1 + \frac{m}{M_r}\Phi_r(vt,\boldsymbol{\Lambda})\Phi_r(vt,\boldsymbol{\Lambda})\right]\ddot{q}_r(t) + \frac{2vm}{M_r}\Phi_r{}'(vt,\boldsymbol{\Lambda})\Phi_r(vt,\boldsymbol{\Lambda})\dot{q}(t) + \\ + \left[\omega_r^2 + \frac{v^2 m}{M_r}\Phi_r{}''(vt,\boldsymbol{\Lambda})\Phi_r(vt,\boldsymbol{\Lambda})\right]q_r(t) = \frac{mg}{M_r}\Phi_r(vt,\boldsymbol{\Lambda})$$ *Eq. 155*

Considering the equation of motion, the situation of $\left|\widehat{\boldsymbol{M}}(t)\right|_{rs} = \delta_{rs}$, $\left|\widehat{\boldsymbol{D}}(t)\right|_{rs} = 0$, $\left|\widehat{\boldsymbol{K}}(t)\right|_{rs} = \omega_r^2\delta_{rs}$ and $\boldsymbol{\Lambda} = \boldsymbol{0}$, then the governing equation of an undamaged beam under a moving force is recovered, while if $\boldsymbol{\Lambda} = \boldsymbol{1}$, then the governing equation of a multi-cracked beam under a moving force is recovered.

The problem can also be generalized by considering the effects of p moving masses each with constant velocity v_j starting from the abscissa z_{m_j}, being $j = 1..p$. The mass that takes longer to get to the end of the beam is mass 1, and this mass defines the duration of the transient analysis $t_f = (L - z_{m_1})/v_1$. In this case:

$$\left|\widehat{\boldsymbol{M}}(t)\right|_{rs} = \delta_{rs} + \sum_{j=1}^{p}\frac{m_j}{M_r}\Phi_s\left(z_{m_j} + v_j t,\boldsymbol{\Lambda}\right)\Phi_r\left(z_{m_j} + v_j t,\boldsymbol{\Lambda}\right)U\left[1 - \left(z_{m_j} + v_j t\right)\right]$$ *Eq. 156*

$$\left|\widehat{\boldsymbol{D}}(t)\right|_{rs} = 0 + \sum_{j=1}^{p}\frac{2v_j m_j}{M_r}\Phi_s{}'\left(z_{m_j} + v_j t,\boldsymbol{\Lambda}\right)\Phi_r\left(z_{m_j} + v_j t,\boldsymbol{\Lambda}\right)U\left[1 - \left(z_{m_j} + v_j t\right)\right]$$ *Eq. 157*

$$\left|\widehat{\boldsymbol{K}}(t)\right|_{rs} = \omega_r^2\delta_{rs} + \sum_{j=1}^{p}\frac{v_j^2 m_j}{M_r}\Phi_s{}''\left(z_{m_j} + v_j t,\boldsymbol{\Lambda}\right)\Phi_r\left(z_{m_j} + v_j t,\boldsymbol{\Lambda}\right)U\left[1 - \left(z_{m_j} + v_j t\right)\right]$$ *Eq. 158*

$$\left|\widehat{\boldsymbol{F}}(t)\right|_{r} = \sum_{j=1}^{p}\frac{m_j g}{M_r}\Phi_r\left(z_{m_j} + v_j t,\boldsymbol{\Lambda}\right)U\left[1 - \left(z_{m_j} + v_j t\right)\right]$$ *Eq. 159*

where U$\left[1 - \left(z_{m_j} + v_j t\right)\right]$ is the Unit Step function that switches off the contribution of the moving masses that reach the end of the beam. Specifically, the U$\left[1 - \left(z_{m_j} + v_j t\right)\right]$ is equal to 1 when $\left(z_{m_j} + v_j t\right) \leq 1$, zero otherwise.

4.3.2 How to evaluate the open cracks distribution at a time instant?

In this part it will be explained how to deal with cracks with time-variant parameters, meaning how to be able to evaluate at any time instant if the crack will be open or closed so that the corresponding analytical expression of the mode shapes for the Damaged or the Undamaged case will be considered in the analysis. To answer this question, two terms should be explained, which are the "cracks distribution" and the "transition instant".

In order to exploit closed-form solutions of the mode shapes to account for the switching cracks, a vector $\boldsymbol{\Lambda}_i$ with entries $\lambda_{i,j}$ equal to 1 if the jth crack is open (damaged), or 0 if the jth crack is closed (undamaged) was added to the analytical expressions for each one of the beam segments of the bridge. If all the cracks are considered as always open during the passage of the moving vehicles, the open crack distribution specified inside the vector $\boldsymbol{\Lambda}$ is not changing. In the case of cracks with time-variant parameters, depending on the axial strain of the beam at the location of the damage, this vector can change at every possible time-step of the analysis causing the opening/closing of one or more cracks. This means, that for every time-step of the analysis, using an unconditionally stable integration scheme, the vector $\boldsymbol{\Lambda}(t)$ is apparently time-dependent and describes a unique crack distribution, meaning a set of entries $\lambda_{i,j}$ with values 0 or 1, specifying the condition of each one of the cracks (open or closed).

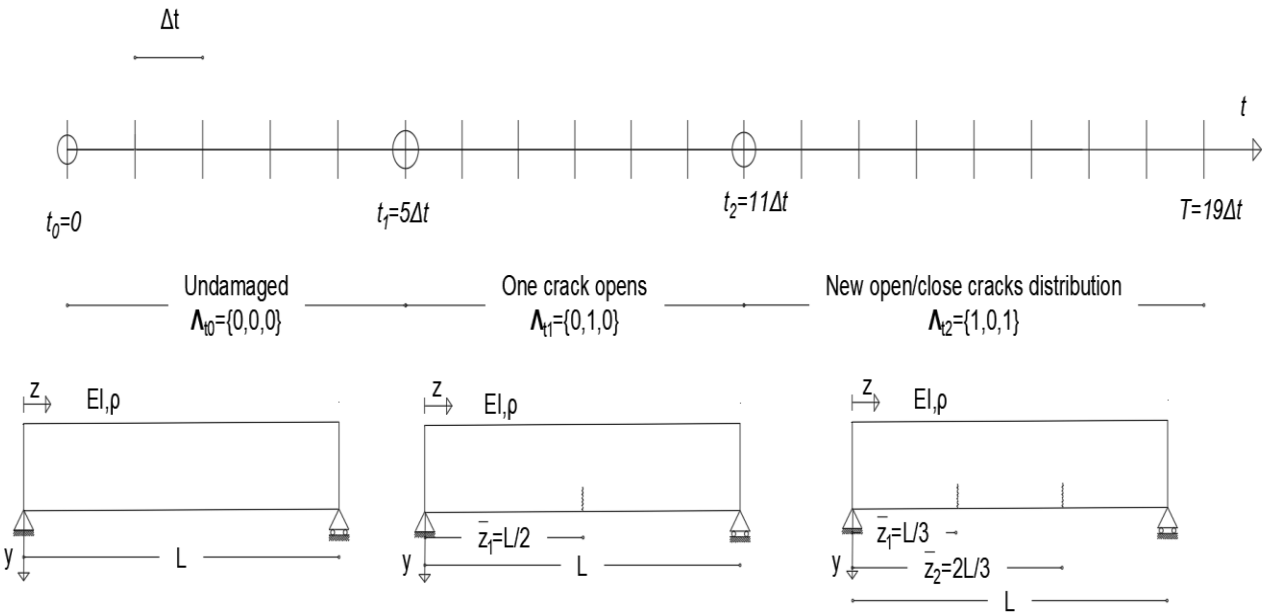

Figure 4. 2: Example of variation of cracks distribution of a beam with three switching cracks over time

As an example, in figure [4.2] the variation of cracks distribution of a beam with three switching cracks is shown. Consider the flexural vibration of the Euler-Bernoulli beam, subject to moving vehicles from time $t_0 = 0$ to $T = 19\Delta t$. Because of the effect of the moving vehicles, the damaged beam will start vibrating transversally and the induced deformed shape at each time step may produce the opening/closing of each of the 3-cracks acting along the beam. There will be a set of time intervals Δt_j which begin at the time instant t_j during which the open cracks distribution is unchanged. The cracks distribution associated with a particular time interval is then described by a vector $\boldsymbol{\Lambda}_{\Delta t_j} = \boldsymbol{\Lambda}(t_j)$. Once a change in cracks distribution is observed a new vector $\boldsymbol{\Lambda}_{\Delta t_{j+1}}$ is computed.

Back to the example in figure [4.2], initially ($t_0 = 0$) all the crack are closed . The time window is subdivided into 19 constant subintervals Δt. At this time window, three transition instants and therefore three time intervals with fixed cracks distribution were obtained, $\boldsymbol{\Lambda}_{t0}$, ,$\boldsymbol{\Lambda}_{t1}$ and $\boldsymbol{\Lambda}_{t2}$. The first transition instant t_0

corresponds to the undamaged case, while t_1 and t_2 are characterized by 1 open crack and 2 open cracks, respectively. Specifically, at $t_1 = 5\Delta t$ the opening of a crack at the midpoint ($\bar{z}_1 = L/2$) occurs, where the $\boldsymbol{\Lambda}_{t1} - \boldsymbol{\Lambda}_{t0} \neq \mathbf{0}$ and that is exactly the reason it is called a transition instant. It means that when the transition instant occurs, the current linear analysis has to be stopped and a new transient analysis with a $\boldsymbol{\Lambda}_{t1}$ cracks distribution has to be considered. *That is why the problem can be considered as a sequence of linear transient analysis, each of which is characterized by a specific open cracks distribution.* The same applies for the transition instant $t_2 = 11\Delta t$ where the closing of the crack at the midpoint and the opening of two cracks at $\bar{z}_1 = L/3$ and $\bar{z}_2 = 2L/3$ occur. Of course, $\boldsymbol{\Lambda}_{t2} - \boldsymbol{\Lambda}_{t1} \neq \mathbf{0}$, and a new cracks distribution ($\boldsymbol{\Lambda}_{t2}$) has to be considered.

As a new transient analysis might begin at different time steps, it requires continuity conditions to be enforced. At each transition instant t_j, two continuity conditions have to be enforced in terms of displacement and velocity response with the cracks distribution before ($\boldsymbol{\Lambda}_{\Delta t_j}$) and at the transition instant ($\boldsymbol{\Lambda}_{\Delta t_{j+1}}$) :

$$u\left(z, t_j, \boldsymbol{\Lambda}_{\Delta t_j}\right) = u\left(z, t_j, \boldsymbol{\Lambda}_{\Delta t_{j+1}}\right) \quad \textit{Eq. 160}$$

$$\dot{u}\left(z, t_j, \boldsymbol{\Lambda}_{\Delta t_j}\right) = \dot{u}\left(z, t_j, \boldsymbol{\Lambda}_{\Delta t_{j+1}}\right) \quad \textit{Eq. 161}$$

These continuity conditions can be used to evaluate the initial conditions for a new linear transient analysis with fixed cracks distributions.

4.3.3 Are the always-open or always-closed cracks distributions the boundaries for the switching crack model?

In this part, the transient analysis of damaged Euler-Bernoulli beams with switching cracks subject to moving vehicles will be performed in order to understand if the always-open or always-closed cracks distribution are the boundaries of this model. It is really important to actually observe the differences of the switching crack model with the well-known damaged model of always open cracks, to be also able to use identification techniques for time-variant damages.

4.3.3.1 Numerical application (4.1) – One switching crack located at the midpoint:

This numerical application concerns the same model described in the paper [21], a simple-supported beam with one crack at the midpoint and at the bottom side of the beam, subject to a moving mass acting on top, in order to verify the computational strategy followed in this thesis project using the unconditionally stable Newmark integration instead of the unconditionally stable step-by-step numerical scheme based on the use of the transition matrix, that was used in the paper.

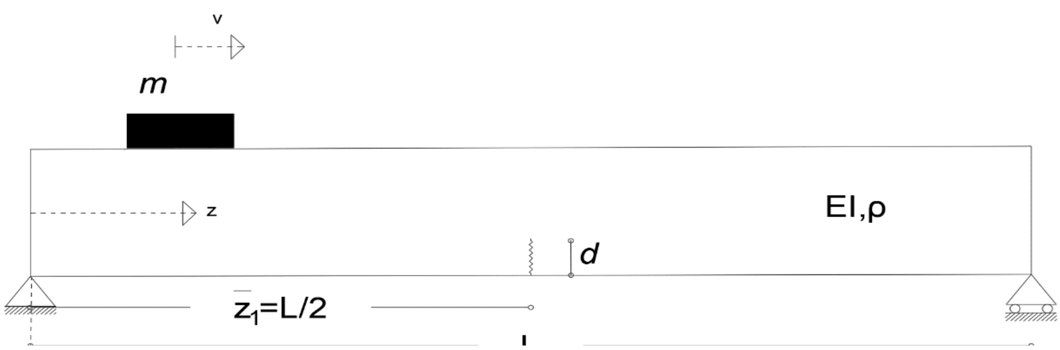

Figure 4. 3: Numerical application (4.1) - Model definition

Table 4. 1: Numerical application (4.1) - Properties of the Beam

Properties	Length - *L* (m)	Density - *ρ* [kg/m^3]	Cross-sectional area – A (m^2)	Young's modulus - *E* (GPa)	Second moment of inertia – *I* (m^4)
Beam	20	7800	0.04	206	1.33*10^{-4}

Table 4. 2: Numerical application (4.1) - Properties of the moving mass

Properties	Mass -*m* (kg)	Speed – *v* (m/s)
Moving mass	1000	5

Table 4. 3: Numerical application (4.1) - Properties of the crack

Properties	Location - $\bar{z}_1$ (m)	Depth *d* (m)	Equivalent stiffness - *K* (kN/m)	Damage parameter – *α* (m^{-1})
Crack	10	0.15	8240	3.33

The computational strategy followed for the transient analysis of damaged slender beams with switching cracks subject to moving masses requires the following steps (also mention in [21]):

1. At $t_0 = 0$ all the cracks can be assumed to be closed or alternatively an initial crack distribution can be assigned, $\boldsymbol{\Lambda}_{t0}$.
2. If the undamaged crack distribution is considered so that $\boldsymbol{\Lambda}_{t0} = \mathbf{0}$, then the analytical expressions for the mode shapes and the corresponding natural frequencies of the undamaged beam are computed. The response of the undamaged beam subject to moving masses is then calculated. Alternatively, the mode shapes and corresponding natural frequencies are calculated using the expressions of the damaged beam.
3. The strain $\tilde{\varepsilon}_{i,j}$ at the center of the jth crack is computed and the Boolean variable $\lambda_{i,j}(t)$ is determined for each time step of the analysis (starting from t_0~~$\lambda_{i,j}($~~) and listed in the array that specified the open/closed status of the n cracks.
4. The first transition instant t_1 occurs when $\boldsymbol{\Lambda}_t \neq \boldsymbol{\Lambda}_{t0}$ and the transient linear analysis has to be stopped.
5. A new mode shape basis is calculated with $\boldsymbol{\Lambda}_{t1}$, and the continuity conditions at the transition instant t_1 are enforced to produce a new set of initial conditions for the second transient linear analysis.
6. The second linear analysis with fixed mode shape basis with $\boldsymbol{\Lambda}_{t1}$ is performed in the next time interval. The response of the damaged beam will be calculated using the mode shapes given by the expressions for the damaged case.
7. The strain $\tilde{\varepsilon}_{i,j}$ at the center of the jth crack is computed again and the Boolean variable $\lambda_{i,j}(t)$ is determined for each time step of the analysis (starting from t_1~~$\lambda_{i,j}($~~)
8. t_2 occurs when $\boldsymbol{\Lambda}_t \neq \boldsymbol{\Lambda}_{t1}$
9. A new transient analysis has to be performed by considering the new mode shape basis with $\boldsymbol{\Lambda}_{t2}$ and new initial conditions
10. Steps 7, 8 and 9 are repeated until the last moving mass reached the end point of the damaged beam

These steps will be followed in this numerical application to produce the dynamic response of the damaged beam. Moreover, the same model will be designed in SAP2000 in order to verify the computational strategy followed in this thesis project with the Finite Element Method with SAP2000. This will happen, examining the always open crack model, as there is a limitation on using SAP2000 for damages with time-variant parameters like the switching crack model. The crack was modelled in SAP2000 by applying a release partial fixity at the crack's location.

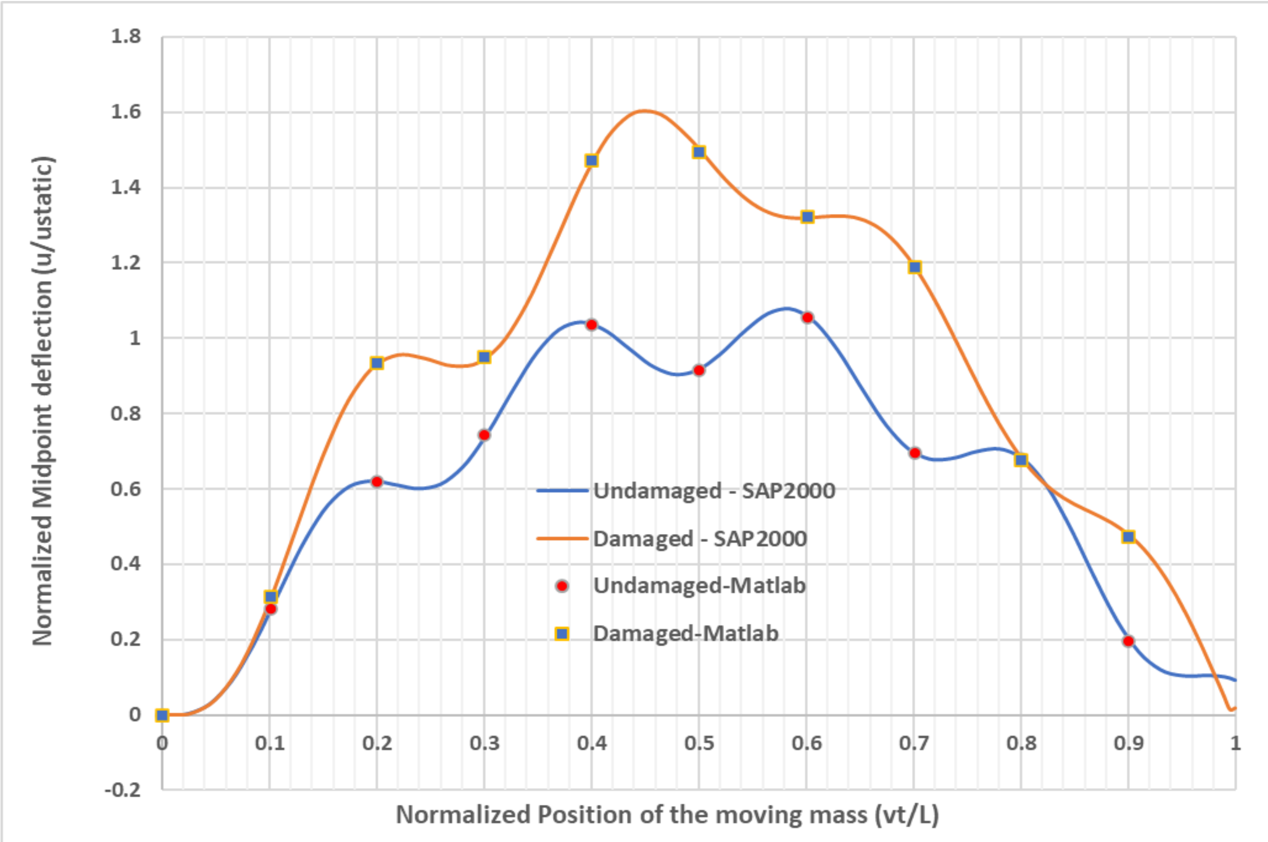

Figure 4. 4: Numerical application (4.1) - Dimensionless transverse deflection versus Normalized position of the moving mass – Comparing results from MATLAB and SAP2000 for the undamaged and always-open crack model

The results in figure [4.4] are expressed in terms of the ratio of the dynamic deflection at the midpoint to the static deflection due to the mass acting on the midpoint, $u/u_{static,max}$, versus the normalized position of the moving mass, vt/L. The static deflection at the midpoint of simply supported beam loaded by the weight of the mass is given by $(\rho A_0 L^3)/(48EI_0)$, where A_0 is the undamaged cross-sectional area and EI_0 is the reference value of the flexural stiffness with I being the second moment of inertia.

It looks like the results coming from the proposed approach, using the unconditionally stable Newmark integration scheme, and the values coming from SAP2000 show a perfect agreement. This means that the proposed expressions could accurately produce the dynamic response of a damaged beam subject to a moving mass, as it was verified using a detailed model with the Finite Element Method. For the analysis, the time variable has been subdivided in 700 time intervals, each of duration 0.0057 sec.

In the same figure, the results obtained for the always open crack are compared to the undamaged results, indicating that the presence of a single crack produces larger amplitudes. In particular, the maximum dimensionless deflection has increased from 1.075 (undamaged) to 1.603 (always open crack).

Moreover, the values coming from the analytical expressions for the eigenfrequencies were also validated in SAP2000. The first four natural frequencies are equal to:

Table 4. 4: Numerical application (4.1) - Eigenfrequencies Undamaged and Damaged case

Eigenfrequencies	Undamaged (rad/sec)	Damaged (rad/sec)
1	7.32	6.34
2	29.28	29.28
3	65.89	58.71
4	117.135	117.135

As expected, only the first and the third natural frequencies are affected by the crack. The second and the fourth mode shapes have a nodal point at the center of the beam, as it has been already mentioned before, where the crack is located, so they remain unchanged.

Next step will be to deal with the switching crack model, to compare with the results coming from the always open or closed crack. The crack will be considered closed at t_0 and then for each time step of the analysis its open/close status will be tested. Moreover, both top and bottom locations are considered.

In figure [4.5] the dynamic response of the damaged case when considering the switching crack located at the top side is plotted. It is observed that the plot of the switching crack model coincide with the plot of the undamaged case. This happens because of the two transition instants t_1 and t_2 found during the analysis. At the transition instant t_1 the crack opens and at the transition instant t_2 the crack closes again, meaning that for the rest of the analysis where the mass is moving on top of the beam, the crack remains closed and the analytical expressions of the undamaged case are used. That is the reason the graph coincide with the one of the always-closed crack.

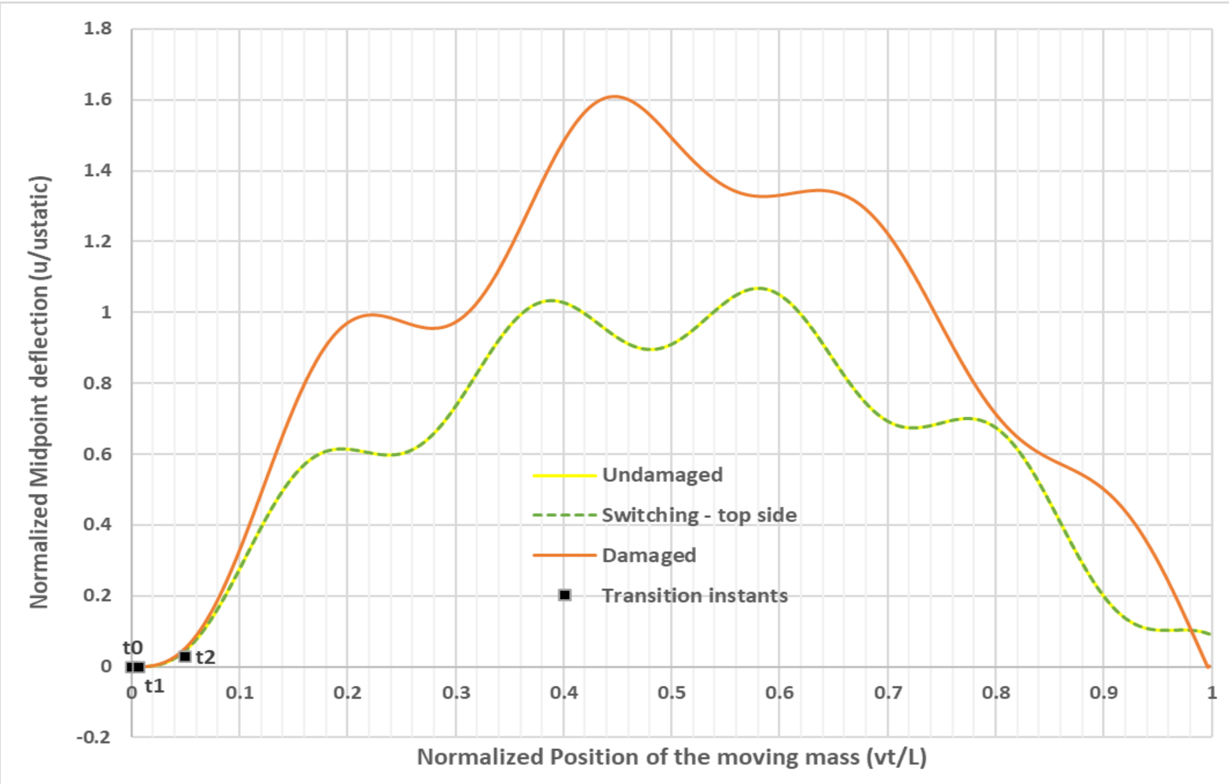

Figure 4. 5: Numerical application (4.1) - Dimensionless transverse deflection versus Normalized position of the moving mass – Comparing results from MATLAB and SAP2000 for the undamaged and always-open crack model and the switching crack located at the top side of the beam

This means that for the case under investigation (crack at the top side of the beam), employing the always open crack model would largely overestimate the transversal vibration.

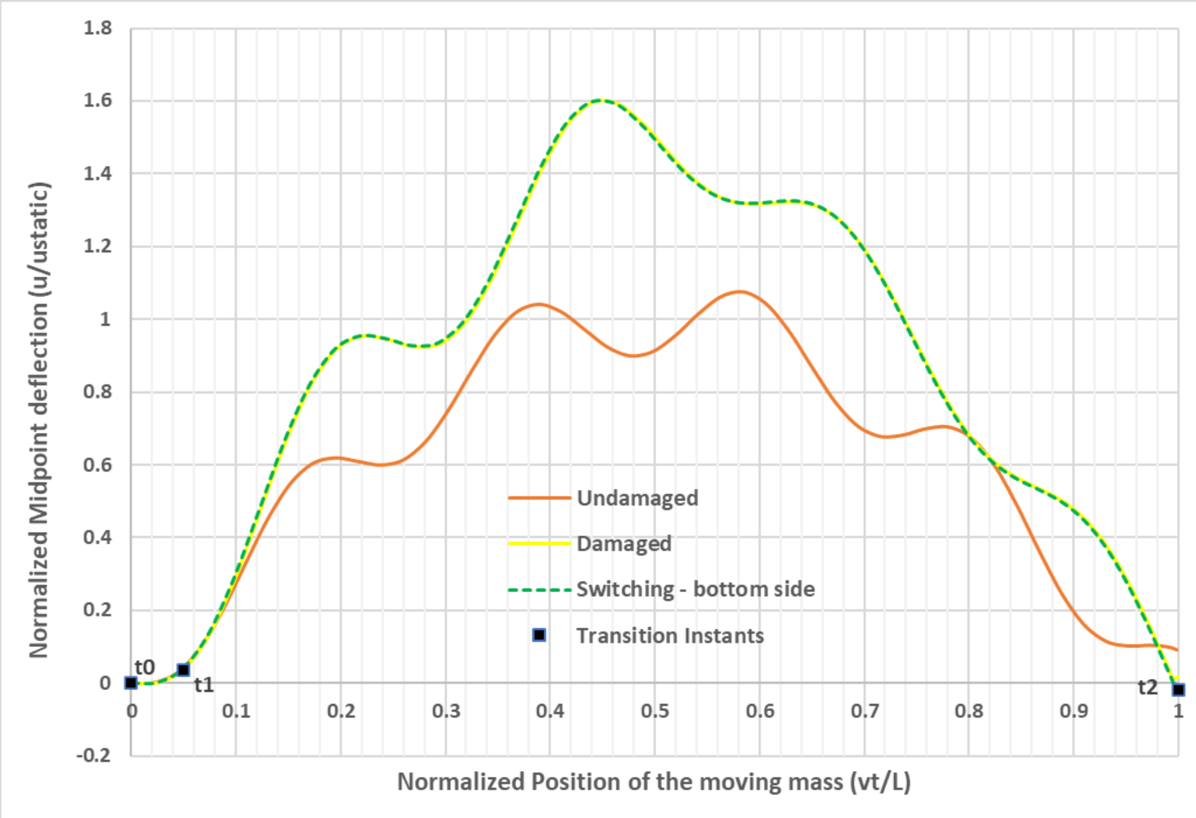

Figure 4. 6: Numerical application (4.1) - Dimensionless transverse deflection versus Normalized position of the moving mass – Comparing results from MATLAB and SAP2000 for the undamaged and always-open crack model and the switching crack located at the bottom side of the beam

In figure [4.6], the dynamic response of the damaged case where the switching crack is located at the bottom side of the beam is plotted, and this time it coincides with the one of the always-open crack. This happens because the transition instants even if they are again two, they occur at different time steps, and the crack remains open for a longer time interval (almost during the whole analysis) leading to a transverse deflection conforming with the one obtained if the crack is considered always opened.

It can be concluded, as stated in [21] that for this case of a simply-supported damaged beam: (i) The crack produces larger deflections, (ii) the side where the crack is located significantly affects the response and (iii) the open crack and undamaged solutions provide, respectively, the upper and lower bounds of the transversal vibration.

It is, indeed, really interesting to also examine the case of multiple cracks present along the beam or multiple masses acting on top of the beam or what changes if flexible boundary conditions are considered, but all of these cases are already presented in [21]. The main conclusions of this research were that:

- The always open crack assumption, widely adopted for many engineering applications, may overestimate or underestimate the transverse response of a damaged beam with switching cracks under moving masses. Therefore it cannot be used as an upper bound on the results yielded by the switching crack model under multiple moving masses

- Including elastic constraints can yield significantly different results compared to the widely adopted simply-supported beam model under a moving mass
- The side where the crack is located can largely affect the response of the damaged beam under moving masses
- The response of a beam with switching cracks under moving masses is not always bounded by the always-open crack model and by the undamaged case; this can be caused by the effect of multiple masses or by the presence of multiple cracks

Moreover, what will be accomplished in this thesis project that has not been presented, is to derive the dynamic response of a damaged beam with switching cracks subject to moving masses, when the complexity of the beam is increased. Actually, the concept of three different beam segment with different properties will again be used in this part. The reason that this will be possible are the new analytical expressions for the mode shapes derived in the first part of this project, aiming to be able to deal with any number of step changes in material along the beam.

4.3.3.2 Numerical application (4.2) – Step changes in material – Switching crack at the midpoint:

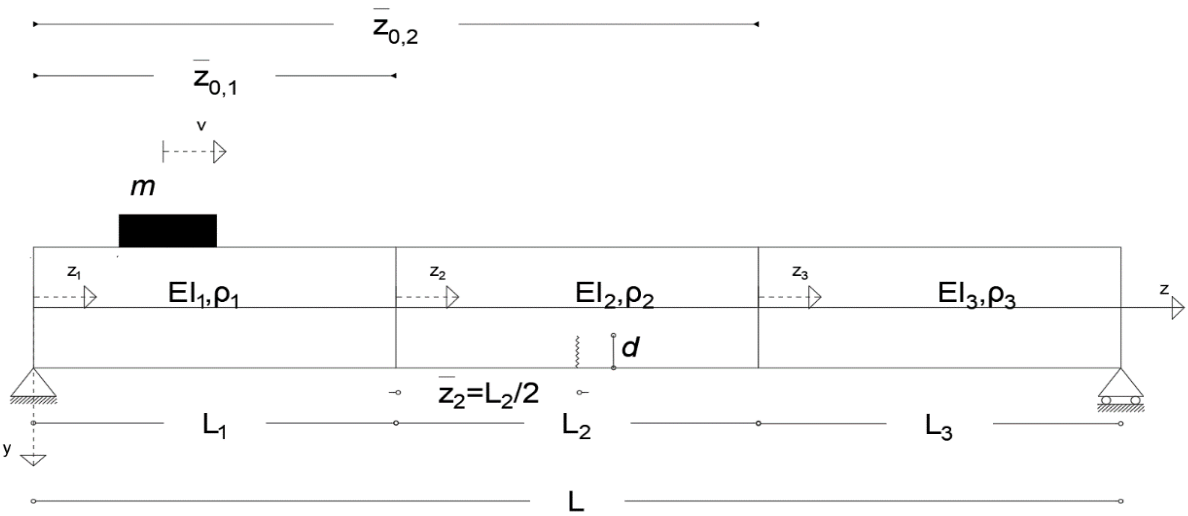

Figure 4. 7: Numerical application (4.2) – Model definition

Table 4. 5: Numerical application (4.2) - Properties of the beams

Properties	*Beam 1*	*Beam 2*	*Beam 3*
Length [m]	10	10	10
Density [kg/m^3]	7800	7400	7000
Young's modulus [kN/m^2]	2.10x10^8	2.00x10^8	1.90x10^8

Table 4. 6: Numerical application (4.2) - Properties of the moving mass

Properties	Mass -*m* (kg)	Speed – *v* (m/s)
Moving mass	1000	5

Table 4. 7: Numerical application (4.2) - Properties of the crack

Properties	Location - $\bar{z}_2$ (m)	Depth *d* (m)	Equivalent stiffness - *K* (kN/m)	Damage parameter – α (m^{-1})
Crack	5	0.15	8000	3.33

A simple-supported beam-type bridge is considered with three different beam segments with different properties. One crack is located at the midpoint and one mass is acting on top of the bridge. In figure [4.8] the results coming from MATLAB using the analytical expressions for the always open crack model and the undamaged case and the results coming from SAP2000 from a detailed model solved with the finite element method, seems to be in perfect agreement. Again, as expected, one singe crack is enough to cause quite larger deflections than the undamaged case.

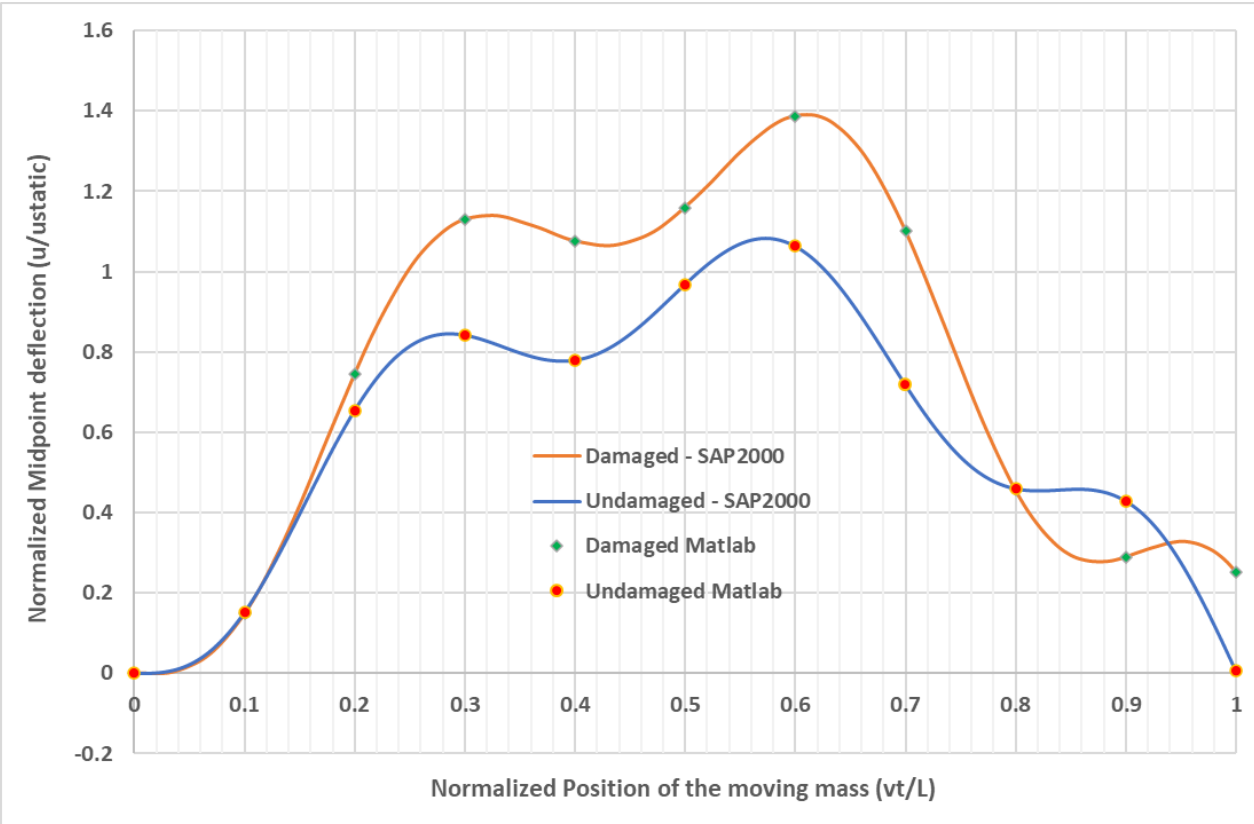

Figure 4. 8: Numerical application (4.2) - Dimensionless transverse deflection versus Normalized position of the moving mass – Comparing results from MATLAB and SAP2000 for the undamaged and always-open crack model

Following now the same computational strategy for solving problems with the switching crack model, the results from both top and bottom location of the crack are considered. The graphs are again expressed in terms of the ratio of the dynamic deflection at the midpoint to the static deflection due to the mass acting on the midpoint, $u/u_{static,max}$, versus the normalized position of the moving mass, vt/L.

In figure [4.8] the case of the crack located at the top side of the beam is considered. As happened with the previous numerical application the plot of the switching crack model coincide with the plot of the undamaged case. In this case there is no transition instant observed, meaning that the crack remains closed for the whole analysis, because of the higher value of bending rigidity EI in the first beam segment.

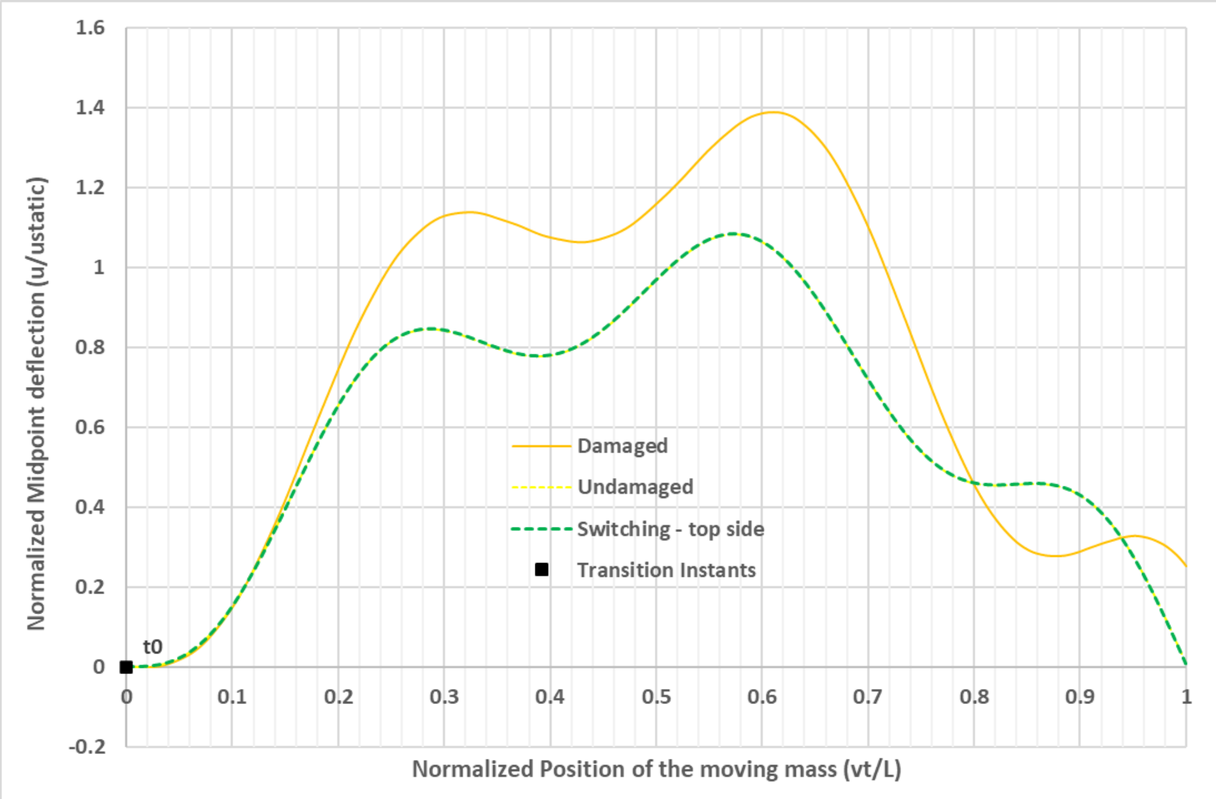

Figure 4. 10: Numerical application (4.2) - Dimensionless transverse deflection versus Normalized position of the moving mass – Comparing results from MATLAB and SAP2000 for the undamaged and always-open crack model and the switching crack located at the top side of the beam

Figure 4. 9: Numerical application (4.2) - Dimensionless transverse deflection versus Normalized position of the moving mass – Comparing results from MATLAB and SAP2000 for the undamaged and always-open crack model and the switching crack located at the bottom side of the beam

In figure [4.9] the case of the crack located at the bottom side of the beam is considered. Two transition instants are observed now, t_1 where the crack opens and t_2 where the crack closes again. This means that the crack remains open for quite a large part of the analysis, so that the plot of the switching crack model now coincide with the one of the always open crack model.

There are no new findings comparing to the last numerical application but it was important to notice that the computational strategy presented, including the analytical expressions derived in this project, is able to deal with any case of beam-type damaged bridge with both time-variant and time-invariant damage parameters. The next numerical application will compare these two categories of damage in terms of identification purposes.

4.4 What would be the differences in damage identification when using the switching crack model instead of the widely adopted always-open crack model?

This part is, indeed, really important as it sums up all the findings of this thesis project in order to deal once again with the main research question "*How to model and identify damages with time-variant and invariant parameters on beam-type bridges under moving vehicle loads*". Until now, numerical applications have been done to prove which would be the optimal measured quantity to detect crack(s), what would be the minimum depth of a crack to be identifiable, and other examples to test different ways of modelling the crack or to increase the complexity of the beam-type bridge. Then, the analytical expressions for the mode shapes were modified to be able to deal with damages with time-variant parameters, introducing a Boolean array which indicates a constant crack distribution for every time step of the analysis. Now it is time to test the switching crack model using the knowledge derived from the identification of the crack for the always-open crack model. The question is, what would change as far as the crack identification is concerned when using the switching crack model instead of the widely considered always-open crack model.

Numerical application (4.3) – One switching crack located at the midpoint – Moving vehicle load as a spring mass system:

The properties for this numerical application are a combination of using the beam and damage properties of the numerical application [4.1], mentioned in [21] but now instead of a moving mass, the vehicle is represented as spring-mass system in order to be able to derive its motion as well as the reaction force acting on top of the beam, measurements that are useful for the crack identification, as it has been shown.

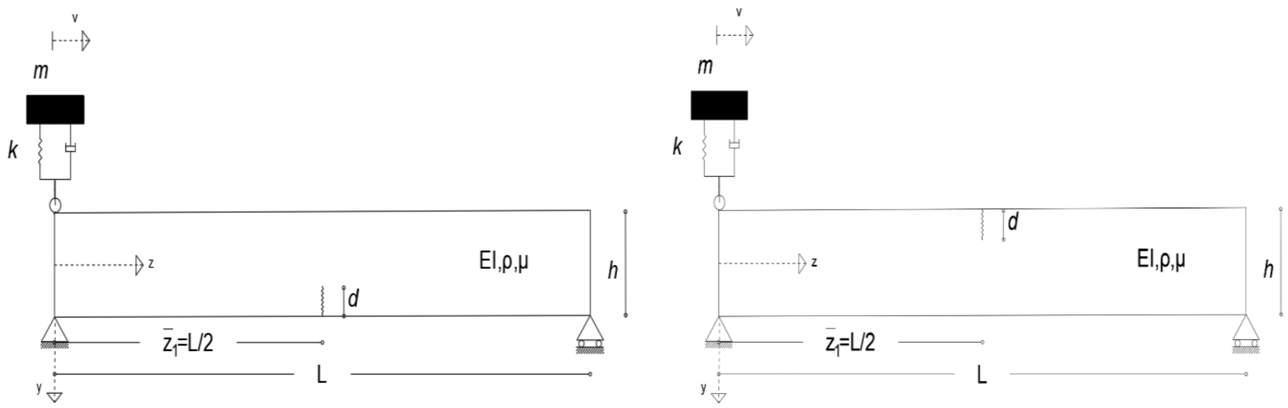

Figure 4. 11: Numerical application (4.3) - Model definition (left): crack located at the bottom side, (right): crack located at the top side

Table 4. 8: Numerical application (4.3) - Properties of the beam

Properties	Length - *L* (m)	Density - *ρ* [kg/m³]	Cross-sectional area – A (m²)	Young's modulus - *E* (GPa)	Second moment of inertia – *I* (m⁴)
<u>Beam</u>	20	7800	0.04	206	$1.33*10^{-4}$

Table 4. 9: Numerical application (4.3) - Properties of the moving oscillator

Properties	Mass -*m* (kg)	Damping – *c* (Ns/m)	Stiffness -*k* (N/m)	Speed – *v* (m/s)
<u>Oscillator</u>	1000	25130	$3.96x10^{6}$	5

Table 4. 10: Numerical application (4.3) - Properties of the crack

Properties	Location - $\bar{z}_1$ (m)	Depth *d* (m)	Equivalent stiffness - *K* (kN/m)	Damage parameter – *α* (m^{-1})
<u>Crack</u>	10	0.15	8000	3.33

For a beam-type bridge with the specific properties, using again a spring-mass system as the moving vehicle instead of a moving mass, the switching crack model and the always-open crack model will be compared as far as the damage identification techniques are concerned. Both top and bottom side of the beam as the location of the crack will be considered, as it has been done before and it was proven that the location could really affect the results. Specifically, for the already found as the optimal measured quantity for crack identification purposes, the moving vehicle's acceleration, the results of its difference with the undamaged case for the time-variant and time-invariant crack parameter, are presented in the figure below:

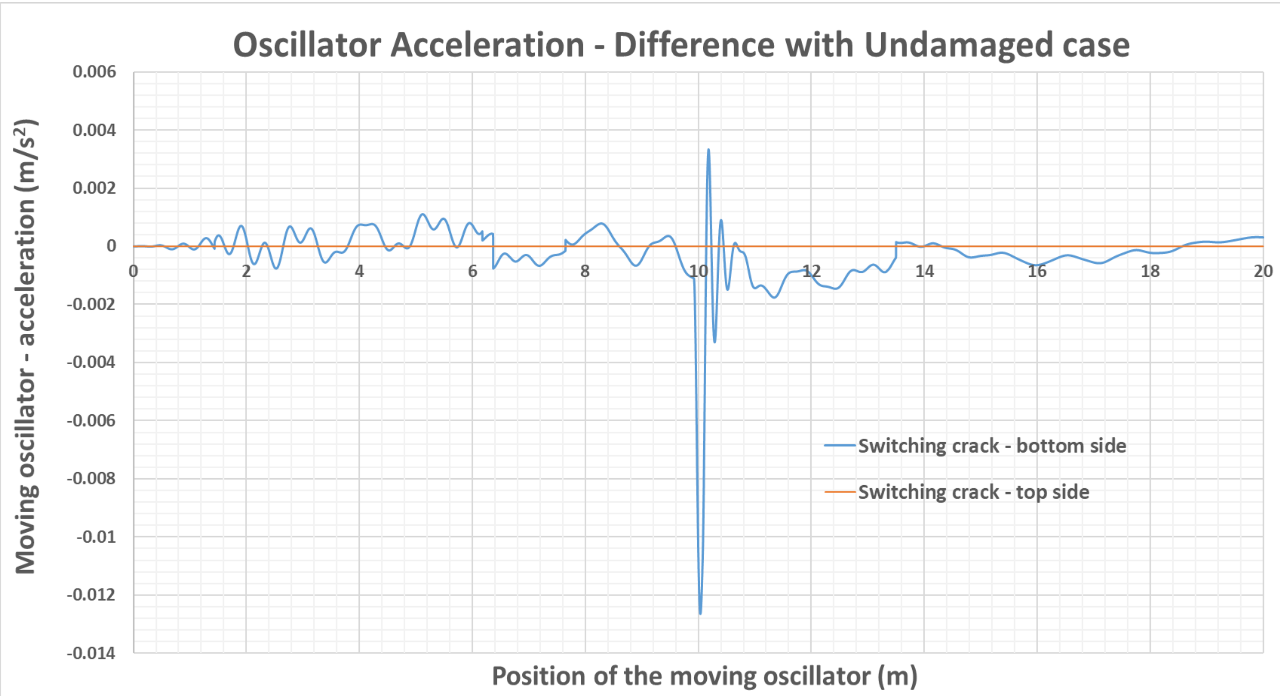

Figure 4. 12: Numerical application (4.3) - Oscillator's Acceleration versus Position of the moving oscillator – Compare different locations for the crack (top/bottom side of the beam)

Figure [4.12] contains, indeed, really important and useful remarks for the identification of crack(s) with time-variant parameters. When the crack is considered as located at the top side of the crack, there is not even one indication that there is a crack present along the beam at all. When the crack is considered as located at the bottom side of the beam, the abrupt fluctuations that were also there for the always-open crack model, could be observed exactly when the moving vehicle passes on top of the location of the crack. This means that when one or more cracks belong to the category of damages with time-dependent parameters, mainly because of one or more vehicles moving on top of the beam and causing time-dependent transversal vibrations, the location of these cracks is really crucial because it could lead wrong estimations about the structural condition of the bridge, and even if it is damaged there would be no sign of identification.

One reason that these results were more or less expected, comes by looking at the expressions of the governing equations that describe these time-dependent problems of a beam subject to moving vehicle loads. What really separates the damaged and the undamaged condition of the beam are the entries of the modal matrices that are included in the equation of motion. The differences of the two conditions come from considering the analytical expressions of the mode shapes, $\Phi_r(vt)$, for the damaged or undamaged state of the beam, that were derived at the beginning of this thesis project. When the transition instants indicate that the crack will be open almost for the whole analysis (as it is happening for the case of the crack located at the bottom side of the beam) then the mode shapes considered will be the ones of the damaged scenario, so also the moving spring-mass system will move on top of a damaged beam and the damage will be identifiable. When the transition instants indicate that the crack will be closed almost for the whole analysis (as it is happening for the case of the crack located at the top side of the beam) then the mode shapes considered will be the ones of the undamaged scenario, so also the moving spring-mass system will move on top of a undamaged beam and there would be no way of identifying the damage.

To sum up, understanding the behavior of damaged beams with cracks with time-variant parameters subject to moving vehicle loads is really important for damage identification. All the main conclusions mentioned here and in the paper [21] about the switching crack model and the identification of switching cracks should be all considered in the field of structural health monitoring of bridges to be able to make accurate and safe suggestions about their integrity.

Discussions and Conclusions

Results discussion

The damage identification techniques for beam-type bridges under moving vehicle loads have been investigated. In order to accomplish that, new analytical expressions for the mode shapes have been derived so that the dynamic response of such models could be calculated in an efficient manner. In these expressions, one can possibly deal with bridges with any number of step changes in material, any number of cracks, arbitrary boundary conditions, along-axis springs and internal rotational and translational springs at the discontinuities, making them a powerful tool for the calculation of the dynamic response of damaged beam bridges. The expressions have been validated with the results of Finite Element models in SAP2000.

Then, using the analytical expressions, it was possible to investigate fast and accurately different damage cases (varying the depth of the crack) to provide, at the end, valuable conclusions about crack dentification techniques. The quantities coming from the measurements from direct and indirect monitoring were compared to find the most sensitive one. Then, the optimal quantity has been tested in a different way of modelling the crack and in a model with step changes in material, so that the proposed method is valid for all these different scenarios.

Finally, damages with time-variant properties have been investigated, proposing a computational strategy that is able to deal with such models and which was verified again with the results from SAP2000. This strategy is based on checking the open cracks distribution at each time step of the analysis, identifying the "transition instants". It is a process which requires enforcing continuity conditions at each transition instant in order to account for the change in the mode shape basis. The reason why this strategy was developed, corresponds to the main objective of this thesis, which is "How to model and identify damages with time-variant and invariant parameters on multi-span beam-type bridges under moving vehicle loads modelled as a spring-mass system".

In this section, each one of the research sub-questions that have been formed in the Introduction part, and its corresponding answer, will be discussed.

In order to derive the new analytical expressions for a closed-form solution of the mode shapes, the question was:

- *How to improve the numerical stability (higher order modes) and accuracy of the closed form expressions?*

That was achieved by making use of generalized functions and local coordinate systems to decrease the expression of the frequency determinant of the jointed Euler-Bernoulli beam and lead to a large elimination of numerical round-off errors on the evaluation of high-order mode shapes.

While comparing different quantities for damage identification purposes, it was found that:

- *Which is the optimal measured quantity to detect a crack?*

The optimal measured quantity to detect crack(s) found to be the moving vehicle's acceleration, as it is by far the most sensitive one to changes in momentum that occur when the vehicle passes by the location of a crack. Other quantities like the reaction force or the oscillator's displacement are also affected at the point that the vehicle reaches the location of the crack but not as much as its acceleration. Changes in the dynamic characteristics (eigenfrequencies, mode shapes) of the beam bridge itself are also affected when damage(s) are present but these values are not so sensitive either.

- *Would the model of the crack affect the identification?*

There is, indeed, a discussion in the literature about the way damages should be modelled. The main objective is how close to reality is each one of these considerations and to aim for the best trade-off between model accuracy and computational cost. In this thesis, two ways of modelling the crack have been considered, an influenced zone (a relatively small segment of the beam) with reduced rigidity because of the presence of the crack (a method developed first and it is considered to capture the physics of the real scenario) and a discrete spring crack model using a massless rotational spring to represent each crack. The damage identification techniques presented in this thesis, as well as the new analytical expressions derived, can be used for both models with the same accuracy and without computational cost.

- *What would be the size of the crack with respect to the size of the cross section to be identifiable? Would the number of cracks affect the identification? Would the complexity of the beam-type bridge (varying rigidity) affect the identification?*

As far as the size of the crack to be identifiable is concerned, it is a relatively difficult question to give a generic answer which holds in every case. In this thesis, considering the specific type of models, described throughout all the different chapters, and their limitations, different lower bounds calculated for each quantity, and different values for each one of these quantities when the way of modelling the crack is changing (see corresponding values in Chapter 3). Furthermore, the remarks of the damage identification techniques discussed in this thesis, are not affected in the presence of more cracks or when the complexity of the bridge increases, making the findings of this project more useful and robust.

In order to be able in this thesis to deal with models with cracks with time-variant properties, the questions and answers were:

- *How to model the switching crack in the Euler-Bernoulli beam? How to exploit closed-form solutions of the mode shapes to account for the switching cracks?*

These questions have been answered by modifying the analytical expressions for the mode shapes, derived in Chapter 2, by introducing a Boolean array which represent the crack distribution for each time-step of the analysis, specifying which crack(s) are open or closed at every time instant. These new expressions have been validated and they are able to incorporate the switching crack model in every type of beam model (models with increased complexity as presented in Chapter 2). An precise computational strategy has been proposed and is based on checking the open cracks distribution at each time step of the analysis, identifying the "transition instants".

- *Are the always-open or always-closed crack distributions the boundaries for the switching crack model?*

The boundary conditions, the presence of multiple cracks or multiple moving vehicles are the ones that found to define what would be the upper and lower bounds of the switching crack model. Another really important characteristic is the location of the crack (bottom or top side of the beam) that plays a crucial role in the dynamic behavior of the time-variant damage.

- What would be the differences in damage identification when using the switching crack model instead of the widely adopted always-open crack model?

What was found, and it was also an important conclusion to answer the main objective of this thesis, is that the location of the crack is also important as far as the crack identification techniques are concerned because there are cases that the crack, even present in the beam, can not be detected at all, in any of the quantities considered in this thesis (see numerical application 4.3). This happens because the opening of a crack in the switching crack model depends on the value of the axial strain at the specific location and at the center of the crack, which means that if the external loads (coming from the vehicles) are not enough to lead to stretching of the fibers at that point, the crack will be considered as always-closed, and cannot be identified.

To sum up, all these research sub-questions were answered throughout this thesis and that was mainly accomplished thanks to the new analytical expressions derived in Chapter 2, that lead to fast and accurate results, surpassing the limitations of Finite Element models like handling cracks with time-varying parameters, remodeling and remeshing whenever a new model is considered leading to high computational cost for parameter investigation.

Limitations

An introduction about the assumptions of the model was given in chapter 1.5, which are necessary to derive all the equations presented in this thesis and have been made because of the specific research scope, restrictions regarding to computational cost or the compliance with the theories. Even if the conclusions of this thesis would not have been considerably changed if considering these limitations, it is important to note that:

- The surface of the bridge is considered as smooth, meaning the roughness of the bridge has not been considered in the governing equations of motion. There are other papers in literature examining different roughness profiles ([22], [23]) and especially their influence on the vehicle's acceleration which is the most sensitive one. The effect of road roughness can also be alleviated by means of filtering techniques, modifying the vehicle's damping, dual connected vehicles, consideration of ongoing traffic and more ([24]) .
- Vehicle's acceleration, which found to be the optimal quantity for damage identification purposes is not so easy to be extracted from real measurements. There is an on-going research about how to deal with environmental and operational uncertainties that have not been addressed and incorporated in the models of this thesis, which is also related to how and where to instrument the vehicle (sensor placement). An interesting paper [24] that includes and explains briefly many different approaches for the simulation, the laboratory tests and the field investigation of the specific problem is highly recommended.

Future Recommendations

Possible future works could improve the damage identification techniques for cracks with both time-variant or time-invariant properties, presented in this thesis, by using probabilistic model updating approaches to be able to include the uncertainties of the measurements. This can be accomplished by using probability density functions (PDF) to the uncertain parameters to end up in the "posterior" PDF which contains both the uncertainty of the prior information as well as the uncertainty in the experimental data ([25]). The new analytical expressions derived in Chapter 2 of this thesis could be used also in these approaches.

Bibliography

[1] An Y, Chatzi E, Sim S-H, Laflamme S, Blachowski B, Ou J. Recent progress and future trends on damage identification methods for bridge structures. Struct Control Health Monitoring 2019;26(10).

[2] Corbally R, Malekjafarian A. Investigating the Contact-Point Response for Drive-By Damage Detection in Bridges. Conference: Civil Engineering Research in Ireland. 2020.

[3] Doebling, S. W., Farrar, C. R., & Prime, M. B., A summary review of vibration-based damage identification methods. Shock and vibration digest, 30(2) (1998), 91-105.

[4] Brownjohn, J., De Stefano, A., Xu, Y.-L., Wenzel, H., & Aktan, A. (2011). Vibration-based monitoring of civil infrastructure: Challenges and successes. Journal of Civil Structural Health Monitoring, 1(3–4), 79–95.

[5] H. Sohn, Effects of environmental and operational variability on structural health monitoring, Philosophical Transactions of the Royal Society A: Mathematical, Physical and Engineering Sciences. 365 (1851) (2007) 539-560.

[6] Giunta F., Cicirello A. On the analysis of jointed Euler-Bernoulli beams with step changes in material and cross-section under static and dynamic loads. Engineering Structures, Vol. 179, Issue 1, 2019, p. 66-78.

[7] Koplow MA, Bhattacharyya A, Mann BP. Closed form solutions for the dynamic response of Euler-Bernoulli beams with step changes in cross-sections. J Sound Vib Ed 2006;295:214–25.

[8] Torabi K, Afshari H, Najafi H. Vibration analysis of multi-step Bernoulli-Euler and Timoshenko beams carrying concentrated masses. J Solid Mech Ed 2013;5:336–49.

[9] Failla G, Santini A. A solution of Euler-Bernoulli vibrating discontinuous beams. Mech Res Commun Ed 2008;35:517–29.

[10] Lin RM, Ng TY. Exact vibration modes of multiple-stepped beams with arbitrary steps and supports using elemental impedance method. Eng Struct Ed 2017;152:24–34

[11] Gonçalves PJP, Brennan MJ, Elliot SJ. Numerical evaluation of high-order modes of vibration in uniform Euler-Bernoulli beams. J Sound Vib Ed 2007;301:1035–9.

[12] Xu W, Cao MS, Ren Q, Su Z. Numerical evaluation of high-order modes for stepped beam. J Vib Acoust Ed 2013;136:89–102.

[13] Friswell, M.I. , Penny, J.E.T. , 2002. Crack modeling for structural health monitoring. Struct. Health Monitor. 1, 139–148 .

[14] Pesterev, A. V., Bergman, L. A., Tan, C. A., Tsao, T.-C. and Yang, B., 2001. "On equivalence of the moving mass and moving oscillator problems," ASME paper No. DETC01/VIB-21518.

[15] Dimarogonas, A. , 1996. Vibration of cracked structures: a state of the art review. Eng. Fract. Mech. 55, 831–857 .

[16] Bilello, C., Bergman, L., 2004. Vibration of damaged beams under a moving mass: theory and experimental validation. J. Sound Vib. 274 (3?5), 567–582.

[17] Chondros, T. , Dimarogonas, A. , Yao, J. ,1998. A continuous cracked beam vibration theory. J. Sound Vib. 251, 17–34 .

[18] Pala, Y., Reis, M., 2013. Dynamic response of a cracked beam under a moving mass load. J. Eng. Mech. 139 (9), 1229–1238.

[19] Fu, C., 2014. The effect of switching cracks on the vibration of a continuous beam bridge subjected to moving vehicles. J. Sound Vib. 339 (0), 157–175.

[20] Ariaei, A., Ziaei-Rad, S., Ghayour, M., 2009. Vibration analysis of beams with open and breathing cracks subjected to moving masses. J. Sound Vib. 326 (3?5), 709–724.

[21] A. Cicirello, "On the response bounds of damaged Euler-Bernoulli beams with switching cracks under moving masses, International Journal of Solids and Structures, vol. 172-173,pp. 70–83, 2019.

[22] Y. B. Yang, Y. C. Lee and K. C. Chang, Effect of Road Surface Roughness on Extraction of Bridge Frequencies by Moving Vehicle, Interaction and Multiscale Mechanics, Vol. 5, No. 4 (2012) 347-368.

[23] A. Gonzalez, E. J. O'brien, Y.-Y. Li, and K. Cashell, "The use of vehicle acceleration measurements to estimate road roughness, "Vehicle System Dynamics, vol. 46, no. 6, pp. 483–499, 2008.

[24] Yang, Y.B. and J.P. Yang. (2018). "State-of-the-Art Review on Modal Identification and Damage Detection of Bridges by Moving Test Vehicles." International Journal of Structural Stability and Dynamics, 18(02).

[25] Lye, A. Cicirello, E. Patelli, Sampling methods for solving Bayesian model updating problems: A tutorial, Mechanical Systems and Signal Processing 159 (2021) 107760, ISSN 0888-3270.

[26] E. Simoen, G. De Roeck, G. Lombaert, Dealing with uncertainty in model updating for damage assessment: A review, Mechanical Systems and Signal Processing, Volumes 56–57, May 2015, Pages 123-149.

[27] G. Muscolino, A. Palmeri, and A. Sofi, "Absolute versus relative formulations of the moving oscillator problem, "International Journal of Solids and Structures, vol. 46, no. 5,pp. 1085–1094, 2009.